CODEN:LUTMDN/(TMMV-5150)/1-116/2016

LUNDS UNIVERSITET
Lunds Tekniska Högskola

Investigation of a package laminate by nanoindentation

- A study of polymer-aluminum adhesion and the effect of Free Fatty Acids

Oskar Korpås

Lund 2016

DIVISION OF PRODUCTION AND MATERIALS TECHNOLOGY
LUND INSTITUTE OF TECHNOLOGY, LUND UNIVERSITY

Abstract

This thesis has been carried out at the department of production and materials engineering at Lund University in cooperation with Tetra Pak. The goal has been to investigate a package material by nanoindentation with a focus on polymer-aluminum adhesion. Common paper board packages encountered in daily life for storing a wide variety of products often consists of several different layers to ensure an optimal overall performance of the package. On the inside of the package is usually a polymer layer to enhance the food-contact properties. When extra barrier properties against outside influence (e.g. oxygen, light) is needed an aluminum layer is often added. Good adhesion between these two layers is important since a lack of adhesion might affect the quality of the packaged product negatively. Specifically, Free Fatty Acids has been observed to significantly decrease the polymer-aluminum adhesion in in package laminates. It is therefore the goal of this thesis to investigate if nanoindentation can be used to investigate this adhesion and how it is affected by Free Fatty Acids. Nanoindentation is a technique in which a sharp indenter is pressed into the material using very small loads resulting in indentation depths on the order of hundreds of nanometers which enables the investigation of mechanical properties (e.g. hardness) of multilayer structures and thin films. Samples were investigated in three main ways: normal indentation, scratch test and cross-sectional indentation. First, the indents were made normal to the polymer surface and analyzed for hardness. It was found that the hardness of the polymer layer was possible to measure using nanoindentation with a value of approximately 15 MPa, although with significant variation. It was also found that holding time (the time in which load is held constant at maximum load before unloading) influenced the results more than the loading rate.

Next the adhesion was investigated by scratch test and cross-sectional indentation. This was done on samples submerged in acetic acid and untreated samples. The polymer was scratched with a linearly increasing load in order to try to induce delamination and the displacement of the indenter during scratch was analyzed for irregular behavior. Also, topography of the surface before and after scratch were measured and the difference were taken as a measure of plastic deformation. Scratch tests were unable to find any measures of adhesion. However, scratching a sample that had been submerged in acid for two days showed a behavior where the surface had become very flat and the material became significantly softer but very little plastic deformation occurred. This effect disappeared one day after the acid was removed, where the effect reverted back to the one for non-acid-treated samples. The third method was to make indents into the polymer-aluminum interface. These indents were analyzed qualitatively by analyzing the loading curves for irregularities as well as quantitatively by analyzing the hardness. These tests did not find any measure of adhesion. However, there was problems with getting the indent in the interface as there were problems with indentations ending up offset a few microns. This is probable due to too high surface roughness from insufficient sample preparation. All acid treated samples showed this problems and could therefore not be compared with the non-acid-treated samples in a satisfactory fashion.

Acknowledgement

This thesis has been done as a part of the education to Master of Science in mechanical engineering. The work has been carried out at the department of production and materials engineering in cooperation with Tetra Pak.

I would like to first direct a big thank you to my supervisor from Tetra Pak, Jan Wahlberg, for taking the time and meet to discuss the findings of the experiments and the intricacies of packaging materials. Also your great effort of proof reading the report over and over to make sure it's up to standard is something I am very grateful for. An equally great thank you I would like to direct to my supervisors from the department of production and materials engineering, Johan Persson and Jinming Zhou for always taking the time to discuss experimental approaches, findings and the interesting and complex field of nanoindentation. Off course a thankyou goes to my examiner Jan-Eric Ståhl for guiding me through the details of getting the report approved. I would also like to take the opportunity to thank all the people I've met along the way of writing this thesis. From the fika room discussions to Wednesday floor ball to the roommates at "plattan", you all made my time writing this thesis truly awesome!

Throughout all the years of pursuing my dream of becoming an engineer I've met a lot of friends along the way. While you are far too many to list here, I would still like to make an effort to direct a thank you to all of you.

Lastly, I would like to express from the bottom of my heart my sincerest gratitude to my family who have always supported me through my whole education. Without your support this would not have been possible.

Lund, Maj 2016
Oskar Korpås

1 Introduction

In 2015, the food waste in the European Union was estimated to 88 million tonnes with a cost of 143 billion euros [1]. Furthermore, one of the factors mentioned to be involved in food waste includes storage and transport. Increasing the shelf life of the products can therefore decrease food waste and thereby take a step towards a more sustainable way of living. In order to increase the shelf life of foods, an important aspect to consider is the performance of the package. A common method to improve the performance of the package is to create multi-layer laminate packages where each layer has a specific task instead of just one material to handle all problems. Although this demands a higher number of different materials, the use of several materials with optimal properties for each specific problem may actually decrease the amount of material needed, thus decreasing the environmental impact of the package.

However, the use of a laminate package makes determination of the interaction between the packaged food and package more difficult as the overall performance of the package is a combination of the specific performance of the individual layers and the interaction between the layers. For example, in high performance carton packages there is often a polymer layer closest to the packed food and an aluminum layer between the polymer and paper board. In order to determine the performance of the package both the polymers food contact properties as well as the polymer and aluminum layers barrier properties and the adhesion between the two layers need to be considered. Tetra Pak has discovered that the adhesion between the polymer and aluminum layer is affected negatively when storing contents with a high content of Free Fatty Acids (FFA). To this day there exists no reliable method to accurately determine the adhesion between the layers in a package laminate. The Peel test is the most commonly used method to investigate adhesion in package laminate applications. However, this method has a series of limitations and problems, especially apparent in laminates with strong adhesion and/or weak polymer layers.

Nanoindentation is a relatively new technique to measure mechanical properties (e.g hardness) on a small scale by pressing a sharp indenter into the material a few hundred nanometers. This makes it possible to measure the properties of thin films and multilayer structures without the influence of the underlying substrate. Although the most common properties to measure with the nanoindentation technique is hardness and elastic modulus, the technique enables many other properties to be investigated.

The aim of this thesis is to investigate the mechanical properties of a paperboard laminate using nanoindentation in a package laminate application. Specifically the adhesion between the polymer and aluminum layers and the effect of Free Fatty Acids is to be investigated.

1.1 Objective

The main objective of this thesis is to investigate the mechanical properties of the layers in a package laminate and its dependence of Free Fatty Acids using the nanoindentation technique. A big focus is put on finding a way to measure the polymer-aluminum adhesion and how this adhesion is affected by the presence of Free Fatty Acids. The specific objectives of this thesis is to:

- Investigate the previous scientific work relating to nanoindentation and adhesion measurements of a package laminate.
- Investigate the mechanical properties of the layers in a package laminate using nanoindentation.
- Investigate the polymer-aluminum adhesion properties in a package laminate using nanoindentation.
- Investigate how the polymer-aluminum adhesion properties change due to contact with Free Fatty Acids, using nanoindentation.

1.2 Scope and limitations

A significant part of the thesis is to investigate how the nanoindentation technique can be used in investigations of a package laminate. To achieve that some limitations have been made and are summarized below:

- Investigation of mechanical and adhesion properties are measured solely using nanoindentation. No comparative measurements using other techniques (e.g. Peel test) have been performed.
- Two paperboard laminates with different thickness of the inner polymer layer has been included in the experiments and one laminate without paperboard has also been included. The materials have been supplied by Tetra Pak.
- Hardness have been calculated using the instruments built-in software.
- No chemical analysis have been performed.

2 Background

In this chapter, a background to some important materials, techniques and other considerations are presented. First, a description of a typical carton package laminate and its production is presented. This is followed by a discussion on the theory of polymer-aluminum adhesion and common methods for measuring adhesion. Also an overview of the nanoindentation technique and the challenges of using it in polymeric materials are presented. Also, some common properties to measure are presented. The chapter finishes with a literature study that aims to investigate the scientific basis for polymer-aluminum adhesion testing using nanoindentation.

2.1 Basics of a carton package laminate

There are a lot of requirements on a package other than just being able to contain food in desired portions. The package must also protect the food from outside influences and inform the user [2]. The outside influences can be divided into 3 main categories: chemical, biological and physical [2]. Chemical protection minimizes the exposure to gases (typically oxygen), moisture and light. Biological protection includes the barrier to microorganisms, insects and other animals. The mechanical protection involves shielding the content from loads and other outside influences [2].

The main advantage of a carton package compared to other available packages is its rigidity, resistance to shock, the ability to produce it in different shapes, as well as its price [2, 3]. However, plain paperboard has a few problems that need to be addressed in order for a carton package to be fully successful. First of all, paperboard has bad properties regarding contact with food where its tendency to soak moisture from products and thereby decreasing structural integrity makes it unsuitable for applications with direct contact with food, except for some dry foods [4]. Instead, an internal layer, sometimes several, is added to the inside of a carton package [2]. This inner layer has many different objectives, where the main tasks are to protect the paperboard from soaking, stop negative outside influences such as gases (e.g. oxygen), moisture (e.g. water vapor) and light as well as providing the ability to make the package sealable [2].

The most common type of materials used for contact with food are the polyolefins (eg. Polyethylene and polypropylene) due to their heat-sealability and water barrier properties [5]. Specifically, polyethylene is the polymer most used for co-extrusion with paper board due to its low cost and processability [6]. Between the polymer layer and the paper board is sometimes a barrier layer which might be a polymer or metal. Common polymers used as barrier layers in package applications include polyamide (PA), EVOH, PET, PvdC, HDPE, and PP [7]. It is also common to use an aluminum layer as a barrier layer [2]. While polymers have limited barrier properties, aluminum is an almost perfect barrier although practical limitations

occur when producing the package such as porosity or micro-holes [4, 8]. An image showing the different layers in a paperboard package is shown below.

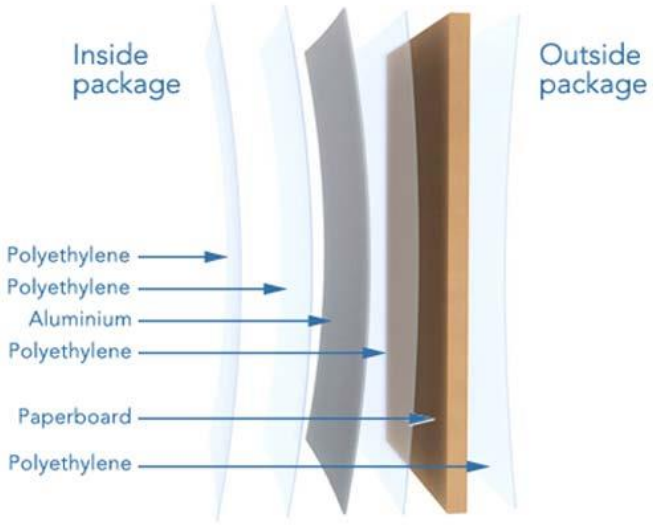

Figure 2.1 *Image showing the general appearance of a paperboard laminate investigated in this thesis (reprinted with permission from Tetra Pak).*

2.2 Production of a carton package

The process of applying one or several films onto other films or substrates is achieved by the process of lamination but within lamination there exists a variety of methods. In this chapter adhesive lamination an extrusion coating will be discussed followed by a discussion of surface treatments.

2.2.1 Adhesive lamination

Adhesive lamination connects two layers by applying an adhesive tie layer between two materials followed by pressing them together assuring sufficient contact between the materials and adhesive layer [9]. The materials can be polymeric film, metallic foil, paperboard etc. [9]. The important properties of the adhesive to ensure good adhesion is mainly its ability of bonding to the materials to be joined and good mechanical properties [10]. Bonding strength is mainly governed by chemical bonding (e.g. presence of acid-basic groups in the interface region) and molecular interlocking while the mechanical properties of importance is most importantly the plasticity properties [10]. A variety of adhesives exist and enercon lists them in the following categories [10]:

- Solvent-based.
- Non solvent-based.

- Water-based.
- Radiation-curable.
- Combination radiation curable.

Each adhesive has a list of polymers to which it can be applied and thereafter there is a big possibility to further mix and find the best formula for the specific application [10]. There are often more desired properties to take into consideration than bonding strength when selecting adhesive, of which can be mentioned barrier properties, optical transparency, electrical properties, heat resistance properties etc. [10]. There are different types of adhesive lamination processes of which two main configurations can be mentioned: wet adhesion and dry adhesion. The processes are shown below:

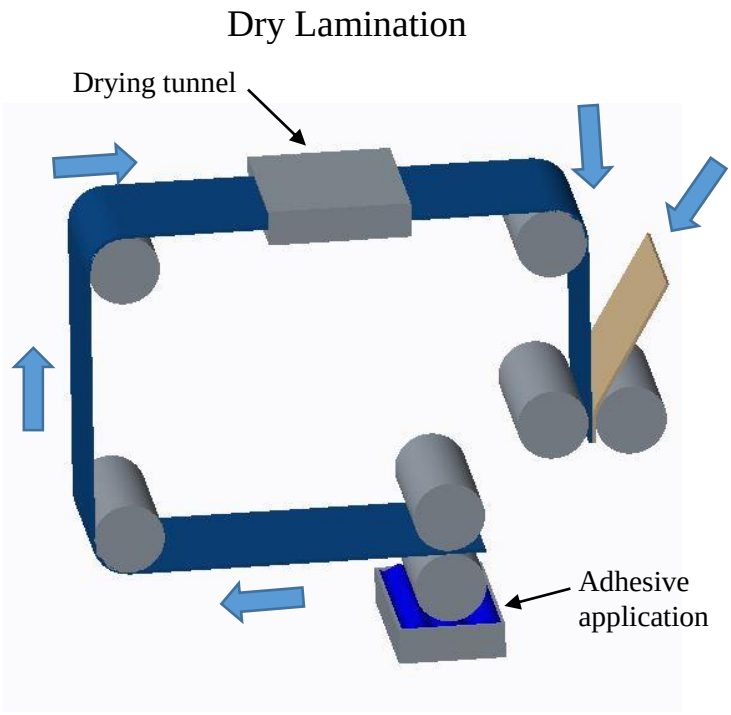

Figure 2.2 *Image showing the conceptual appearance of the dry lamination technique.*

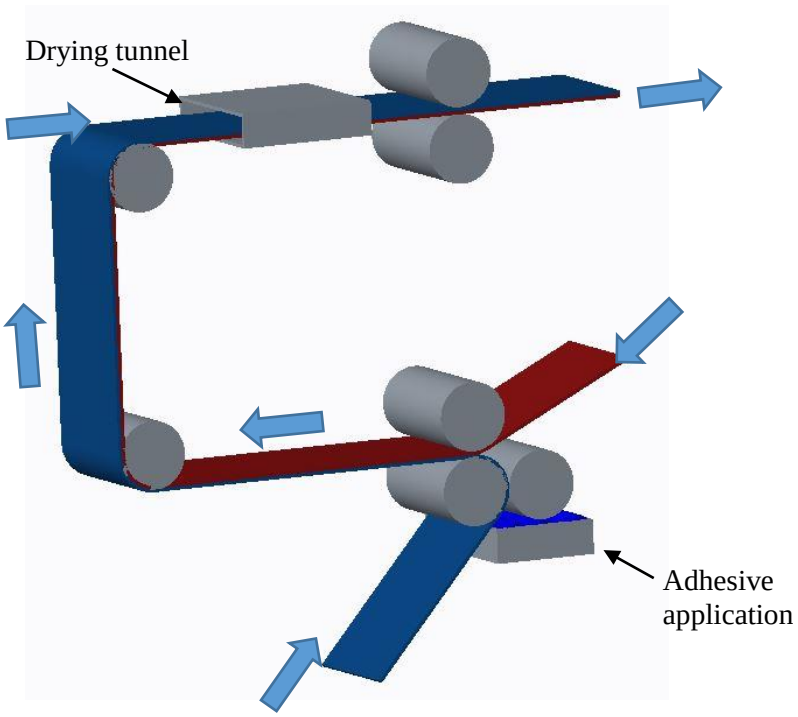

Figure 2.3 *Image showing the conceptual appearance of the wet lamination technique.*

2.2.2 Extrusion coating/lamination

The process of extrusion coating/lamination is a process in which a polymer is melted and extruded through a die onto a substrate which can be for example polymeric film, metallic foil, paper board etc. [11]. The extruded polymer can be applied on one side of a material called extrusion coating or between two materials called extrusion lamination. There is also a possibility to extrude several materials at once called co-extrusion [11]. Images illustrating these techniques are shown in Figure 2.4 below.

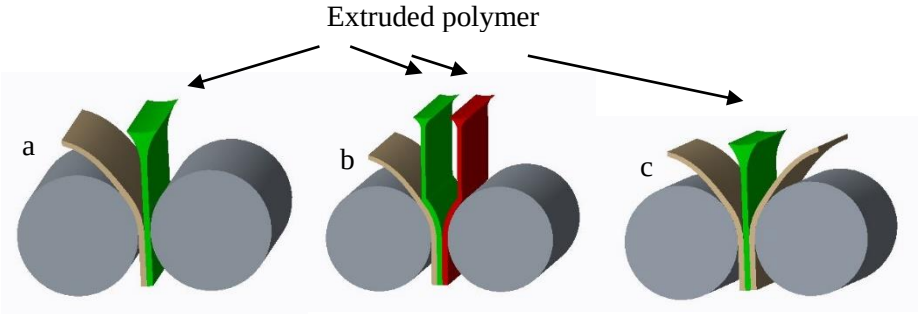

Figure 2.4 *Image showing the conceptual appearance of the a) extrusion coating technique, b) co-extrusion technique and c) extrusion lamination technique.*

A system for extrusion of polymers is a complex system, but can be described as follows: First the individual polymers are supplied in the state of granulates and thereafter simultaneously molten and transported forward under pressure via a transporting screw towards the shaping unit [12]. There is a lot of parameters to control in order to get optimal result, such as melting temperature, injection pressure and injection speed [13]. Thereafter, the molten polymer is pressed through a die onto the substrate where it is pressed between revolving chill rolls.

There are two basic ways of constructing the shaping unit, either via a feed block followed by a single manifold die or by a multiple manifold die [14]. The feed block collects the molten polymers and stacks them on top of each other prior to entering the die. There might arise problems in a feed block due to the viscoelastic behavior of polymers. This is especially apparent if the polymers have a big difference in viscosity, where the issue of encapsulation might occur. This means that the polymer with the lower viscosity might flow around the one with higher viscosity and if the cavity is long enough, encapsulate it. Therefore, polymers should if possible be stacked with polymers of similar viscosity [14].

Usually plates are inserted parallel to the flow in the cavity where the polymers are stacked to divide it into a couple of areas with equal area in order to ensure that the velocity of the different layers are equal [7]. In the case of different viscosity the geometry of these plates can be altered to hinder the viscosity induced problems in a method called profiling [7]. An image of a feed block is depicted in Figure 2.5

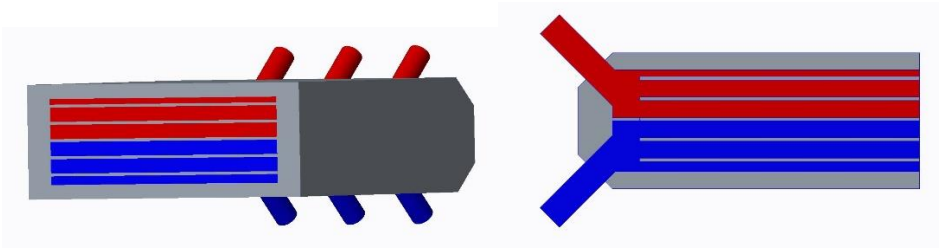

Figure 2.5 *Image showing the conceptual appearance of a feed block.*

If problems with viscosity cannot be solved using profiling, changing stacking order, changing materials or similar, a solution is to switch the feed block-single manifold

die assembly to a multimanifold die instead [7]. In a multimanifold die the streams of molten polymers are transported separately to the point where they are all pressed to the desired thickness [7]. An image of a multimanifold die is shown in Figure 2.6

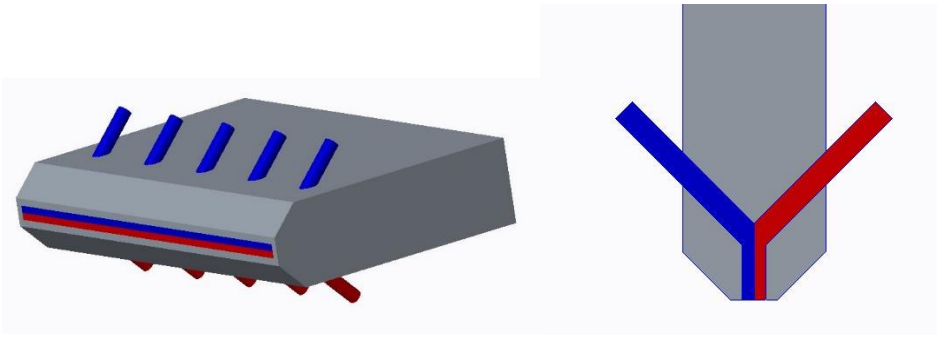

Figure 2.6 *Image showing the conceptual appearance of a multimanifold die.*

2.2.3 Surface treatments

Usually, polymers have poor adhesion properties due to a lack of acidic-basic groups on the surface rendering lamination with other materials difficult [15]. This draws the need of a surface treatment prior to lamination. The most commonly used methods includes corona discharge, plasma treatment and flame treatment [6].

The corona discharge works by putting a film of, for example, polymer or paperboard close to an electrode and applying a high voltage to the electrode. When the voltage is high enough the air is ionized around the electrode creating a blueish glow. This glowing region is a plasma containing ions, electrons, excited molecules, heat and light [16]. This plasma will oxidize the surface that is to be treated. The plasma is created as stray electrons around the electrode move towards the electrode and on its way collide with air molecules either knocking the electron out from the molecule or lifting it to a higher energy shell creating an excited molecule. The excited molecule is unstable and transforms into ions, thereby creating the corona [16].

Plasma treatments can be viewed as a process in which a stable plasma is created with more process parameters than the corona discharge method, for example because of the possibility to mix different gases to ionize in order to get the desired surface properties of the material to be treated [15].

Flame treatment uses, as the name suggests, a flame to increase the surface properties. This is done by several different factors, of which one is a plasma created by the flame [6]. Also, in the case of paperboard, the flame can burn of fibers extending out of the surfaces otherwise risking to puncture or in other ways minimize the adhesion of the laminated layer [6].

In extrusion coating/lamination the adhesion of the molten polymer and substrate needs to be optimized. It is often necessary to treat the molten polymer to ensure the existence of polar groups to ensure adhesion to the substrate. This can be done by high melting temperatures (300-320 °C) and a distance from the substrate long

enough that ensures that the polymer has time to oxidize [6]. However, high temperatures might lead to problems with odor and other shelf-life problems with the product to be packaged. Instead, ozone treatment is used where ozone is produced and transferred to the polymer melt between the die and lamination point, also called the nip [11].

2.3 Food-package interaction

To increase the shelf life of a packaged product the food-package interaction needs to be investigated. There are both the concern of components going from the package to the food as well as matter going from the food into the package. Multiple reports have investigated the components migrating from the plastic layer to the food, such as solvents, reaction by-products, additives and monomers [17].

Ilia Rodushkin & Astrid Magnusson reported that the transportation of aluminum from the package to the food when storing orange juice is negligible [18]. Also, as mentioned earlier the aluminum foil is an excellent barrier against gases and light [4, 19] adding to the picture that it is more important to focus on the matter going from the food into the package and its interaction with the different layers when investigating a package laminated with aluminum foil. One common problem regarding the food-package interaction is the migration of aroma compounds from the packed food into the inner polymer layer. As the polymer absorbs these aromas, the taste disappears from the packaged product [20].

There are a number of factors involving the shelf-life of a product, where the transportation of different compounds is of great importance. This food-package interaction can be divided into three different categories [21]:

1. Permeation of compounds through the package.
2. Migration of substances from the packaging material into the packed food.
3. Sorption of compounds from the food into the polymer.

The sorption of compounds include the sorption of flavors and aromas into the inner polymer layer that creates an off-taste due to lost flavor and therefore limiting shelf life [21]. It also includes the migration of chemicals from the package into the packed food. In the case of paperboard packages this mostly includes the solvents and adhesives used for production and lamination [20]. Research about the migration and sorption behavior in package applications has been relatively extensively researched and mathematical expressions, such as diffusion equations, have been developed [17]. Although interesting, it is beyond the scope of this report. There sometimes also exists a combined effect between the sorption and migration. Willige [22] reported that as LDPE absorbed flavor compounds it swelled and thereby significantly increased the oxygen permeability.

The migration of compounds into the package also creates the risk of the compounds decreasing the adhesion between the protective layers, and in worst case causing total delamination and thereby risking the quality of the packaged product.

Specifically, acids are well known to cause adhesion problems and a number of studies exists on different acids affecting aluminum foil laminated paperboard packages. Olafsson has published a series of reports regarding the adhesion performance of paperboard laminates subjected to acids [21, 23, 24]. The studies show that for a 3wt% solution in water of acetic, propionic, citric and lactic acid total delamination occurs after a few days for acetic acid with a recovery to 50 % of initial adhesion for acetic acid while propionic acid showed total delamination after 8 days with no signs of recovery. Citric and lactic acid and water showed no change in adhesion [24].

Also oleic and acetic acid were mixed in a fatty food simulant of rapeseed oil and water mixture where the mixture with both oleic and acetic acid had the highest absorption and migration rate and a total delamination occurred after 4-7 days for all emulsions [21].

Furthermore a study of the influence of acetic acid showed that a solution of 3wt% acetic acid in water delaminated the interface in 3-4 days while a solution of 1wt% showed little effect in 4 weeks. In the last study unsaturated fatty acids were mixed in a solution of water/sls/ethanol and thereafter stored in laminated carton packages for 4 weeks. The study showed that monounsaturated fatty acids were absorbed 2-4 times better than polyunsaturated and delamination occurred within 2 days. Polyunsaturated fatty acids were less uniformly absorbed but caused severe decrease in adhesion followed by an increase in adhesion to 50-60% of the initial adhesion. Moreover, for the acids used in that sub-study the adhesion decreased to half of the initial adhesion and remained that way throughout the experiment. The rate of delamination did not seem to be directly proportional to the amount of absorbed fatty acid [23].

2.4 Free Fatty Acids

Free Fatty Acids (also denoted as FFA) are characterized as a long hydrocarbon chain with a carboxyl group COOH at the end of the chain. FFA can be either saturated having only single bonds between the carbon and hydrogen atoms in the chain, or unsaturated having at least one double bond in the chain [25]. Sometimes the distinction is made between monounsaturated acids having only one double bond and polyunsaturated having two or more double bonds [25].

FFA are often described using a system where the first number reveals the number of carbon atoms in the molecule followed by the number of double bonds separated by a colon. Sometimes a parenthesis also follows revealing the position of the double bonds. As an example eleosteric acid is written as 19:3(9,13,15) [26].

2.5 Adhesion in package applications

2.5.1 Basic theory of adhesion between polymer aluminum

The most important bonding for joining polymer-aluminum (and most other inorganic surfaces) are believed to be the acid-base bonding [27]. There are two main theories describing acid-base relationship, the Brönsted theory and the Lewis theory where the Brönsted theory explains acids and bases as proton donors and acceptors whereas the Lewis theory explains acid and bases as electron donors and acceptors [28]. Although convenient when describing aqueous solutions, the Brönsted theory is a bit limited compared to the Lewis theory since it requires the presence of a proton [28].

Using the Lewis theory, an acid then reacts with a base by sharing electrons thereby creating a bond [29]. There are three different types of acid-base substances, consisting of monopolar acting either completely acidic or basic, bipolar acting both acidic and basic and apolar being inert and neither acidic nor basic [30]. Interesting to note is that water is bipolar, although not particularly strongly acidic or basic [27].

The definition of how strongly acidic or basic a specific substance is, can sometimes be tricky and demand caution. In simple aqueous solutions, for example the aforementioned water, there's usually not too much problems, since the content can be measured and the mixing is fairly uniform leading to quantitative expressions being developed [31]. In the case of solid surfaces, however, quantifying the strength is a bit more challenging. The strength can be seen as the sum of the functional groups but on the same surface there can be many different functional groups with different strength and both acidic and basic which can be unevenly distributed [30]. The functional groups strength depend on what molecules they are attached to and what they are surrounded by, and also there is often other substances not related to the surface material that contribute, such as contaminants [30]. There sometimes also occurs problems where the functional groups cannot bond with the other functional group due to the large widespread appearance of one or both of the

molecules that prevents them from coming close enough [30]. Sometimes the structure of the surfaces comes into consideration, for example a very finely porous surface can prevent the functional groups from reaching each other [30].

In the case of the metal surface, the metal oxide layer is usually the one most responsible for creating an acidic/basic layer [31]. There is a range of both acidic and basic groups on this metal oxide driving adhesion. O anions can act as Lewis bases while cations act as Lewis acidic sites whereas the OH anions can act both as a Lewis acid/base or a Brönsted acid/base [31]. The most important factor in determining if the resulting effect of a surface is acidic or basic is according to Van Den Brand the metal cation [31]. As exemplified by aforementioned author in "on the adhesion between aluminum and polymer", the strong electron accepting behavior of the Si cation in the SiO_2 oxide renders the oxide (via reasoning that will not be detailed here) as a resulting basic oxide whereas the relatively weak Mg cation in the MgO makes it acidic [31].

Although water is a weak acid and base, it has been observed that bonds between metal oxide and organic coatings are not stable in the presence of water [31]. There has been discoveries that water can travel through a polymer layer and cumulate at the interface between a polymer and metal surface decreasing adhesion. Several explanations have been proposed, of which can be mentioned the possibility of water to replace the relatively weak hydrogen-bonds between the polymer and metal as has been shown by van den Brand [31]. Also shown by the same author is a three step process in the case of an epoxy-aluminum laminate which can be described as follows [31]:

1. In the first step water diffuses through the polymer layer and accumulates in the interface decreasing adhesion.
2. An oxyhydroxide layer starts to grow at the aluminum surface.
3. The oxyhydroxide layer connects to the epoxy layer increasing adhesion and stops to grow due to a lack of water at the interface. This layer shows stronger bonding than the initial state thereby increasing adhesion. The oxyhydroxide layer is more stable against water decreasing the amount of water able to diffuse to the metal oxide interface and since the bonds are stronger they cannot as easily be replaced by the water.

2.5.2 Currents test methods

There exists many possible methods for measuring adhesion, but according to Kücükpinar [32] all techniques relevant to packaging today was summarized by Mittal in the late 1980's. According to Kücükpinar [32] the most common technique for measuring adhesion in package applications is the peel test which is why that technique will be discussed in more detail compared to the other techniques described in this chapter.

Mittal published a report named *Adhesion measurement in thin films* [33] in which methods deemed suitable for determining adhesion of thin films were described. The descriptions in that report will be the source for the methods described below

unless otherwise mentioned. However, the listing in this chapter does not aim to be comprehensive, but rather give a glimpse of some of the methods the author of this report considers relevant. It should be noted that the previously mentioned report is focused on thin (< 1μm) metallic films and therefore might have excluded some methods suitable for other setups, such as polymeric coatings.

2.5.2.1 Direct pull off

This method works by connecting a rod perpendicular to the film, for example by gluing, after which the specimen is inserted into a tensile testing instrument where force is applied to the connecting rod so that the loss of adhesion causes the film to be lifted from the substrate. A value of the adhesion is then obtained as the force required to remove the film from the substrate. Care must be taken so that the connecting rod is connected at 90 degrees towards the film. Also, the method of joining the connecting rod to the film must be significantly stronger than the adhesion between the film and the substrate. The value obtained cannot be seen as the pure adhesion since the mechanical properties of the film and connecting rod and the connecting joint between the two will influence the obtained result.

2.5.2.2 Moment or topple method

This method is similar to the previous method but instead of subjecting the rod to tension, a force is applied to the rod parallel to the surface of the film, thereby resulting in a moment at the surface of the film causing deadhesion when it's sufficiently high. The moment required to remove the film from the substrate is then obtained as a measure of the adhesion.

2.5.2.3 Scotch tape method

The first step in this method is to apply a piece of tape to the film thereafter subjecting the tape to tensile stress parallel to the film. The film can then be either be completely peeled off, not peeled off at all or partially peeled off. This is mostly a qualitative method mostly capable of screening films with poor adhesion.

2.5.2.4 Peel test

The peel test is the most commonly used test for adhesion testing in package applications and can be performed in a tensile testing machine. Its basic description is that after a strip of the bonded material of interest is inserted in the machine to be used, force is applied at the end of one or both of the laminated materials, thereby "opening the strip". The test can be performed at any angle, where zero degrees corresponds to the direction parallel to the strip pointing out of the end where force is to be applied. However, three basic types of test exists, the T-peel test, the 90° peel test and the 180° peel test. The 90° and 180° peel test are preferably used when a flexible material is bonded to a rigid substrate. The rigid material is fixed and the other film is then pulled in a 90 or 180 degree angle. In the T-peel test both materials are attached to a separate tensile tester clamp and thereafter pulled in the opposite direction from each other. The pulling motion is programed to be done at a fixed rate and the force required to split the two materials divided by the width of interfacial zone is then taken as the measurement of adhesion.

2.5.2.5 Tangential shear or lap shear method

A piece of glass is glued to the film and then force is applied to the glass plate parallel to the film thereby causing loss of adhesion. The applied force needed to make the film lose connection to the substrate is then a measurement of adhesion.

2.5.2.6 Scratch or stylus scribe method

In this method an indenter is drawn across the surface with an increasing load until the film is completely removed from the substrate, creating a ”channel” down to the substrate with no film present. The load at which all of the film has been removed is a measure of the adhesion

2.5.3 Limitations and problems

Ideally, adhesion measurement should be a direct measurement of the forces between the two materials bonded together, although that is hard to achieve in reality due to practical considerations. Mittal [33] proposed the term practical adhesion as

$$practical\ adhesion = basic\ adhesion - (loss\ of\ adhesion\ due\ to\ internal\ stress) \pm effects\ or\ defects\ or\ extraneous\ processes\ introduced\ by\ the\ test\ procedure$$

Where basic adhesion is the “true adhesion” depending only on the bonding forces. In peel test measurements, what is obtained is the practical adhesion and a factor influencing the output can be for example the mechanical behavior of the films during loading. The force required to de-adhere the layers can be the sum of overcoming the interfacial forces as well as deformation of the film(s) [32, 34]. Also the loading conditions may influence the obtained value such as the loading rate [34]. Another major problem is that preparation of the sample can affect the obtained value, for example in order to get hold of the layers in the laminate one must use some method to extract them from the laminate. Such a method can be to heat-seal a polymer strip onto the films and apply force to the heat sealed polymer. This introduces more uncertainties as the response from the Peel test is now also depending on the mechanical properties of the heat sealed polymer strip and its adhesion to the original layer to be tested [32, 34].

2.6 Nanoindentation

2.6.1 General introduction

As the materials used today are getting more complex and the situations in which they are expected to operate get increasingly demanding, the need for more advanced test methods to drive this development forward emerge. One such method is the nanoindentation technique, which is a relatively new technique first being developed in the 1980's [35]. The theory behind the nanoindentation is to use a sharp indenter to press into the material, from which various mechanical properties can be obtained (e.g. hardness, modulus of elasticity) [36]. The procedure is in principle similar to conventional hardness testing techniques (e.g. Vickers, Brinell) but with some key differences. First of all, the loads applied (and thereby indentation depths) are much smaller. As the name implies, indentation depths are measured in the order of nanometers and the applied loads on the order of micro or millinewtons [36]. Secondly, while common hardness measuring techniques usually only measure the properties relating to the maximum indentation depth, nanoindentation devices almost exclusively continuously measure the indentation parameters (e.g. depth and load) throughout the experiment called *depth sensing indentation*. This enables the ability to measure more properties than in a conventional hardness tester [36].

Nanoindentation has several advantages compared to an ordinary hardness testing instrument. An obvious application where its advantages becomes apparent is when mechanical properties of multilayer structures are of interest. Where conventional hardness tests due to its high forces and big indenter area would get a result dependent on the mechanical properties of all the different layers, the nanoindentation makes it possible to measure the mechanical properties (e.g. hardness and elastic modulus) of the individual layer [36]. Analogously, nanoindentation enables the measurement of the properties of thin films. Due to the lack of neighboring molecules the mechanical properties of thin films are different than those of the bulk material [37].

Also, due to the sharp indenters and small indentation depths, nanoindentation can be used to measure the variation of properties due to the microstructure of the material. For example, for materials with a microstructure consisting of different phases indents can be aimed measuring the properties of the specific phase excluding the influence from surrounding phases and grain boundaries [38]. Nanoindentation instruments often include a nano-scratch module in which the indenter is moved along the surface of the material. This can be used to measure for example wear properties or adhesion properties in multilayer materials [36].

The applications for nanoindentation are numerous and more applications are found as the nanoindentation technique is gaining more attention and popularity. It is the purpose of this chapter to explain the basics of nanoindentation together with an overview of experiments carried out previously that can be of interest for the investigation of mechanical and adhesion properties of a package laminate.

2.6.2 Nanoindentation and nano-scratch properties

Table 2.1 *Table of selected properties to investigate using nanoindentation.*

Hardness
Elastic modulus
Creep
Plasticity/ Elasticity
Surface adhesion
Topography
Yield strength
Structure changes
Wear resistance

Although hardness and modulus are the most common properties when investigating mechanical properties by use of nanoindentation there are a variety of other properties of which a selection have been summarized in Table 2.1 and below follows a description of those properties.

2.6.2.1 Hardness

The hardness and elastic modulus is obtained by the widely used theories by Oliver & Pharr [39] in which the hardness is assumed to be

$$H = \frac{P_{max}}{A} \tag{1}$$

where H is the hardness, P_{max} is the maximum load and A is the projected area of contact. The area is calculated via indenter geometry and the contact depth, h_c, which is related to the total indentation depth as

$$h_c = \beta h - \frac{\varepsilon F}{S} \tag{2}$$

where β and ε are constants related to indenter geometry, h is total indentation depth, F is the load and S is the stiffness, visualized as the slope of the initial unloading curve, as depicted in Figure 2.8. S can also be expressed as

$$S = \frac{dP}{dh} \tag{3}$$

2.6.2.2 Elastic modulus

As is the case with hardness, the elastic modulus is calculated using the methods developed by Oliver & Pharr [39] showed in eq. 4-5 where E_r is the obtained modulus when considering the elastic behavior of both the indenter and sample. E_i and υ_i are elastic modulus and poissons ratio for the indenter tip whereas E_s and υ_s are elastic modulus and poissons ratio for the sample. S is the stiffness, as explained in eq. (3)

$$E_r = \frac{\sqrt{\pi}S}{2\sqrt{A}} \tag{4}$$

$$\frac{1}{E_r} = \frac{1-{v_i}^2}{E_i} + \frac{1-{v_s}^2}{E_s} \tag{5}$$

Figure 2.7 shows a schematic image of a residual indent with some important measures and Figure 2.8 shows a schematic load-unload diagram.

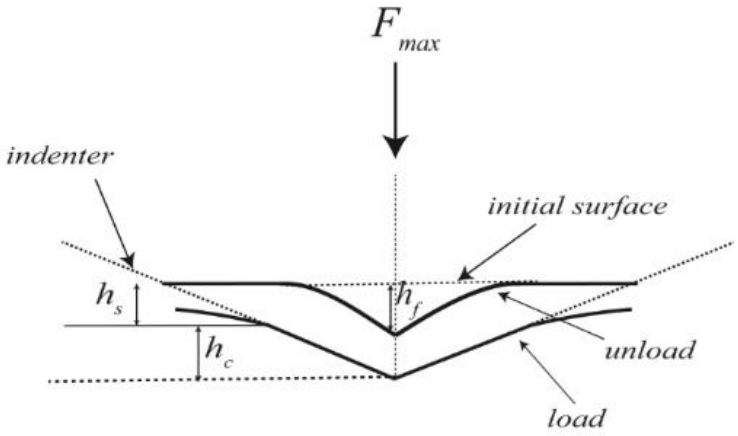

Figure 2.7 *Schematic image of a residual indent in nanoindentation. Image acquired from Cinar et al. [40].*

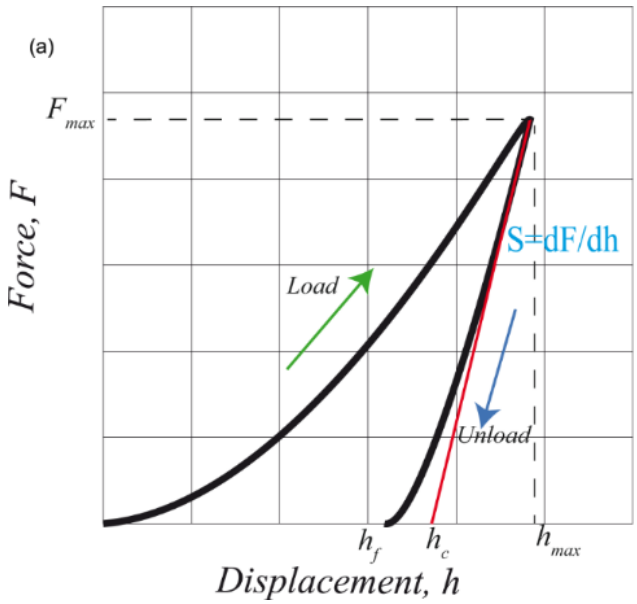

Figure 2.8 *Schematic image of a load-unload curve in nanoindentation. Image acquired from Cinar et al. [40].*

2.6.2.3 Creep

Creep is especially apparent in polymers due to their viscoelastic behavior, where the displacement into the material is dependent not only on the load applied but also the amount of time the load has been applied [41]. This behavior may affect the experiments negatively if not accounted for. Often, the hold time is held sufficiently long for the creep behavior to wear off or at least stabilize to an extent where it influences the readings as little as possible [42]. There is also a possibility to investigate the creep properties of the tested material using nanoindentation. In a report by Fang & Chang [43] the below formula for modeling creep was used

$$\sigma = k\dot{\varepsilon}^n \tag{6}$$

Where σ is the contact stress, $\dot{\varepsilon}$ the strain rate and n is the stress exponent for creep. The strain rate as proposed by Briscoe et al. [44] can be expressed in terms of loading rate as

$$\dot{\varepsilon} = k_2 \cdot \frac{\dot{h}}{h} \tag{7}$$

Where h is the displacement of the indenter and $\dot{h}$ is the displacement rate of the indenter. If instead loading rate is the used parameter strain rate can be expressed in terms of the loading rate $\dot{P}$ as [44]

$$\dot{\varepsilon} = k_2 \cdot \left(\frac{\dot{P}}{h \cdot \frac{\partial P}{\partial h}} \right) \tag{8}$$

The expression for contact stress is then put into a log scale thereby obtaining [43]

$$\log \sigma = \log k + n \cdot \log \dot{\epsilon} \tag{9}$$

Describing a linear relationship between log σ and log $\dot{\varepsilon}$ where n represents the slope. This was proved to be valid for polycarbonate film in the above mentioned report by Fang & Chang [43] where contact stress had a linear relationship with contact strain rate in a log-log diagram from which the parameters k and n was obtained.

2.6.2.4 Plasticity/ Elasticity

In an indentation sequence, the indentation depth can be divided into an elastic part and a plastic one. If the unloading curve follows the loading curve the deformation is purely elastic. In a report by Beake & Legget [45] a plasticity index, I_p, proposed by Briscoe [44] as

$$I_p = \psi_p/(\psi_p + \psi_{e)} \tag{10}$$

Was used, where ψ_p is the plastic energy which can be visualized in a load-unload diagram as the area between the loading and unloading curve, and ψ_e is the elastic energy which can be visualized in a load-unload diagram as the area between the unloading curve, a vertical line from the point of max depth and the horizontal line

at zero load. This plasticity index can thereafter give information about how much of the deformation is elastic and plastic.

2.6.2.5 Yield strength

Yield strength is usually performed by a tensile test where load is applied in such a manner that the sample is subjected to tension and the stress-strain curve can be analyzed to determine where deformation is plastic. For thin polymeric films, however, setting up a tensile test might be difficult, especially if the polymeric film in question is bonded other materials. Instead, indentation tests can be carried out where yield strength is related to hardness through a numerical relationship. Although first developed for metallic materials, according to Strojny et al. [46] the hardness for glassy polymers can still be expressed as a linear function of yield strength as

$$H = k \cdot \sigma_{ys} \tag{11}$$

where k is a material specific parameter and σ_{ys} the yield strength. Another method used in the same report referred to as an *imaging method* the size of the residual indent and pile-up is taken as a measurement of the size of the plastic zone and is thereafter related to the yield strength by

$$\sigma_{ys} = \frac{3P_{max}}{2\pi c^2} \tag{12}$$

Where P_{max} is the maximum load and c is the size of the plastic zone.

2.6.2.6 Structure changes

Nanoindentation test can also be used to extract structure changes of the material, such as the glass transition where the modulus will decrease rapidly when the polymer goes from the glassy state to a rubbery state. This was done by Spinks et al. [47] where the glass transition temperature was predicted at a value in relatively close accordance to the value known from literature.

2.6.2.7 Surface adhesion

Apart from previous methods which can be seen as measuring properties comprising the whole material, nanoindentation also provides an opportunity to measure properties more related to the properties regarding the surface. For example, Cakmak et al. [48] studied the surface characterization of reactor-thermoplastic-polyolefin co-polymers with focus on investigating the surface "stickiness". The method pursued was to set the stickiness as the adhesion between indenter tip and sample surface which is visible in the unloading curve as negative force readings in the unloading curve since the adhesion prohibits the indenter from retracting due to the adhesion between tip and sample surface.

2.6.2.8 Topography

It is also possible to measure the surface topography of a sample. This is done by scratching the surface with a very small load (on the order of 0.01 mN). As the indenter encounters a hill it must move up in order to keep the load constant and

analogous it must move down if it encounters a valley. This produces a curve that shows the surface topography which can then be analyzed for surface roughness.

2.6.2.9 Wear resistance

The wear resistance properties are possible to investigate using nanoindentation. In a report by Beake & Legget [45] the difference in scratch resistance between uniaxially and biaxially drawn PET-films were investigated. The materials were scratched three times with a scanning after each scratch to determine the residual plastic deformation from the scratch. The plastic and total depth were measured and it was concluded that the resistance to wear followed the ratio of hardness to the elastic modulus.

2.6.3 Important parameters in nanoindentation

Table 2.2 *Important parameters in nano-scratch.*

Max load (or depth)
Loading rate
Unloading rate
Holding time

It can be important to have some knowledge in the parameters involved when performing a nanoindentation experiment and its consequences. As the nanoindentation instrument can be used both in a load controlled manner (setting the max load) and depth controlled one (setting the max depth) the parameters are naturally different depending on in which mode it is set [36]. For a load controlled experiment the natural parameter is the max load whereas in a depth controlled one the max depth is the important parameter [36]. It should be noted that although the machine can be operated in a depth controlled mode, most nanoindentation machines are built so that they are load controlled. For example: when discussing the sensitivity of a nanoindentation device, minimum indentation depth is not a relevant specification since the nanoindentation devices are built to be able to apply as small forces as possible, with the penetration depth as a response to the load applied [36].

Another parameter to determine is the loading and unloading rate, meaning the rate at which the load is applied and decreased. Also important is the holding time as earlier mentioned. In a report by Fang & Chang [43] the nanoindentation characteristics of polycarbonate film was investigated and it was found that an increase in applied load decreased the modulus and hardness as did an increase in hold time. Also, an increase in loading rate increased the modulus and hardness.

2.6.4 Important parameters in nano-scratch

Table 2.3 *Important parameters in nano-scratch.*

Max load (or depth)
Load rate
Total scratch length
Length of max load

Similar to nanoindentation an important parameter in the nano-scratch experiment is the max load or max depth paired with loading rate, although the unloading rate does not have as pronounced role. Also important is the scratch length which can aid in setting the loading rate by setting the max load and the scratch length thereby obtaining the loading rate.

A nanoscratch experiment usually consists of three parts: pre-scan, scratch and post-scan. During pre-scan the topography prior to the scratch sequence is analyzed. During scratch the indenter is scratched along the sample. During post-scan the topography of the residual scratch groove is measured.

2.6.5 Nanoindentation in polymers

Although nanoindentation has become a common method for investigating the mechanical properties of small dimension samples [49] there still exists some problems regarding the experiments of polymeric materials [42]. The obtained values for for example hardness and modulus when using the method of Oliver & Pharr, previously explained, tend to be exaggerated compared to expected values [42]. The biggest contributor to this problem and other general problems encountered in nanoindentation of polymers is believed to be the viscoelastic behavior of polymers that the Oliver & Pharr method does not account for [50]. The viscoelastic behavior mainly manifests itself as a time dependent load behavior such as creep [41]. Specifically, it has been reported in literature of a ”nose” in the loading curves when the indentation depths increase although the applied load is decreased producing a negative slope which cannot be used for calculations of mechanical properties [42]. To rid these problems it is possible to develop a viscoelastic material model from which calculations of mechanical properties can be performed. A lot of studies exists on producing such material models for different materials [51], but developing such a model lies outside the scope of this report. However, some actions can still be made in order to try and minimize the influence of the viscoelastic behavior for example by using long holding times [51] or otherwise tweak the experimental parameters.

Another problem usually encountered is pile-up where the indented material bulges up along the indenter. This leads to a greater contact area than what the indentation depth implies, therefore inducing misleading values [50]. However, this phenomena can be minimized by using smaller indentation depths [51].

Adhesion between tip and sample material results in the problem of the material restraining the indenter from retracting in the unloading state which then decreases the experienced load on the indenter tip, thereby increasing the stiffness [48]. There is also a problem with determining the shape of the indenter. Hochstetter et al. [52] discovered that experiments on determining the tip defect, i.e. The deviation from a perfectly sharp tip, were significantly different depending on if the experiments were carried out on fused silica or polymers. This is similar to the problem of determining the zero point of the sample, where the used zero point yields an applied load (usually some tens of micronewtons), which in the case of a relatively soft polymer means that the indenter will have to be pressed in a non-neglible distance [42].

2.6.6 Experimental overview

In a report Djokić et al. [53] the mechanical properties of chitosan/poly(ethylene oxide) (PEO) films were investigated using nanoindentation. The Oliver & Pharr method was deemed suitable since the indentation depth was small in comparison to the film thickness. Further, a line scan of the residual indent was made together with measures of surface roughness where the surface roughness was deemed low enough to perform indentation tests and the absence of considerable pile-up and sink in behavior of the residual indent ruled the obtained results reliable.

Although the material is different from the one to be investigated in this thesis, there are some interesting conclusions to draw from it. First, reducing the substrate effect is important, especially since the material to be investigated has a smaller film thickness and different substrates with different properties than the polymer film of interest. A common rule of thumb to avoid substrate influence is that the indentation depth should be less than 10 % of the film thickness [54]. Another approach is to calculate a substrate correction as was done in a report by Strojny et al. [46]. In order to do this the properties of the substrate must be well known, for example by indentation tests. This procedure is not possible in this thesis due to the complex nature of the layers beneath the polymer film of interest, but there should be no problems following the rule of thumb.

Further, the investigation on surface roughness is interesting since the material investigated in this thesis suffers from a high surface roughness. Strojny et al. [46] proposed that the effect of surface roughness on indentation response is due to the difference in contact area which is especially apparent if the indenter geometry is big compared to the surface irregularities. Similarly, Cakmak et al. [48] explains a high scatter in indentation tests with surface roughness and correlates a flat rise of the initial loading curve to indenting on the top of a hill and a steep rise to indenting on a valley. Although the surface roughness probably cannot be altered, it is important to keep in mind going forward the potential effect it might have.

As reported earlier, the behavior of polymers during indentation demands caution when analyzing the results, and this is especially true for the polyethylene polymer investigated in this thesis since it is a relatively soft polymer. An attempt to rid some of these problems is to use a continuous stiffness measurement technique (CSM) where a small sinusoidal load is superimposed during the loading part, rendering the

mechanical properties a response to this sinusoidal loading rather than the unloading part of the base loading curve. Although an interesting technique, the use of such a technique would be more suited if the pure material properties were sought after rather than the adhesion characteristics and would require a lot of calibration and time for finding the optimal method and parameters. Since the scope of this report is not purely aimed at extracting the mechanical properties of the polymer film alone the use of CSM is not pursued from an early stage, but it should be kept in mind if extracting properties get tricky or a more precise and accurate value of the mechanical properties of the polymer is sought.

Other than indentation tests, the nanoindentation technique also offers the possibility to perform nanoscratch tests where for example the adhesion between two materials can be investigated. Liu et al. [55] studied the adhesion of different coatings on PET substrates using nanoscratch where one of the coating tested was an aluminum film of 200 nm thickness using both a berkovich (three-sided pyramid) and a conical indenter. The surface of the aluminum were scratched with a linearly increased load with a maximum load of 5 mN. The loading curve was then investigated together with microscopic studies using an electron microscope. The loading curves showed no signs of irregularities that would indicate delamination and neither did the microscopic studies. However, for the tests with more brittle materials coated on to the polymer delamination was found.

The microscopic images did reveal the presence of a ridge along the edges of the residual scratch groove, and no signs of chipping or cracking were visible. Although the scratch tests were performed on a metallic surface, the phenomena of built up ridges has been reported also for polymers as Cheneler et al. [37] proposes three different wear mechanisms of polymers by scratching: grooving, plowing and chipping. Grooving creates a residual groove with a cross-section similar to the one of the indenter while plowing creates a groove with pile-up along the edges. Chipping is the mechanism where particles are released from the sample during the scratch sequence. These phenomena are shown in Figure 2.9.

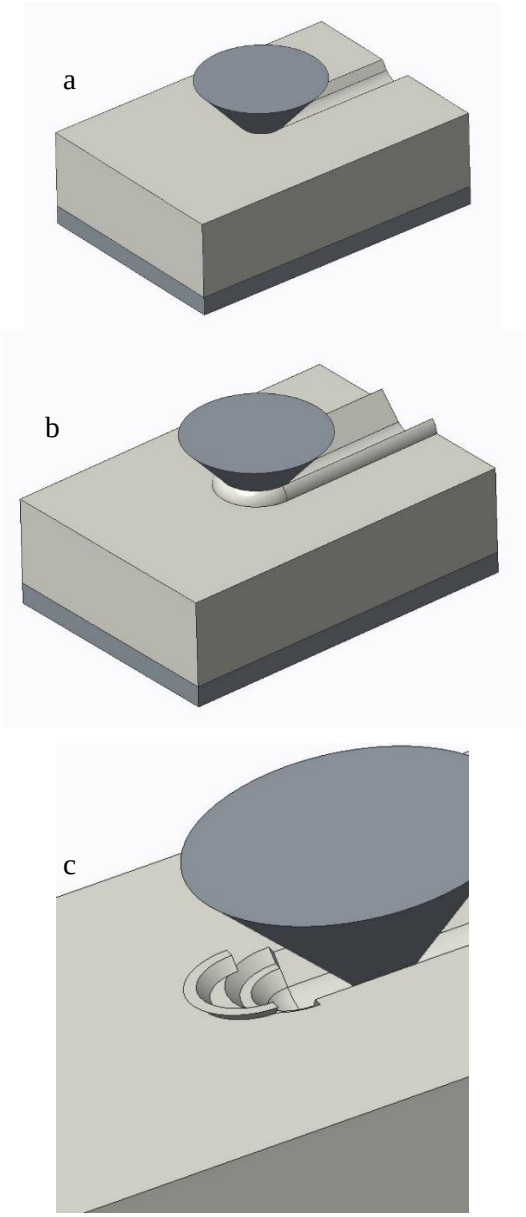

Figure 2.9 *Image showing three scratch mechanisms during scratching: a) grooving, b) ploughing and c) chipping.*

In another nanoscratch experiment Kassavetis et al. [56] studied the adhesion between a PET film coated with an AlO_x layer where the length of elastic deformation was noted as the part in the loading curve where the pre-scratch, post-scratch and scratch curves started to deviate from each other. At further increase of scratch length (and thereby load) the scratch curve evens out to a plateau before continuing its increase in scratch depth. Microscopic studies showed three stages:

first small cracks occur traveling outwards from the residual groove at an angle from the scratch direction. These were also seen in the previously mentioned report by Lieu et al. [55] and was then called “fishbone pattern”. Then as the load is increased the residual groove is further cracked and fragmented in bigger pieces. Finally bigger pieces are de-adhered from the PET film. The width of the residual scratch groove was measured and found to increase throughout the scratch sequence.

Summarizing these two nanoscratch articles, it is interesting to note that both induce delamination by scratching the inorganic film and measure the ability of the polymer film to hold the fragmented pieces. In the case of the material in this thesis scratching the inorganic layer is not possible, and as the article by Liu et al. [55] suggest, inducing a crack in the aluminum might be difficult anyway, rendering it an unattractive way of investigating adhesion.

However, there are some differences in that article to the premises in this thesis that need to be contemplated: firstly, the thickness of the aluminum layer is significantly lower in the experiment than the one to be tested (200 nm compared to some micrometers). It is possible that the very thin layer that has been sputtered on to the polymer film acts differently than the cold rolled aluminum foil used in packaging applications due to mechanical properties being different due to the different manufacturing techniques. Further, whereas the sputtered aluminum film consists purely of aluminum the foil used in packaging applications is usually alloyed with other materials possibly affecting the properties. Interestingly, experiments were performed using both a berkovich indenter probable to induce cracks and a conical indenter more probable to introduce shear stress in the polymer-aluminum interface, without any detectable delamination.

When investigating the adhesion regarding metallic and/or ceramic materials, cross-sectional indentation is sometimes used. The idea behind cross-sectional indentation is to indent into the interface between the two materials, either at the interface or a distance from the interface into the substrate. Unfortunately, this literature study has not found any studies using cross-sectional indentation regarding polymeric materials. However, de-adhesion in cross-sectional indentation often occurs as a crack starts in the substrate and propagates to the interface causing loss of adhesion. A similar approach exists for adhesion tests where a polymer film has been coated onto a brittle substrate (e.g. glass) where an indent is made normal to the polymer surface through the polymer thickness inducing a crack in the underlying substrate that causes deadhesion. The size of the delamination “blister” can then be measured and used as an adhesion measurement [57].

Analogous to the reasoning about the nanoscratch articles, it is doubtful if the aluminum foil is brittle enough to create a crack that can de-adhere the polymer film. Also, this is doubtful due to the fact that the aluminum foil is in turn bonded to soft layers such as a polymer and paperboard which might provide a bit too much flex. However, it is possible that a similar approach can be performed in cross-sectional tests where perhaps the indent can be aimed in the aluminum layer and possibly transferring the energy to the interface to create delamination.

2.6.7 Conclusions

Surface roughness have proved to be of importance when analyzing results since this creates a scatter in the obtained results. However, altering the surface roughness without affecting the mechanical properties is not deemed possible, so instead focus is on analyzing the results such that the effects of surface roughness is accounted for and does not lead to any misleading conclusions.

Some reports exist on methods using the brittle nature of the substrate (e.g. glass) to induce a loss of adhesion to the coated polymer. This is however not deemed a suitable approach due to the rather ductile and flexible behavior of the substrate in this case but rather the behavior of the soft substrate should be kept in mind during experiments and analysis of the results.

Scratch test of a brittle aluminum oxide coating on a PET substrate showed delamination with a proceeding cracking behavior of the aluminum oxide whereas the aluminum coated on a PET substrate showed no delamination and no cracking behavior. Although the absence of delamination of the aluminum film might seem discouraging, scratch is still considered a viable option due to some differences in experimental procedure such as film thicknesses, production procedure and the fact that the report focuses on scratching the aluminum surface whereas the procedure in the package laminate case would have to be on the polymer surface.

No reports on cross-sectional indentation regarding polymers have been found, but it is considered a viable option regarding the adhesion test in this thesis due to the relatively thick polymer layer. Where other studies often deal with simpler material structures such as a thin brittle metal coating on a thicker polymer substrate or vice versa, the complex multi-layer appearance of the material in this thesis makes the use of methods based on a normal-indentation more difficult, and the cross-sectional approach is therefore pursued.

3 Method

The experimental stage in this thesis can be divided into two main steps: a first step performed on a paperboard laminate and a second step with a laminate free from paperboard. The first step with the paperboard laminate can be seen as an introductory study where some general approaches and parameters were tested. Three general methods were pursued:

- Normal indentation.
- Cross-sectional indentation.
- Scratch test.

The normal indentation meant producing indents normal to the polymer surface. Five indents were made for each combination of max load, loading rate and holding time. Results were analyzed for optimal parameter values and hardness of the polymer. Cross-sectional indentation meant aligning the sample so that indents were made parallel to the polymer surface. Indents were thereafter made in the interface between the polymer and aluminum layer. A big part was finding a way to consistently aim the indents into the interface. Loading curves of the indents were studied qualitatively for any irregularities indicating delamination or any other possible adhesion-related property. Also, results were analyzed in terms of hardness as this could possibly be a measure of adhesion. Also, images of the residual indents were captured. Scratch tests were performed by aligning the sample in the same way as for the normal indentation experiments. Thereafter the surface were scratched with a linearly increased load with a preset loading rate until a preset max load was reached.

Due to some problems encountered during the initial experiments the test material was changed to a material without paperboard. The problems that caused the change to a paperboard free material was mainly the concern that during scratch tests the paperboard provides flex when the indenter comes close to the polymer-aluminum interface, thereby prohibiting the indenter to reach the interface or induce enough shear stress for it to delaminate. The other issue was that it was observed that during sample preparation of the cross-sectional samples the paperboard soaked the water used as a lubricant in the wet grinding which led to delamination of the polymer and aluminum layers.

As in the preliminary study cross-sectional indentation and scratch tests were conducted in order to investigate the adhesion. No normal indentation was performed since focus was put on scratch test and cross-sectional indentation as they were deemed more probable to show adhesion properties.

For the cross-sectional experiments, after some initial experiments to investigate the general behavior using ordinary single indents, multi-point indentation was pursued. This is a technique in which, during the same indentation sequence, the load is applied to the first max load thereafter unloaded to a preset percentage of the max load. Thereafter the load is applied to a load higher than the previous max load and thereafter repeating the procedure until reaching the last load at which point the load

is completely unloaded. This creates fairly identical geometrical premises for different maximum loads where hopefully a threshold load/depth can be obtained where delamination or other interesting behavior occurs.

For the scratch test, the first step was to perform single scratch tests to get a sense of the material behavior and optimal parameters. Thereafter multipass wear tests were conducted. This is a technique in which the surface is scratched repeatedly in the same track with the goal of increasing the depth of the residual groove every repeat eventually creating delamination or reaching the aluminum surface.

4 Experimental

4.1 Introductory tests

4.1.1 Material

The material used in the introductory test was comprised of two different paper board laminates, throughout this report referred to as 5781 and 6031. The principal appearance of the materials are Polymer-Aluminum-Polymer-Paperboard-Polymer, where the adhesion between the two first layers were to be investigated. Both materials have an expected thickness of the aluminum layer of 6 µm and the 5781 material has an expected polymer thickness of 19 µm added with a tie layer closest to the aluminum of 6 µm resulting in a total thickness of 25 µm. The 6031 material has an experienced polymer thickness of 12 µm added with a 6 µm tie layer resulting in a total thickness of 18 µm. the thicknesses are summarized in Table 4.1. The thickness of the polymer layer is in good accordance with results acquired via microscopic studies depicted in Figure 4.1

Table 4.1 *Summary of the polymer and aluminum thicknesses of the two different samples used in the introductory tests.*

Material:	**Thickness of Al-layer:**	**Thickness of polymer layer:**
5781	6 µm	6 µm (adhesive layer) + 19 µm
6031	6 µm	6 µm (adhesive layer) + 12 µm

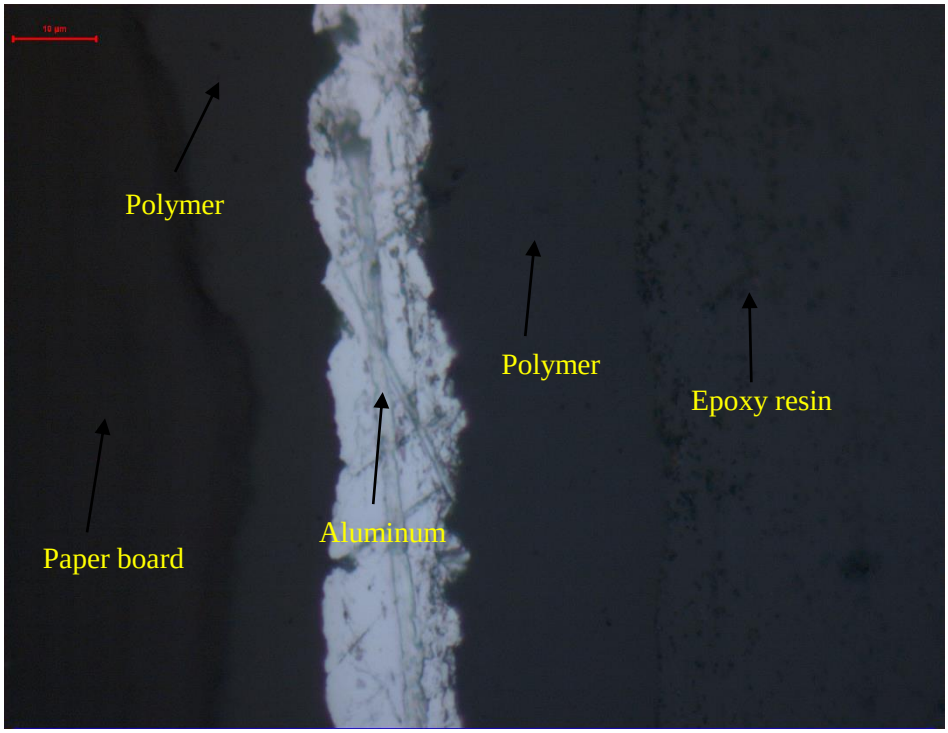

Figure 4.1 *Image of the cross-section of material 5781 with the paper board to the left and epoxy resin to the right. The polymer-aluminum interface on the right side of the aluminum layer is the one to be investigated. The scale in the left upper corner is 10 μm.*

4.1.2 Normal indentation

A strip of material was cut out from the provided material sheet using scissors and placed on the sample holder so that the surface of the polymer was normal to the indenter axis. Indentations were then set up with three different values of *max load*, *loading time* and *holding time*, respectively. The loading time was set equal to the unloading time. A row of five indents with a spacing of 50 µm between each indent was made for each combination of parameters. The spacing between each row was 50 µm. A list of values for the different parameters can be seen in Table 4.2

Table 4.2 *Table of parameters used in normal indentations in introductory tests.*

Parameter	Values	Unit
Max load	0.5, 0.7, 0.9	mN
Loading time	30, 60 , 90	s
Holding time	60, 120, 180	s

Along with the loading-unloading curves the hardness from each indent was acquired through the software provided with the nanoindentation device. The

hardness values were analyzed with regard to max load, loading time and holding time in order to determine the effect of those parameters on the results.

4.1.3 Cross-sectional indentation

Strips of material were cut out using scissors and molded into an epoxy sample so that the strip was parallel to the indenter axis. The samples were then polished first using rotating sandpaper discs (last step 4000 grit) with water as lubricant followed by diamond paste (3 µm particle size) with a water and oil based lubricant finished by etching with active oxide suspension. As there was observed a tendency for the polymer layer to delaminate from the aluminum and the epoxy, a hypothesis were established that the water used as lubricant was responsible. Therefore the number of steps used was kept to a minimum and the amount of water used during the polishing was also minimized. This produced samples without visible delamination between the polymer and aluminum layers but there was still a gap between the polymer and epoxy that was not overcome and were therefore used in the indentation experiments.

Indents were made with varying parameters and a method for aiming the indent squarely at the polymer-aluminum interface was developed. Max loads of 2 mN, 3mN and 5 mN were used and holding times of 60 s and 90 s was used. The loading time was kept at 60 s for all indentations.

Images of the aim of the indent as well as an image of the residual indent was acquired. Further, the loading-unloading curves together with the behavior during holding time was analyzed for behavior that could indicate delamination. Also hardness was acquired for the indents.

4.1.4 Scratch test

A strip of material 5781 was cut out from the material sheet using scissors and placed on the sample holder so that the surface of the strip was normal to the indenter axis. Five scratches with a length of 1500 µm and different max loads were made. The max loads were 10, 20, 30, 40 and 50 mN. Each scratch sequence included three steps: pre-scratch, scratch and post-scratch as described in the background section.

The results were plotted as indentation depth versus scratch distance for the pre-scan, scratch and post-scan and also a plot was made where the scratch depth subtracted with the pre-scratch was plotted. The graph were then investigated for signs of delamination or signs of the indenter reaching the aluminum layer.

4.2 Tests on samples without paperboard

4.2.1 Material

The material used in the experiments is a three layer structure with the basic structure: polymer-aluminum-polymer. The polymer on "the inside" (the layer of interest in adhesion investigations) consists of a 6 µm adhesive layer (closest to the aluminum) followed by a 9 µm LDPE layer and a 10 µm LDPE layer. This results in a total polymer thickness of 25 µm. The other side has a 20 µm LDPE layer without any adhesive layers.

The acid applied to the samples were a solution of 12 volume percent acetic acid in water (bought in grocery store, called distilled/white vinegar, in Swedish "ättika")

4.2.2 Cross-sectional indentation

The samples for cross-sectional indentation were produced by molding a cylindrical piece of epoxy resin which was thereafter cut in half and a strip of material was then glued onto the newly cut surface. The component was then inserted back into the mold and the empty half was filled with epoxy resin. Thereafter the sample was wet grinded in steps with the final step being a 4000 grit paper followed by etching with active oxide suspension. Two samples were submerged in acid one day.

First indentation was performed with single indents as for the introductory experiments. At this stage some general indentation behavior of the material and parameter values were tried out. Thereafter experiments were done with the multi-point indentation technique. The two loading schedules for the multi-point indentation were 0.1, 0.30, 0.75 and 1 mN and 0.5, 1, 1.5 and 2 mN, summarized in Table 4.3.

Table 4.3 *Summary of the two loading schedules for the multi-point indentation during cross-sectional indentation.*

	Load cycle 1	**Load cycle 2**	**Load cycle 3**	**Load cycle 4**	**Load cycle 5**	**unit**
Loading schedule 1	0.1	0.3	0.5	0.75	1	mN
Loading schedule 2	0.5	1	1.5	2	-	mN

4.2.3 Scratch test

Strips of material were cut out using scissors and glued onto the sample holder. A suitable area to perform scratches where the surface was flat without visible surface irregularities were marked with a marker pen. Some parameters were tested in an initial stage and from there it was concluded that a maximum load of 50 mN ramped

with a loading rate of 0.75 mN/second during a scratch length of 1500 µm were the main parameters to be used in most scratch experiments including the wear tests.

Table 4.4 *Summary of the main parameters used in the scratch experiments on samples without paperboard.*

Max load	Loading rate	Scratch length
50 mN	0.75 mN/s	1500 µm

Acid were applied to the sample in a variety of ways. Firstly, it was attempted to apply acid as the sample was mounted on the sample holder, by enclosing a part of the material using adhesive putty. This was unsuccessful since the acid was not contained but instead floated under the created walls. Secondly, a strip of material was put over a plastic jar and gently pushed down creating a "cradle" in which the acid was poured. This method was also unsuccessful due to evaporation of the acid. Attempts were made to overcome this problem by covering it with plastic foil but those attempts were unsuccessful. Lastly, strips of material was submerged in acid for one and two days.

It should be clearly noted that even after one day of submersion the samples had almost completely lost adhesion between the polymer and aluminum on "the outside" (the side that is not of interest in measuring adhesion) and was therefore stripped away by hand before mounting on the sample holder. Although this eliminates the possibility of a flexing polymer layer between the aluminum layer and sample holder possibly creating a better chance of delaminating the polymer, the same procedure cannot be performed for the non-treated sample so caution must be made when comparing the results from acid treated and non-acid treated materials.

5 Results

5.1 Introductory tests

5.1.1 Normal indentation

Indentations normal to the surface were made in order to investigate the behavior of the polymer film and to see if any conclusions could be drawn about the behavior of the polymer in respect to max load, loading rate and holding time and try to find any indications on the optimal parameters. Loading time and unloading time (the time to indent to max load and retract the indenter from max load to zero load, respectively) were set equal and three different loading times (denoted lr in the graphs) were investigated: 30, 60 and 90 seconds. Three different holding times (the time at which the maximum load is kept constant as it is reached, denoted ht in the graphs) were investigated: 60, 120 and 180 seconds. For each combination of loading rate and holding time three max loads were investigated: 0.5, 0.7 and 0.9 mN. For each combination of loading time, holding time and max load five indents were made. A typical load-unload response is shown Figure 5.1. In order to make the result clear the hardness data have been listed in regard to max load, loading rate and holding time.

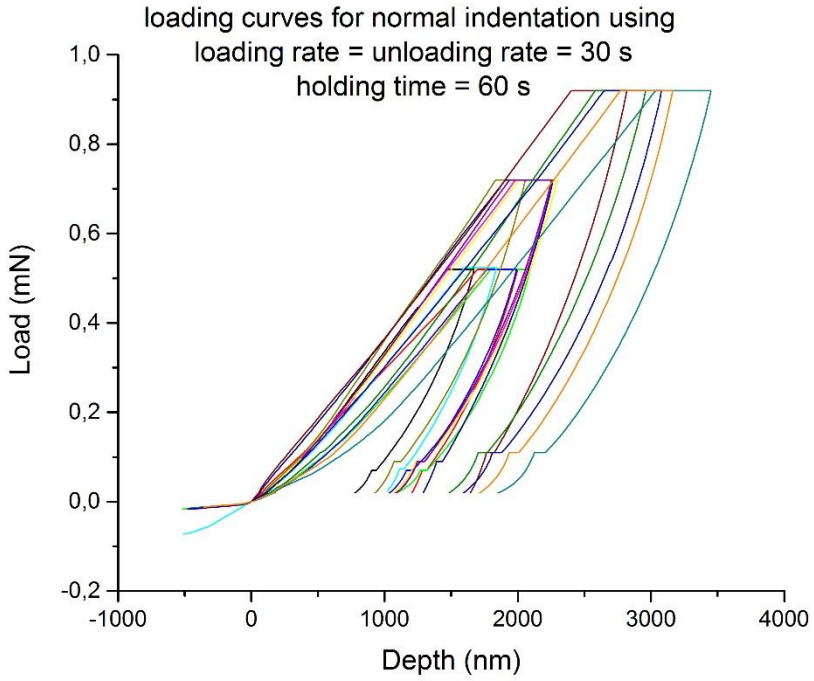

Figure 5.1 *Typical load-unload curve for the normal indentation experiment. Loading time 30 seconds and holding time 60 seconds.*

5.1.1.1 Material 5781

In Figure 5.2 hardness response grouped by the specific combination of loading rate and holding time is shown. Each column includes the experiments performed with 0.5, 0.7 and 0.9 mN max load. The experiments with a holding time of 60 seconds seem to have a slightly higher hardness value than those with other holding times. Also, the variation seem to be highest for the experiment with a loading time of 30 seconds and a holding time of 60 seconds. The least variation seem to be shown by the experiment with a loading time of 90 seconds and a holding time of 180 seconds.

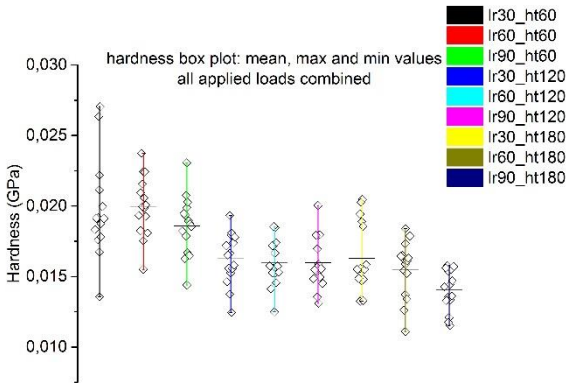

Figure 5.2 *Hardness plots for the different loading time and holding time combinations of material 5781, five indents each for the loads 0.5, 0.7 and 0.9 mN is included in each set of parameter combination.*

In Figure 5.3 only the experiments with a max load of 0.5 mN are shown. Both the highest and lowest value for the lr30 ht60 experiment in the previous graph seem to stem from this experiment. Also, the overall trend is equal here also with the mean hardness for the experiments with a holding time of 60 seconds being higher.

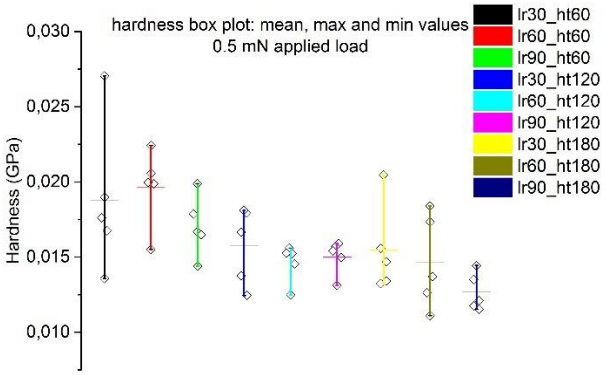

Figure 5.3 *Hardness plots for the different loading time and holding time combinations of material 5781, five indents with the load 0.5 mN is included in each set of parameter combination.*

For the experiments with a max load of 0.7 mN shown in Figure 5.4 the variation for the experiment with the of a loading rate of 30 seconds and a holding time of 60 seconds (the leftmost curve) shows a smaller variation than the previous graph. The mean hardness is still higher for the ones with a holding time of 60 seconds.

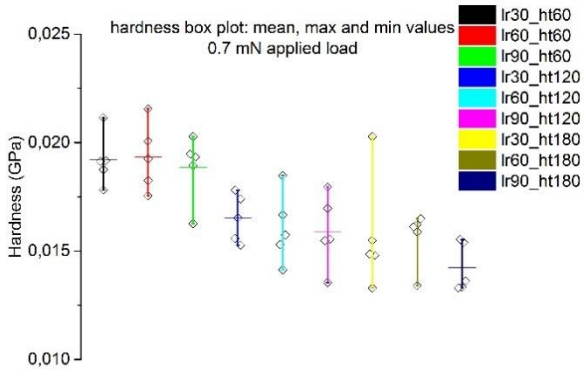

Figure 5.4 *Hardness plots for the different loading time and holding time combinations of material 5781, five indents with the load 0.7 mN is included in each set of parameter combination.*

For the one with a maximum load of 0.9 mN the trend is similar to the previously described graphs with the mean hardness values for the holding time of 60 seconds once again being higher than the rest.

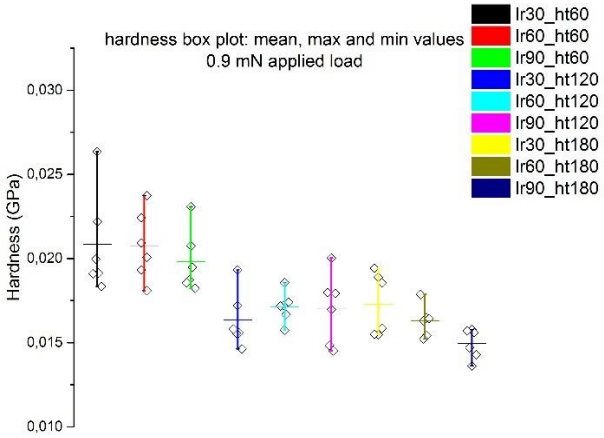

Figure 5.5 *Hardness plots for the different loading time and holding time combinations of material 5781, five indents with the load 0.9 mN is included in each set of parameter combination.*

In order to get an understanding of the influence of loading time and holding time on the hardness response hardness was plotted in regard to loading time (Figure 5.6) and holding time (Figure 5.7). Looking at the effects of loading time there does seem to be a small decrease in hardness with increasing loading time. The variation seem to be similar between the different loading times.

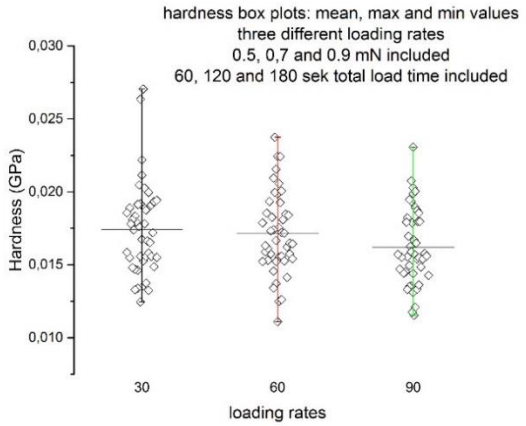

Figure 5.6 *Hardness plots for the loading times of 30, 60 and 90 seconds for material 5781. For each loading time five indents for each unique combination of load (0.5, 0.7, 0.9 mN) and holding time (60, 120, 180 seconds) are included.*

Looking at the effects of holding times there seems to be a trend of decreasing hardness with increasing holding time and this effect seem to be bigger than for the loading time. Also, the variation seem to be slightly smaller for the holding time of 120 seconds and it also lacks the pronounced occurrence of outlier values which the holding time of 60 seconds possesses.

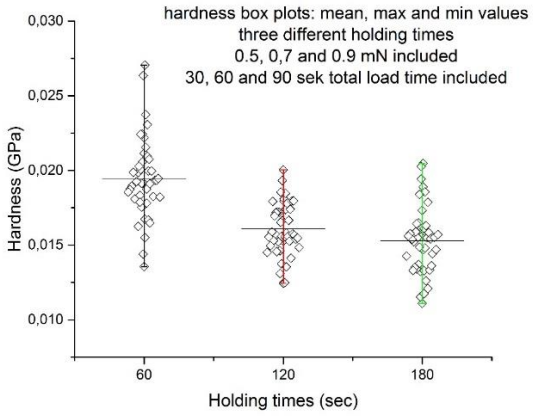

Figure 5.7 *Hardness plots for the holding times of 60, 120 and 180 seconds for material 5781. For each holding time five indents for each unique combination of load (0.5, 0.7 and 0.9 mN) and loading time (30, 60 and 90 seconds) are included.*

5.1.1.2 Material 6031

The hardness response for the material with material number 6031 appears to be a bit different than for the experiments on material number 5781. Looking at the experiments where each combination of loading time and holding time has been separated and all loads are included, the trend seen for material 5781 are not seen.

The hardness for the experiments with a holding time of 60 seconds does seem to be slightly higher than the others although not as significantly as in Figure 5.2 - Figure 5.5. Also, no obvious larger variation can be observed for any of the experimental parameters. Interestingly, the mean hardness is slightly lower than for material number 5781.

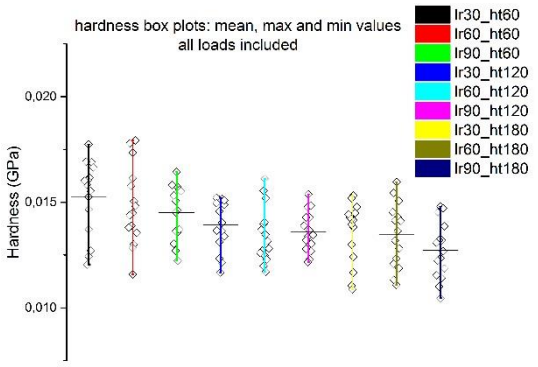

Figure 5.8 *Hardness plots for the different loading time and holding time combinations of material 6031, five indents each for the loads 0.5, 0.7 and 0.9 mN is included in each set of parameter combination.*

For the experiments with a max load of 0.5 mN the hardness is fairly uniform for the different parameters although with a slightly higher hardness for the ones with a holding time of 60 seconds. Also, the mean hardness is lower than 14 Mpa which is a hardness lower than in any of the graphs for material number 5781.

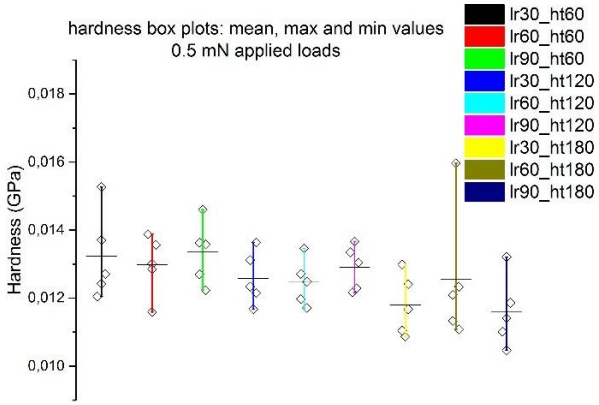

Figure 5.9 *Hardness plots for the different loading time and holding time combinations of material 6031, five indents with the load 0.5 mN is included in each set of parameter combination.*

The hardness for experiments with a max load of 0.7 mN show a higher hardness for a holding time of 60 seconds. However, unlike the experiments for material 5781

the experiments with a holding time of 60 seconds does not show uniform mean hardness, but rather decreases quite rapidly with increasing loading time.

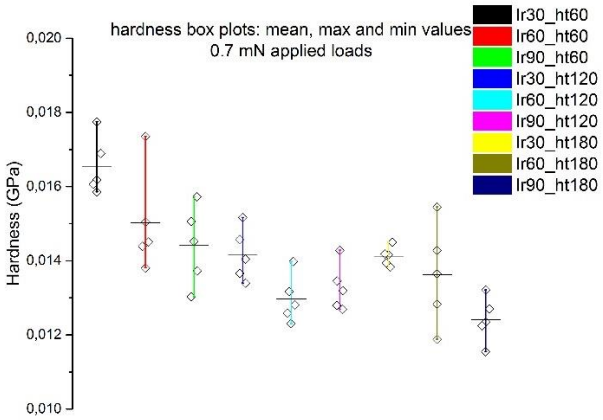

Figure 5.10 *Hardness plots for the different loading time and holding time combinations of material 6031, five indents with the load 0.7 mN is included in each set of parameter combination.*

For 0.9 mN max load the experiments corresponding to a holding time of 60 seconds once again show a hardness higher than the other parameters although without the high similarity between each other as seen for material number 5781.

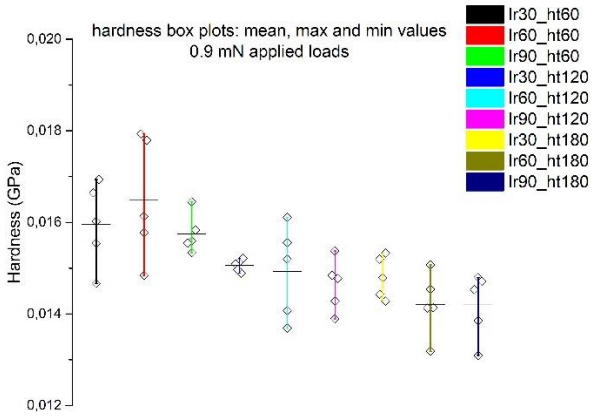

Figure 5.11 *Hardness plots for the different loading time and holding time combinations of material 6031, five indents with the load 0.9 mN is included in each set of parameter combination.*

Looking at the influence of loading time in Figure 5.12 there seem to be a slight decrease in hardness with increasing loading time as for material number 5781. The

variation seem to be slightly smaller for the loading time of 90 seconds although not by much.

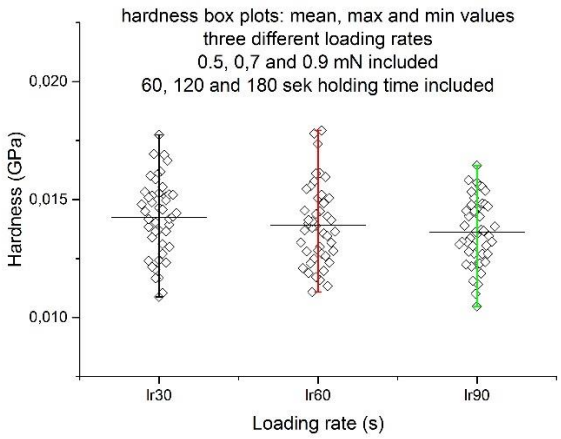

Figure 5.12 *Hardness plots for the loading times of 30, 60 and 90 seconds for the material 6031. For each loading time five indents for each unique combination of load (0.5, 0.7, 0.9 mN) and holding time (60, 120, 180 seconds) are included.*

Looking at holding time, similarly as for material number 5781 the mean hardness decreases with increasing holding time more significant than for loading time. Also, as for material 5781 the variation is smaller for the holding time of 120 seconds.

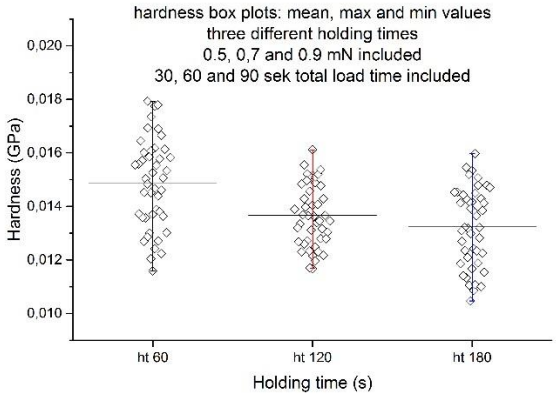

Figure 5.13 *Hardness plots for the holding times of 60, 120 and 180 seconds for material 6031. For each holding time five indents for each unique combination of load (0.5, 0.7 and 0.9 mN) and loading time (30, 60 and 90 seconds) are included.*

For both materials, holding time shows a greater effect on the hardness value than loading time. Also, for both materials, a holding time of 120 seconds yield smaller variation. Therefore, a holding time of 120 seconds seems like a good starting point when choosing experimental parameters. For loading time there it does not seem possible to draw any conclusions about optimal values in future experiments. Worth

noting, hardness decreases with increased holding time and holding time. This is in accordance with literature as Fang & Chang [43] found that hardness and elastic modulus for a polycarbonate film increased with increasing holding time and decreasing loading rate.

5.1.2 Cross-sectional indentation

The results from the cross-sectional indentation are depicted in Figure 5.14 - Figure 5.19. Since the optimal approach was not known from the beginning but rather something to be investigated through the course of the experiments a few indentations have methodological shortcomings manifesting itself in unreliable aim of the indent, where some indents are offset from the interface either into the polymer or aluminum layer. Results from the indentations where these problems have been accounted for are shown in Figure 5.14 - Figure 5.16 and results without this adjustments are shown in Figure 5.17 - Figure 5.19

For the well-aimed ones, four indents were made with the max load of 3 mN and one with 5 mN. The 5 mN indent was noticeably steeper than those for the 3 mN ones. This is probably due to the indent being slightly offset into the aluminum layer thereby experiencing a harder material response than the others. Two of the indents show great correlation through the whole sequence and one indent shows good correlation with these two up to a load of 2 mN followed by a deviation to a more gradual slope. The fourth shows a behavior of the curve quite similar to the others but slightly offset since the curve starts to increase earlier than the others, possibly due to the aluminum layer protruding slightly above the aluminum layer.

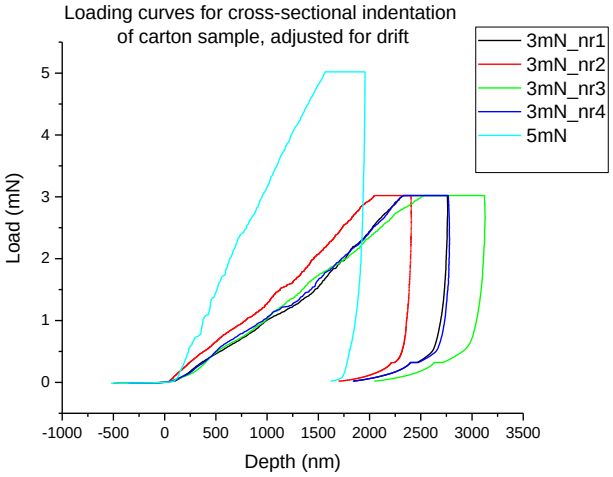

Figure 5.14 *Load-unload curves for five indents into the polymer-aluminum interface of material 5781.*

The related indentation data during holding time shows good correlation between the two curves that were almost identical in the load curves although the rest of the curves do not show the same correlation. The perhaps most interesting results are the ones for the 5 mN indent and the indent that started its deviation before others,

which show spikes in depth curves although a bit differently. While the 5 mN indent show close to vertical leaps in depth the 3 mN one shows a slightly more gradual increase. It is important to note firstly that this might be due to disturbances and errors rather than material behavior, for examples some vibration close to the instrument may cause these disturbances. Reviewing possible material response explanations, it can of course be a sign of delamination but also a sideways flexing of the aluminum layer. It could also be due to localized lack of adhesion close to the indenter tip, for example air bubbles between the polymer and aluminum. However, there is not enough conclusive data to draw any conclusions of whether these irregularities show any significant material behavior or not.

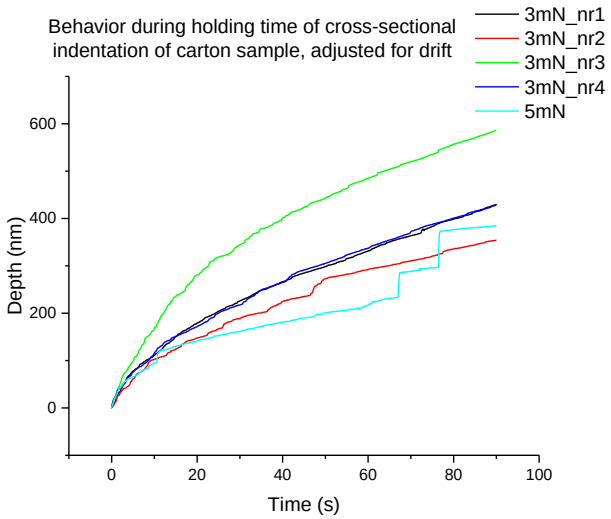

Figure 5.15 *Depth versus time curves during holding time for five indents into the polymer-aluminum interface of material 5781.*

The results were analyzed in terms of hardness and the results are shown below

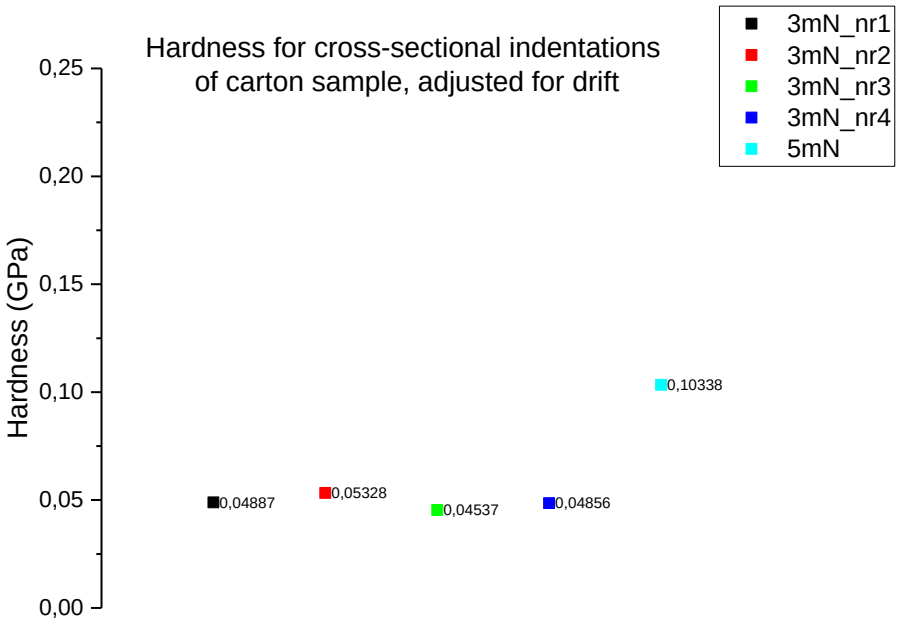

Figure 5.16 *Hardness values for five indents into the polymer-aluminum interface for material 5781.*

It can be seen that as expected the hardness of indent number 1 and 4 is very close to each other with only 0.3 MPa difference. The hardness lies in the range of 45-53 MPa if the 5mN indent is excluded. Comparing it to the hardness for the polymer measured by normal indentation in chapter 5.1.1 it has a considerably higher hardness indicating that the aluminum influences the hardness measurements in cross-sectional indentation.

The load response of the unreliably aimed indents vary significantly more than the accurate ones, with little correlation between any curves which is not surprising given the uncertainties in aim.

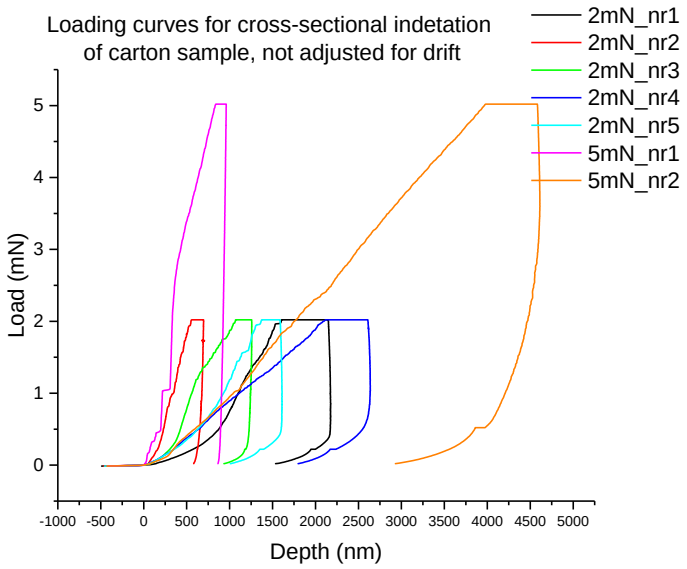

Figure 5.17 *Load-unload curves for five indents into the polymer-aluminum interface of material 5781 with a less accurate aim than those presented in Figure 5.14-Figure 5.16.*

The perhaps most interesting results can be found in the dwell curves where one of the curves makes a significant almost vertical step of approx. 200 nm after about 10 seconds. This could potentially be a sign of delamination although the possibility of errors previously described must be taken into account. Also, one of the curves that show almost no increase in depth starts to show some type of oscillating behavior. This is not expected to be a measure of material behavior but probably caused by some sort of error such as instability in the indentation instrument or outside vibrations influencing the indentation device.

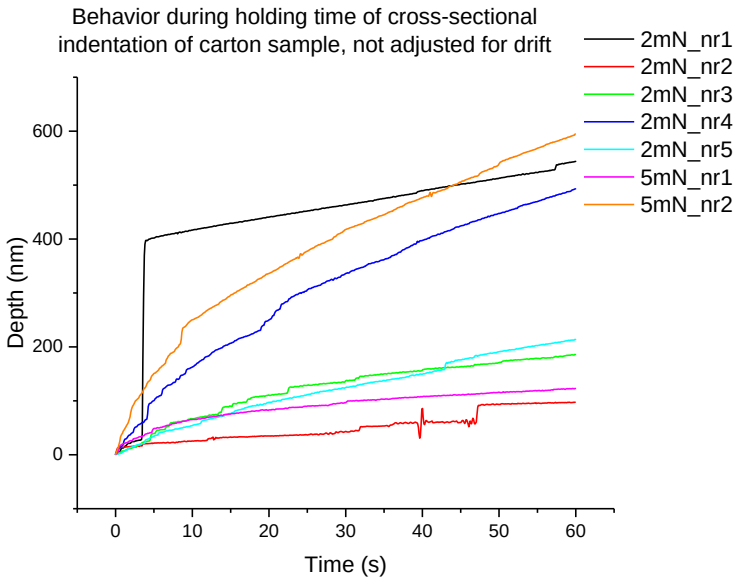

Figure 5.18 *Depth versus time curves during holding time for five indents into the polymer-aluminum interface of material 5781 with a less accurate aim than those presented in Figure 5.14-Figure 5.16.*

When looking at the hardness readings excluding values above 100 MPa as was done for the well-aimed indents the hardness varies between 44 - 65 MPa. The hardness for indent number 1 could not be analyzed, probably due to significant viscoelastic behavior of the polymer, creating a negative slope of the unloading curve.

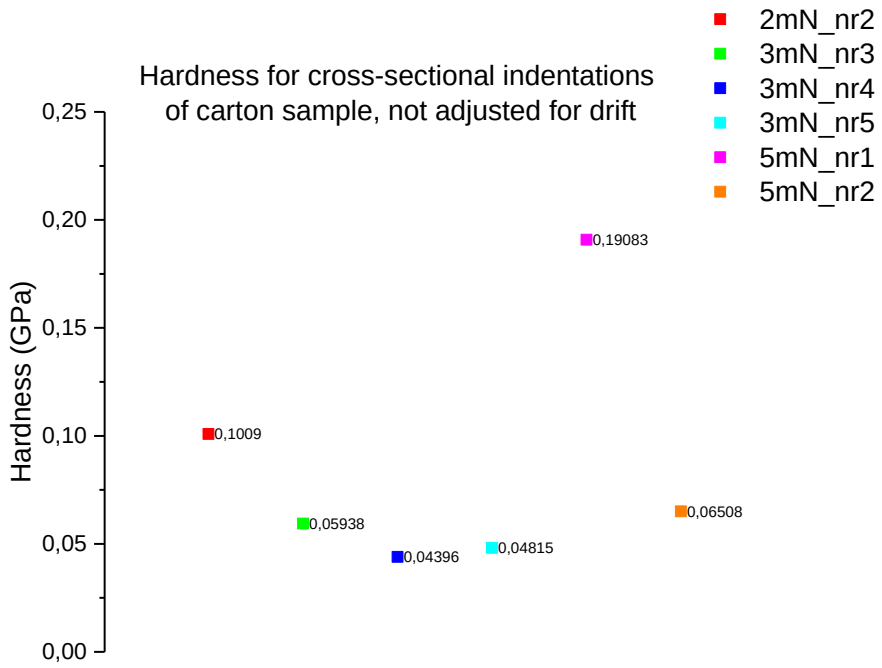

Figure 5.19 *Hardness values for five indents into the polymer-aluminum interface for material 5781 with a less accurate aim than those presented in Figure 5.14-Figure 5.16.*

After the completion of each indentation sequence for the well-aimed indents, an image of the residual indent was acquired in the indentation device's built in light microscope which is depicted in Figure 5.20.

As can be seen in the images, finding a straight section between the polymer and aluminum layer is challenging, and the appearance of the polymer-aluminum interface is different from indent to indent inducing a source of error since the response might be dependent on this geometry as well as the material and adhesion properties. However, it can be seen that the indents has created a half circle in the aluminum layer so the aim seems to be somewhat satisfying.

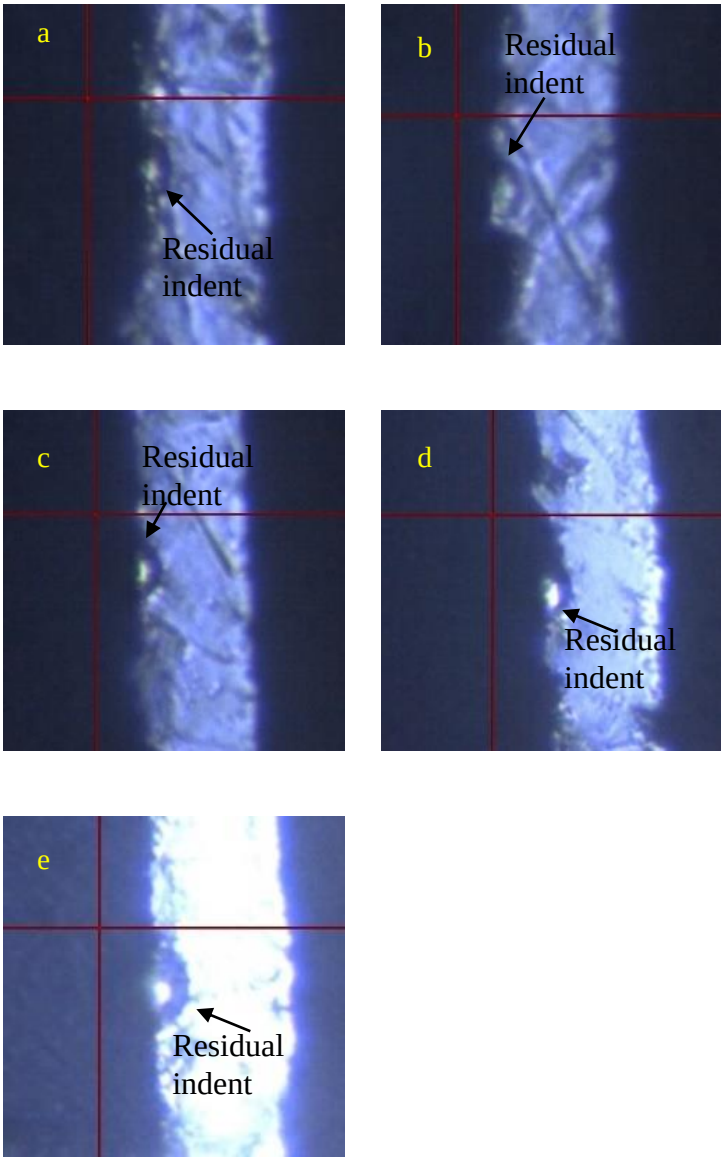

Figure 5.20 *Residual indents for cross-sectional indentations of the carton sample for the indentations: a) 3mN nr1, b) 3mN nr2 c) 3mN nr3 d) 3mN nr4 e) 5mN.*

5.1.3 Scratch test

In Figure 5.21 - Figure 5.25 the indenter displacement for the pre-scratch topography, scratch sequence and post-scratch topography are presented for the different max loads.

In Figure 5.21 the displacement during scratch with a max load of 10 mN is shown. The plastic deformation, which can be seen as the difference between pre-scratch and post-scratch, is small. The displacement during scratch is several orders larger than the plastic deformation, indicating a large elastic part of the deformation.

Further, the profile of the scratch curve and post-scratch follows the profile of the pre-scratch quite well which could indicate that no delamination has occurred.

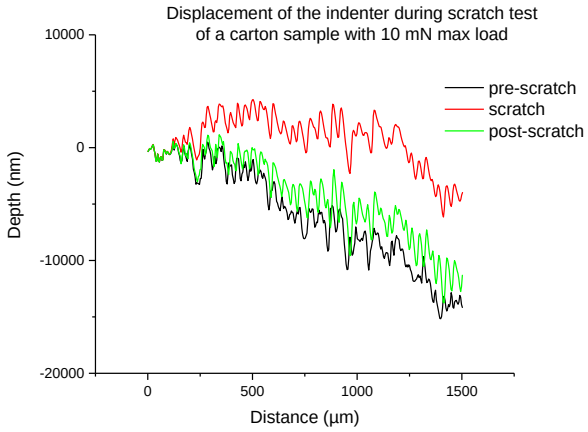

Figure 5.21 *Indenter displacement for the pre-scratch, scratch and post-scrath profiles with 10 mN max load.*

The scratch response for the max load of 20 mN shown in Figure 5.22 shows a bit flatter initial surface profile resulting in the topography closer to horizontal than the

one for 10 mN max load. The post-scratch follows the pre-scratch curve in a similar manner as for the 10 mN one continuing the assumption that no delamination occurs.

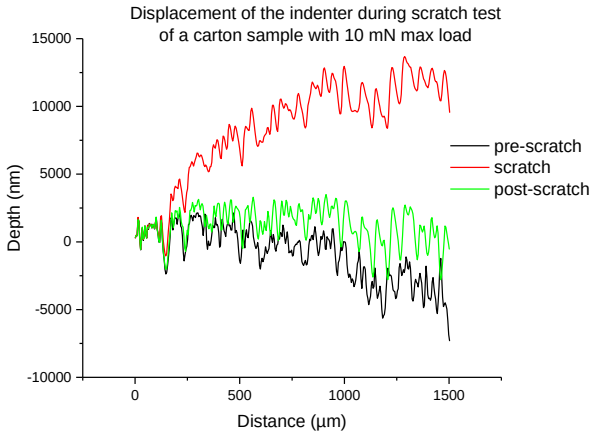

Figure 5.22 *Indenter displacement for the pre-scratch, scratch and post-scrath profiles with 20 mN max load.*

For a max load of 30 mN no new behavior can be seen.

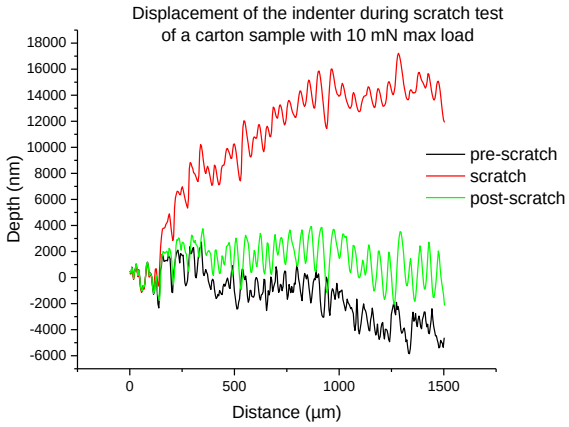

Figure 5.23 *Indenter displacement for the pre-scratch, scratch and post-scrath profiles with 30 mN max load.*

For a max load of 40 mN the plastic deformation starts to increase quite significantly compared to the previous experiments. Also worth noting is that the maximum indentation depth is close to the instruments maximum depth of 20 µm. Although the pre-scratch and post-scratch curves are not as easily compared there is no clear

indications that they deviate from each other in a way that makes delamination plausible.

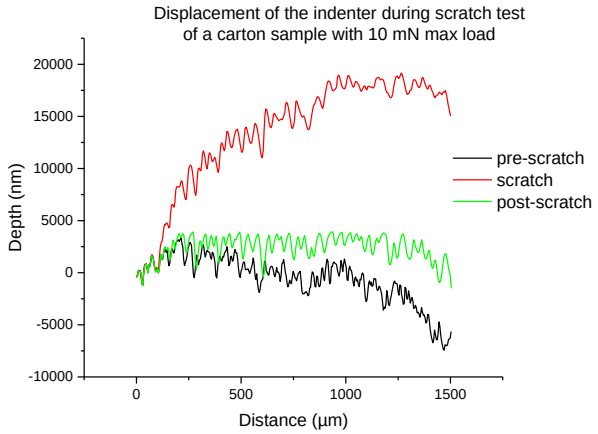

Figure 5.24 *Indenter displacement for the pre-scratch, scratch and post-scrath profiles with 40 mN max load.*

For the 50 mN max load the appearance is slightly different. The scratch curve flattens out after about 1000 µm after which it decreases slightly in the end of the sequence. The depth appears to be below the instruments maximum indentation depth so that is probably not the reason. A possible explanation could be that the increasing load and the uphill appearance of the surface profile balance each other out, thus leading to a horizontal behavior of the scratch curve.

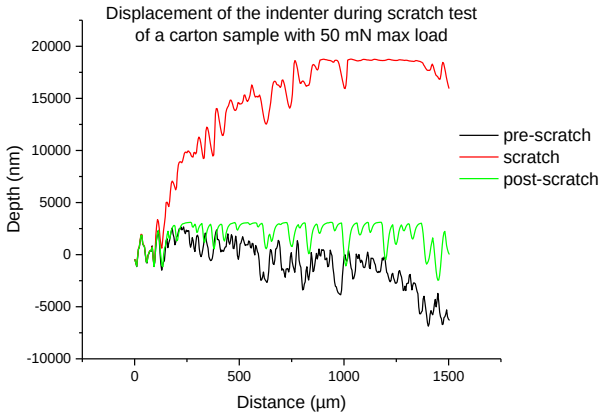

Figure 5.25 *Indenter displacement for the pre-scratch, scratch and post-scrath profiles with 50 mN max load.*

In order to account for the structure of the surface, and instead get a measure of the indenter's depth into the polymer, the displacement of the pre-scratch curve was subtracted from the displacement of the scratch and the results are shown in Figure

5.26. As can be seen all curves show a fairly smooth appearance until a depth of approx. 250 µm after which the curves start showing a more pronounced oscillating behavior. After reviewing Figure 5.21 - Figure 5.25 the distance where the smooth curve transcends into the more oscillating behavior correlates fairly well with the start of the plastic deformation. Interestingly, the correlation between initiation of plastic deformation with applied load are poor but rather the scratch distance seem show a better correlation. This indicate that the strain might have a bigger effect on the plastic initiation than applied load.

The 10 mN max load evens out at 1000 µm due to reaching the maximum load. The 20 and 30 mN mx load show a trend of a fairly straight line with no obvious deviations or irregularities, although the oscillations throughout the scratch sequence are quite significant and might mask such behavior. The 40 and 50 mN curves show a good correlation throughout the experiment. Also worth noting is that the depth of 25 µm at the end of the experiment is just around the expected thickness of the polymer layer. However, no signs of the indenter reaching the aluminum seems to be visible in the scratch curves.

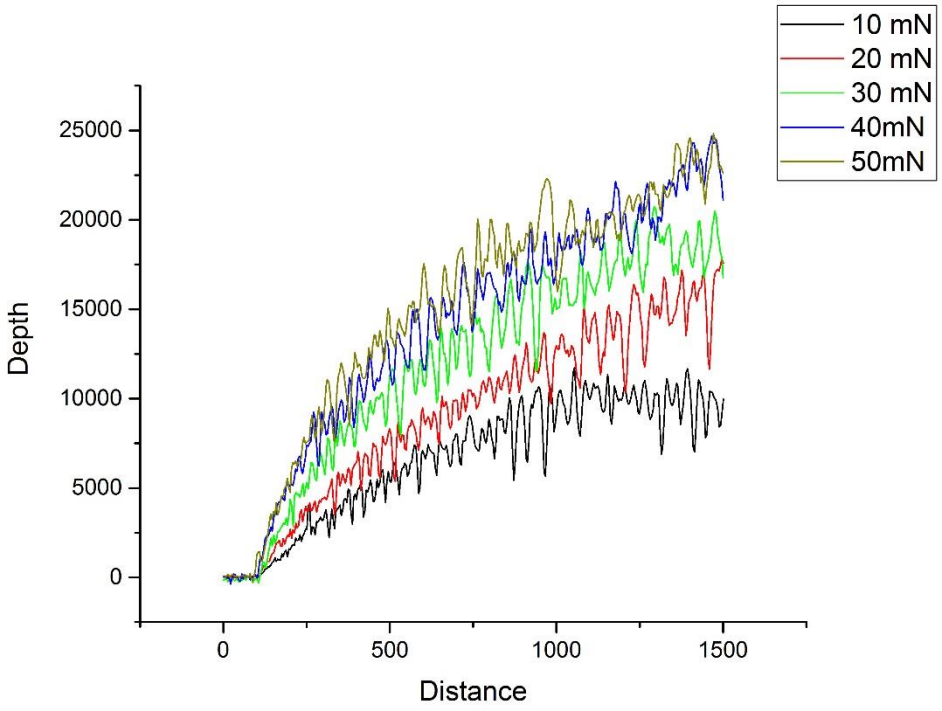

Figure 5.26 *Indentation depth versus scratch distance for the scratch test performed on material 5781. The scratch depth has been calculated as depth during scratch subtracted by the surface topography registered during pre-scratch.*

In Figure 5.27 post-scratch curves have been subtracted by pre-scratch topography. Noteworthy is that the curves representing scratch experiments for 40

and 50 mN max load shows slightly less oscillating behavior. However, no obvious irregularities that could indicate delamination can be seen.

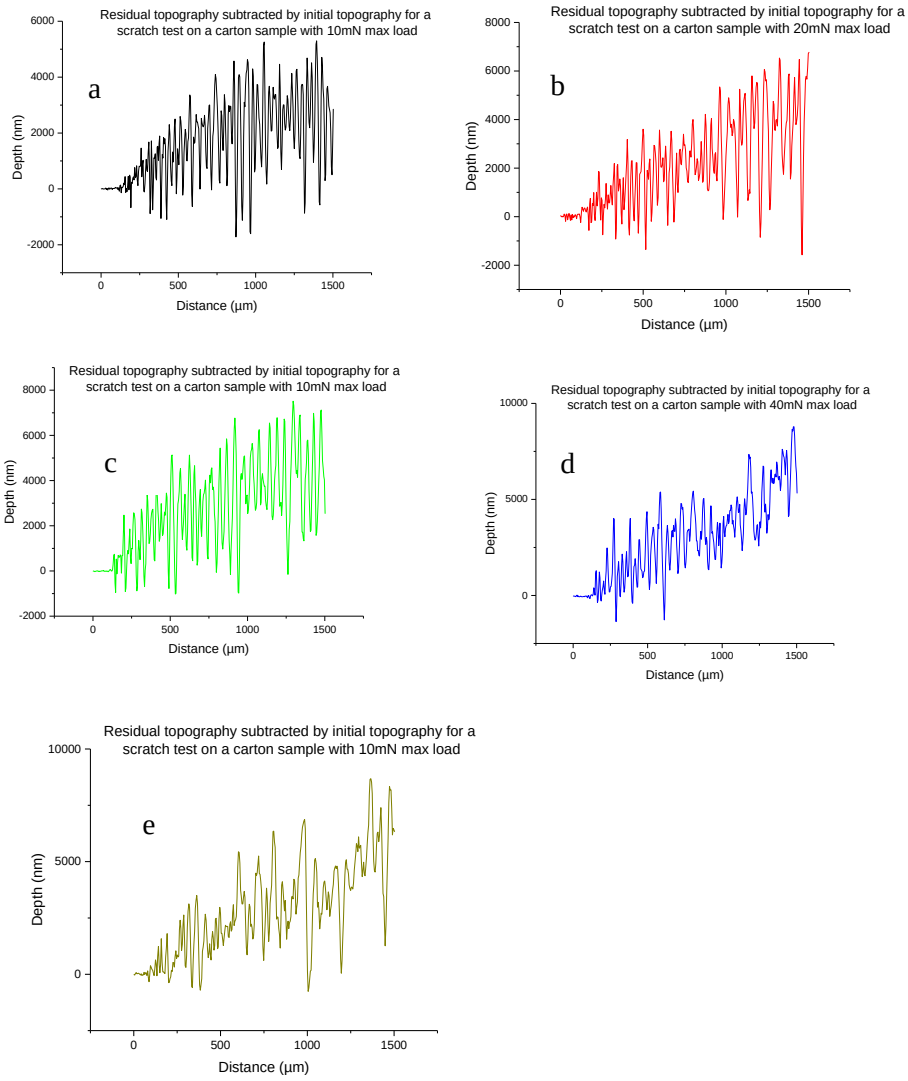

Figure 5.27 *Post scratch curves subtracted by initial topography on a carton sample for a) 10mN max load b) 20mN max load c) 30mN max load.*

5.1.3.1 Residual scratch grooves

Images of the residual scratch grooves were acquired both in the nanoindentation instrument's built-in microscope as well as an external light microscope (Nikon epiphot). Images acquired in the instruments built in microscope are depicted in Figure 5.28 - Figure 5.30 and the images from the external microscope is depicted in Figure 5.31 & Figure 5.32.

In Figure 5.28 at a scratch distance of approx. 200 µm there is a ridge that seems to be pointing upwards along the scratch. It is possible that the polymer is "lifted" at

the back end of the indenter tip thereby creating a ridge, but it could also be an optical illusion.

In Figure 5.29 there is obvious signs of cracks in the formed groove and most of them seem to move from the edge of the groove in a forward direction towards the center of the scratch. Figure 5.30 shows an image of the end of the residual groove for the scratch with 50 mN max load where it has been attempted to focus at the groove to determine if the indenter has reached through the polymer layer. The groove is dark and lacks much of the detail that Figure 5.29 and no sign of the

aluminum layer can be seen, but no conclusive evidence of an intact polymer layer either.

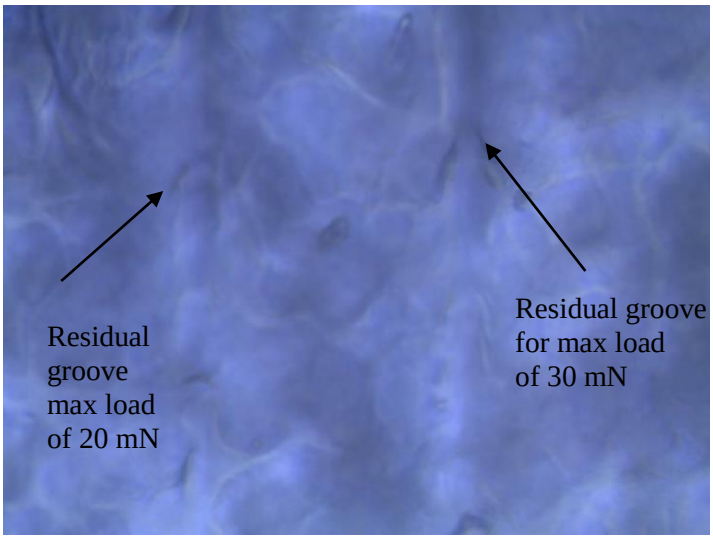

Figure 5.28 *Image of the residual scratch groove of the scratch with a max load of 20 (to the left) and 30 mN at a scratch distance of 200 μm. Acquired in the built-in microscope in the nanoindentation instrument.*

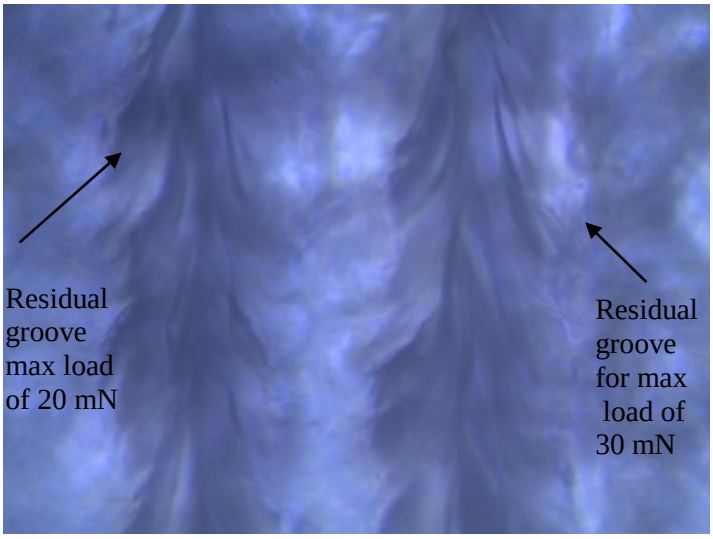

Figure 5.29 *Image of the residual scratch groove of the scratch with a max load of 20 (to the left) and 30 mN at a scratch distance of 1100 μm. Acquired in the built-in microscope in the nanoindentation instrument.*

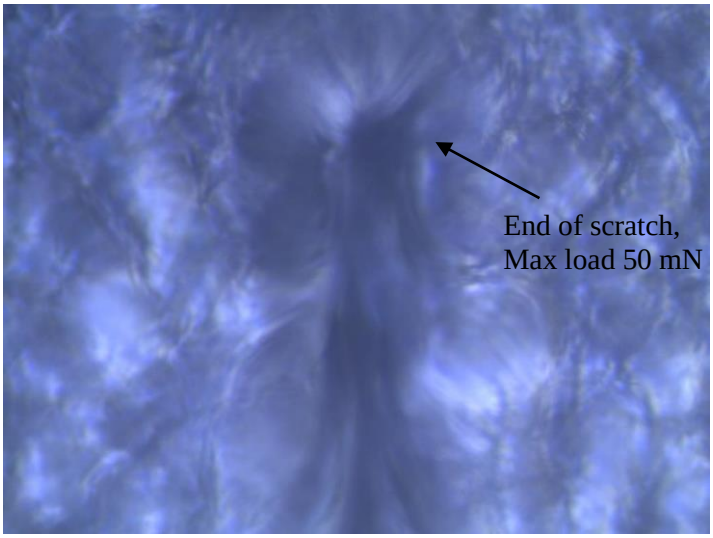

Figure 5.30 *Image of the residual scratch groove of the scratch with a max load of 50 mN at the end of the scratch. Acquired in the built-in microscope of the nanoindentation instrument.*

In Figure 5.31 and
Figure 5.32 images acquired in an external light microscope are depicted. In Figure 5.31 a textured surface is in focus and a groove with cracks/wrinkles is present. In Figure 5.32 an air bubble right next to the residual groove has been focused. Since the surface away from the groove is out of focus there is some indication of the polymer piling up along the groove. Further, it seems as the polymer layer can be followed from the edge of the groove to the middle of the groove without any signs of a broken polymer layer. However, closer to the end of the scratch the bottom of the groove was not visible so determination if the indenter has reached the aluminum layer seems difficult.

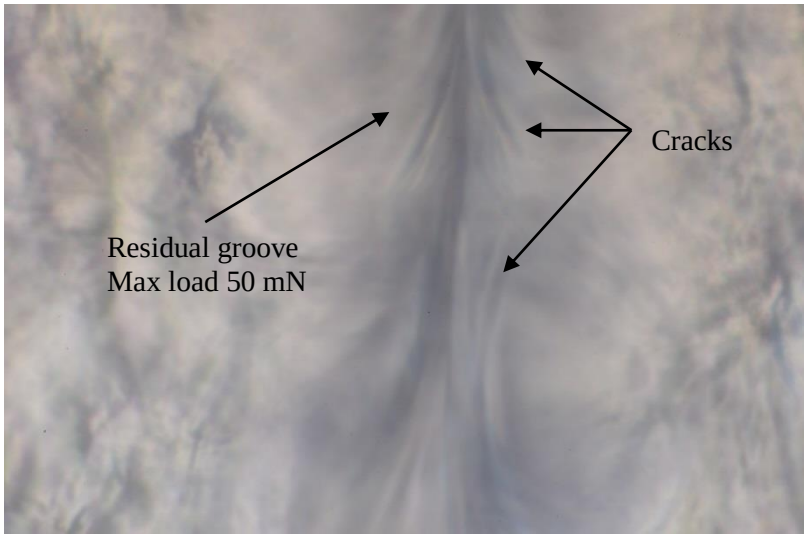

Figure 5.31 *Image of the residual scratch groove of the scratch with a max load of 50 mN acquired from an external light microscope.*

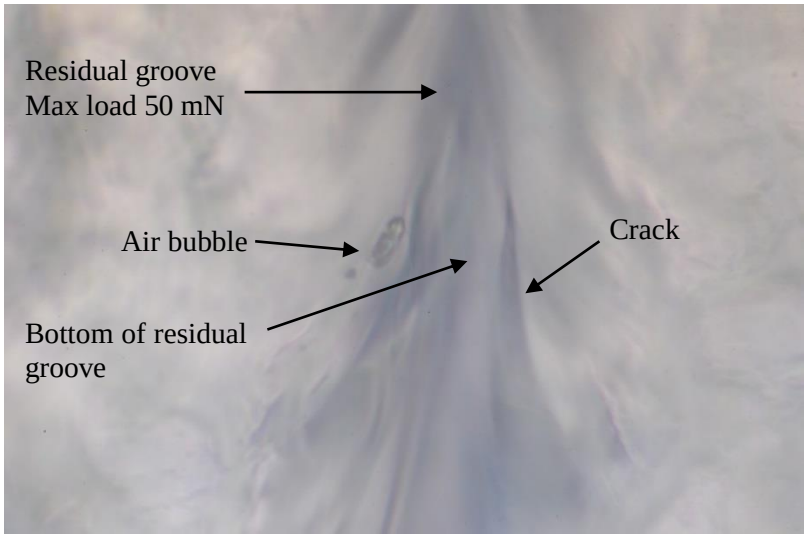

Figure 5.32 *Image of the residual scratch groove of the scratch with a max load of 50 mN acquired from an external light microscope.*

5.2 Tests on samples without paperboard

5.2.1 Scratch test

Figure 5.33 shows plots where three separate scratch tests has been performed on untreated samples with 30, 40 and 50 mN max load with almost equal loading rates (the 30 mN has 0.7 mN/s whereas 40 and 50 mN has 0.75 mN/s) in order to investigate the influence of max load on the scratch response. As a result the 30 mN experiment has a shorter scratch length. The bottom curves represents the residual topography of the scratch measured as the surface topography after the scratch subtracted with the surface topography before the scratch and can be seen as the plastic deformation. The top curves represents the displacement of the indenter from starting position subtracted with the topography of the initial surface and can be seen as a measure of how deep into the material the indenter reaches during scratch

As can be seen there is good correlation between the scratch responses for all three loads indicating that max load in the chosen interval seem to have a negligible effect. No tests has been performed on the influence of loading rate, but it could be an interesting topic.

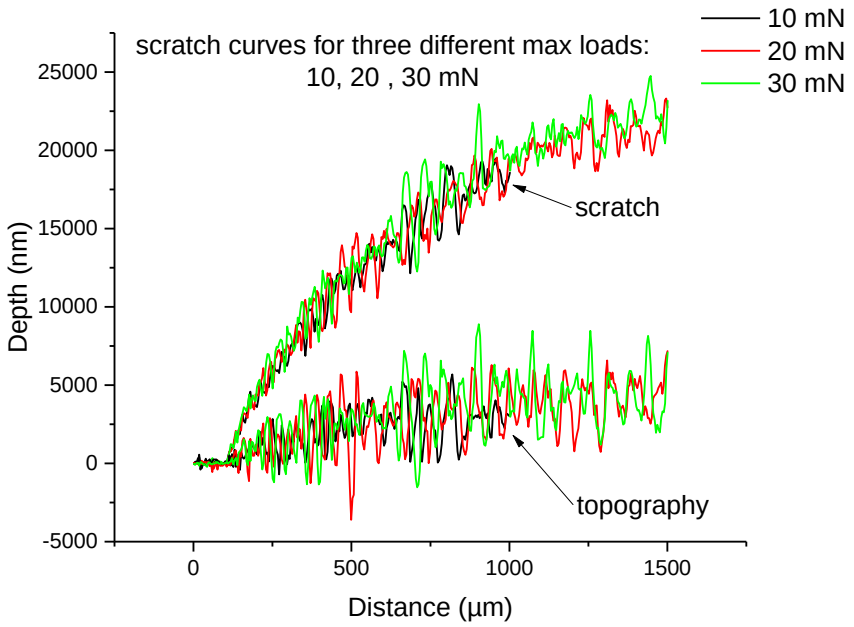

Figure 5.33 *Scratch curves with 30, 40 and 50 mN max load, respectively, on a sample non-acid treated sample.*

In Figure 5.34 a five times wear test has been performed where after the first scratch there is almost no plastic deformation. For scratch number 2-5 the scratch curve

goes flat after about 1000 µm due to the instrument reaching its maximum indentation depth.

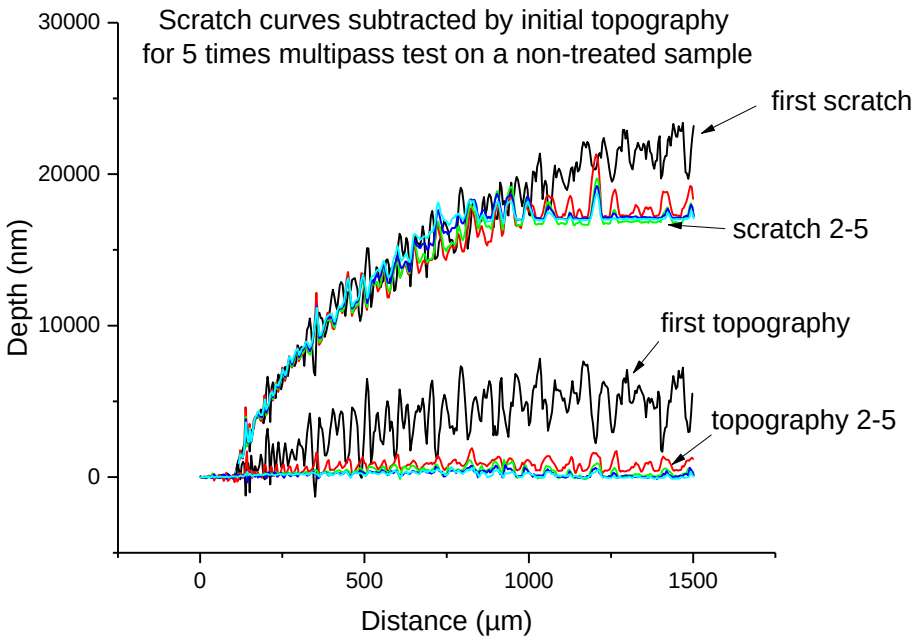

Figure 5.34 *Five time wear test on a sample not treated with acid where the sample has been scratched three times in the same groove.*

Figure 5.35-Figure 5.36 show the scratch response for the experiments where acid has been applied normal to the surface as the sample has been folded as a "cradle" and stored for one day. It should be mentioned that the acid evaporated quickly despite attempts to rid the problem and at some points all acid was completely evaporated thus decreasing the time the sample was actually applied to the sample and also inducing the risk that the effect of the acid disappears when the acid is gone. As for the non-treated material the plastic deformation after the first scratch is very small and shows the same overall appearance as the non-treated sample with no behavior that suggest any change in adhesion or mechanical properties.

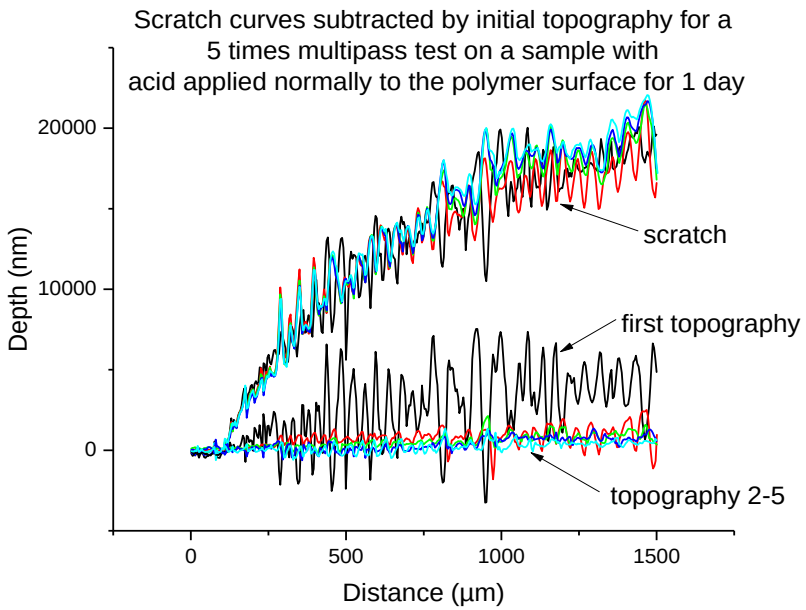

Figure 5.35 *Five time wear test for a sample treated with acid one day normal to the polymer. Same procedure with experimental parameters and visualization as in Figure 5.33.*

A ten times wear test was also performed and is shown in Figure 5.36. It should be noted that this was performed the day after the five times wear test so it's possible that possible acid influence has disappeared. The plastic deformation is very small after the first scratch with exception for pass number nine where there is a little bit more deformation although not extensive.

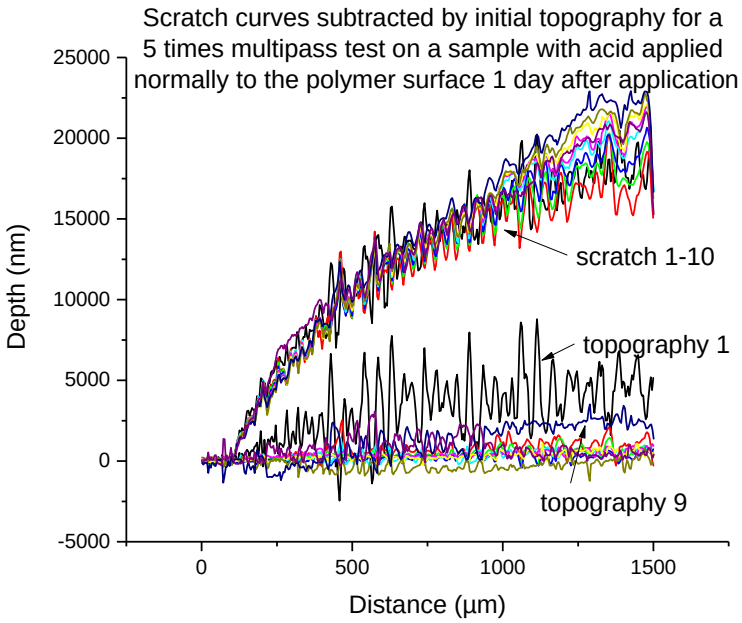

Figure 5.36 *Ten time wear test for a sample treated with acid one day normal to the polymer, one day after the acid was removed. Same procedure with experimental parameters and visualization as in Figure 5.34.*

Figure 5.37 - Figure 5.38 shows the scratch response for a sample that has been submerged in acid for 1 day and the scratch response the day after. It is of importance to once again stress that the polymer layer on the side that is not of importance lost the adhesion to the aluminum layer and was removed before it was mounted to the sample holder, potentially influencing the resulting scratch response. Similarly to the previous experiments the plastic deformation is insignificant after the first scratch and there is nothing indicating a loss of adhesion or change in mechanical properties. Also, the experiment performed the day after shows the same behavior and no difference can be observed, indicating that the acid has had no effect or at least none detectable by the technique.

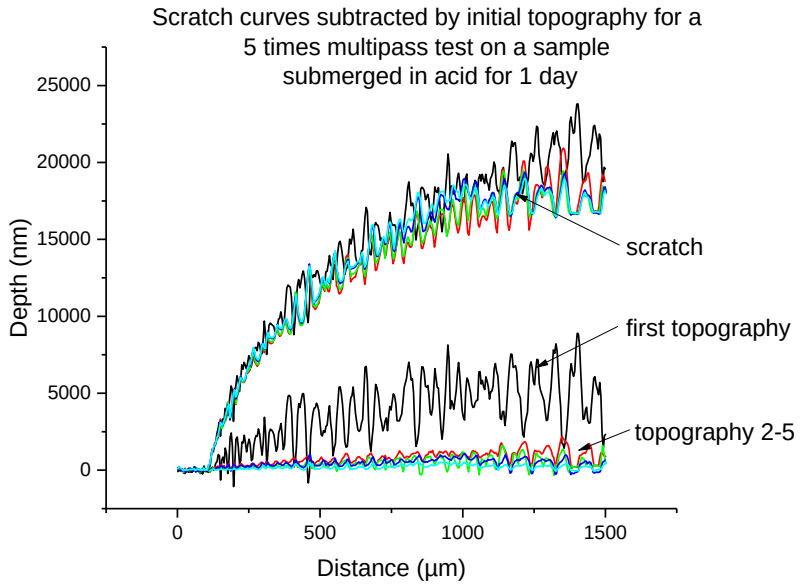

Figure 5.37 *Five time wear test for a sample submerged in acid one day. Same procedure with experimental parameters and visualization as in Figure 5.34.*

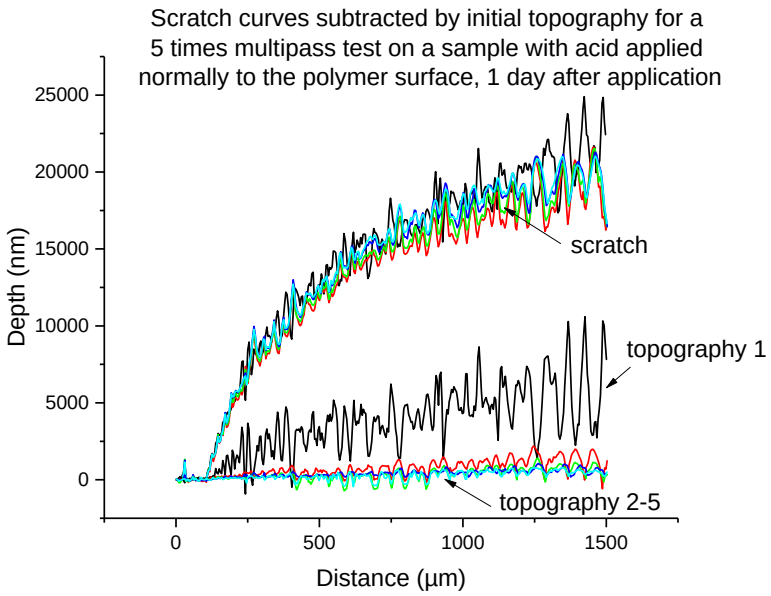

Figure 5.38 *Five time wear test for a sample submerged in acid one day. Same procedure with experimental parameters and visualization as in Figure 5.34.*

Figure 5.39 - Figure 5.42 show scratch curves where the sample has been submerged in a jar of acid for two days. The scratch curves show significant difference from

previous experiments where the surface topography prior to and after scratch tests shows an almost completely flat behavior. Important to note is that contrary to the previous experiments in these graphs the scratch curves and post-scans have not been subtracted by the surface topography. Instead it shows the displacement of the indenter from its starting position. The topography scans show the initial topography prior to the start of the experiment coupled with the topography scans after each scratch sequence. This is due to the flat pre-scan topography and lack of plastic deformation which yields the previous approach unnecessary.

The scratch curve shows almost no resistance to the scratch as the indenter sinks in rapidly to the maximum depth limit of the instrument without much resistance thereafter continuing at this level with no changes. The same behavior occurs for the wear tests with five, ten and fifteen passes, with a very small plastic deformation on the order of 100 nm between each scratch which in the end results in a measurable total depth but significantly smaller than the previous ones. Interesting to note is that the pre-scratch curve is included and show the same flat appearance as the post-scratch curves. Since the adhesion is unlikely to influence behavior of the topography scans this is probably due to a change in properties of the polymer. For example, polymers are known to swell and become rubbery as they come in contact with solvents [58]. This could also explain the very rapid descent into the polymer during the scratch if the hardness of the polymer has been reduced by the acid. The response during scratch is probably a combination of the mechanical properties of the polymer and the adhesion, thus a loss of adhesion could yield as steeper descent into the polymer. It is however highly unlikely that a loss of adhesion could be solely responsible for the close to instant descent to the max limit, and a method for isolating the possible adhesion influence seem difficult to find.

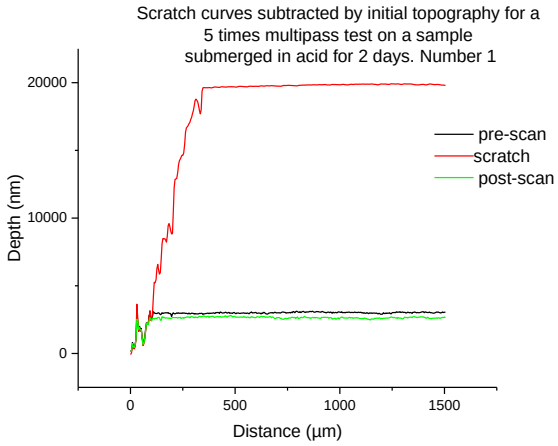

Figure 5.39 *Single scratch test for a sample submerged in acid two days. Subtraction with initial topography has not been performed.*

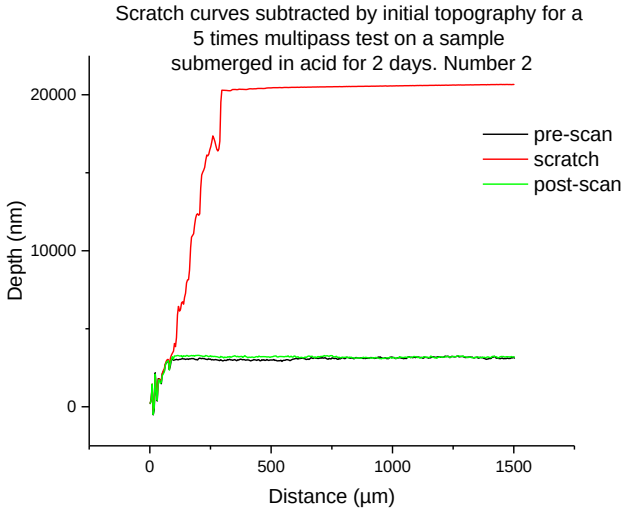

Figure 5.40 *Single scratch test for a sample submerged in acid two days. Subtraction with initial topography has not been performed.*

a

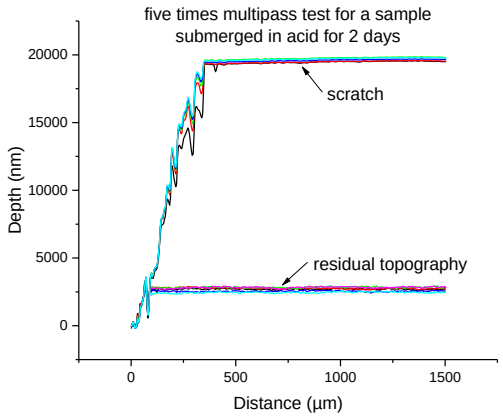

b

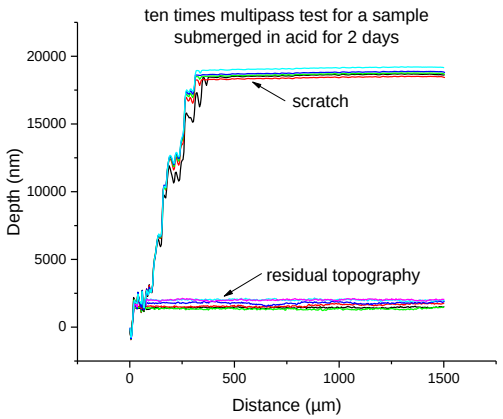

c

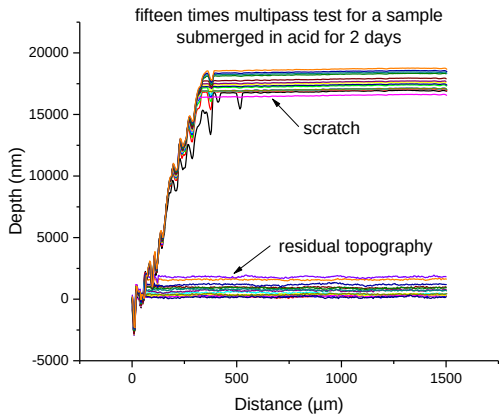

Figure 5.41 *Wear test for a sample submerged in 2 days, scratched a) five times, b) ten times, c) fifteen times.*

Figure 5.42 shows a scratch experiment performed on the same sample with the same experiment details as for those in Figure 5.39 - Figure 5.41 one day after the acid has been applied. Interestingly, it does not show any of the behavior in the previous experiments, but rather similar to the experiment of the untreated sample.

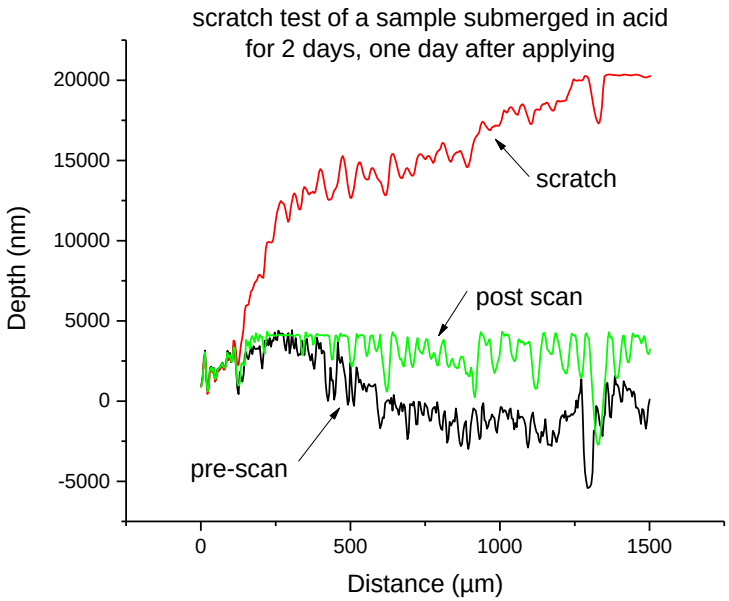

Figure 5.42 *Single scratch of a sample submerged in acid for two days, tested one day after the acid was removed.*

5.2.1.1 Residual scratch grooves

Unfortunately, due to some mistakes residual images were not acquired for all scratch tests, so comparison is somewhat difficult but some comparisons can still be made and images of residual grooves are shown in Figure 5.43

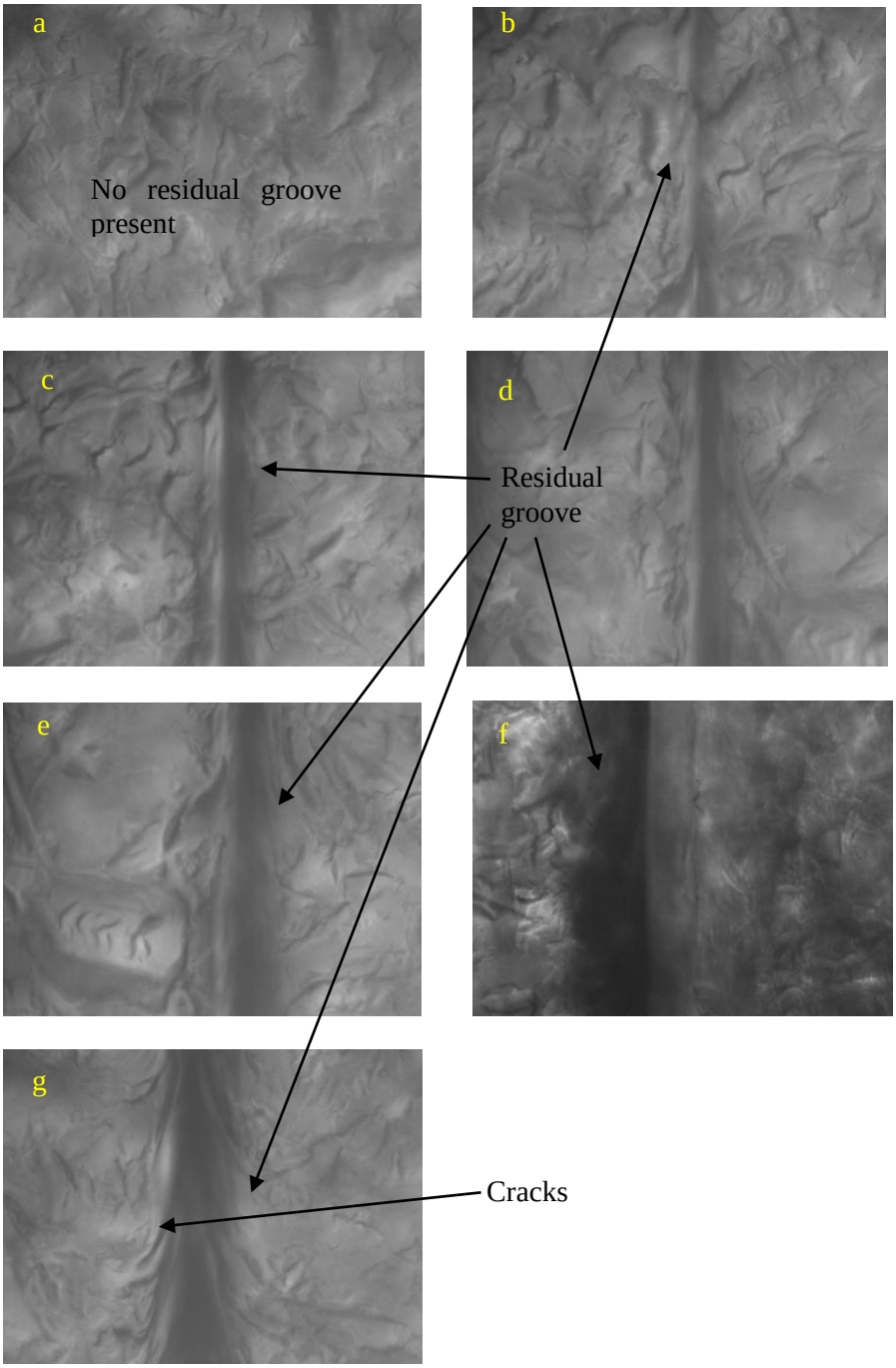

Figure 5.43 *Residual grooves at the scratch length of approx. 1200 µm of the scratches corresponding to a) 2day single nr1 b) 2day single nr2 c) 2day 5x d) 2day 10x e) 2day 15x f) cradle 10x g) 1day single.*

The depth for the scratch tests with a sample submerged for two days read from the scratch curves in Figure 5.39 - Figure 5.42 shows a depth of approx. 300 which is very close to the theoretical resolution limit for a light microscope of approximately 250 nm [59]. However, the residual grooves for the single scratches shows a groove for the whole scratch length for scratch number 1 and a groove along the first 500µm for scratch number 2. This is consistent with the behavior of the scratch curves in Figure 5.43. Whether the small depth of approx. 300nm is measured correctly in the nanoindentation instrument and actually visible in a light microscope or a result of the topography scan understating the actual depth is hard to determine.

The residual grooves of the samples submerged for two days seem to show that the grooves of multipass tests are wider than for the single ones. However, the grooves belonging to the samples submerged for two days seem to be narrower than for the other acid application techniques. This is consistent with the scratch curves. Unfortunately, as it was not apparent at the time, no measure was performed on the width of the groove but it could be a useful measure of the plastic deformation in the future as a complement to the post-scratch curves. It is for example possible to do topography scans across the groove or measure in the built-in microscope.

5.3 Cross-sectional indentation

Figure 5.44 shows the loading curves for a multi-point indentation experiment for the first max load of 0.05 mN. It is important to note that the instrument uses a surface-finding load of 0.05 before applying the load. Therefore, only the behavior after the load of 0.05 mN is of interest. Further, this load is added to the other experiments so that the reading on the y-axis show a max load 0.05 mN higher than expected. The loading curves for 0.05 mN show a small spike in depth and another curve show an oscillating behavior.

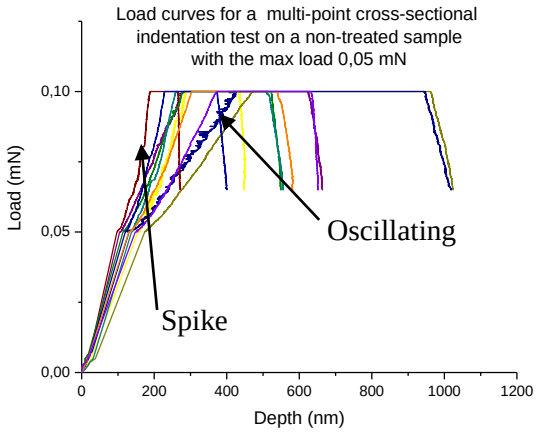

Figure 5.44 *Load curves for multi-point indentations of a non-treated sample (sample 3) with the max load of 0.05 mN.*

In Figure 5.45 curves with the max load of 0.3 mN is presented. There is a rather large variation and the curve that showed an oscillating behavior in the previous graph shows an oscillating behavior in this graph. Further, one curve shows spike in depth although it's another curve than for the 0.05 mN max load.

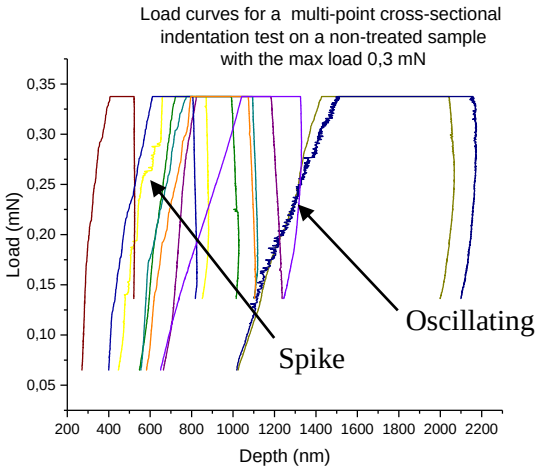

Figure 5.45 *Load curves for multi-point indentations of a non-treated sample (sample 3) with the max load of 0.3 mN.*

For the 0.5 mN max load there is the same oscillating behavior for the oscillating curve in the previous experiment and another curve also shows some oscillating behavior. There does not seem to be any spike in depth, but rather there seems to be a distinct change in slope. There can also be seen a division of the curves into three different groups with a low depth, medium depth and high depth.

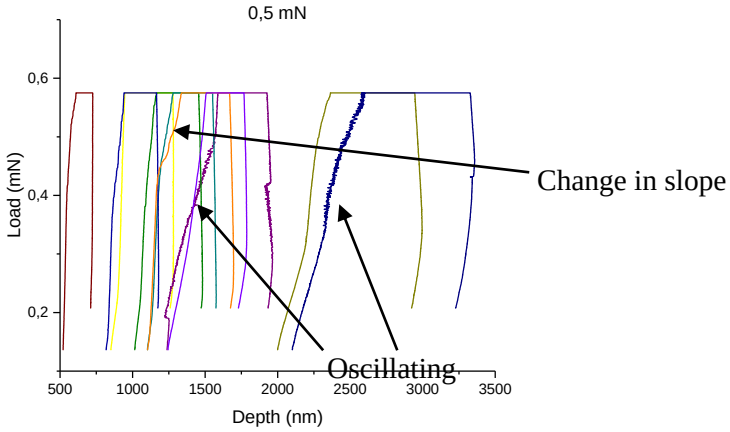

Figure 5.46 *Load curves for multi-point indentations of a non-treated sample (sample 3) with the max load of 0.5 mN.*

For the curves corresponding to the max load of 0.7 mN there does not seem to be any oscillating and a sudden increase in depth seem to occur although it appears to be a bit smoother than for the previous ones.

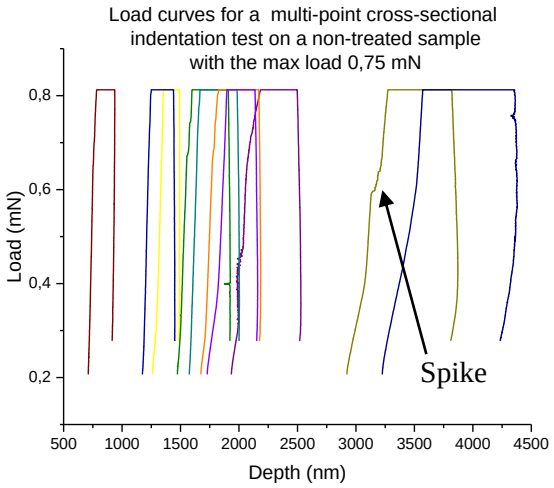

Figure 5.47 *Load curves for multi-point indentations of a non-treated sample (sample 3) with the max load of 0.7 mN.*

For the 1 mN max load there seem to be some very small oscillating behavior and one spike in depth a bit bigger than previously seen. The variation is bigger than for any of the previous loads.

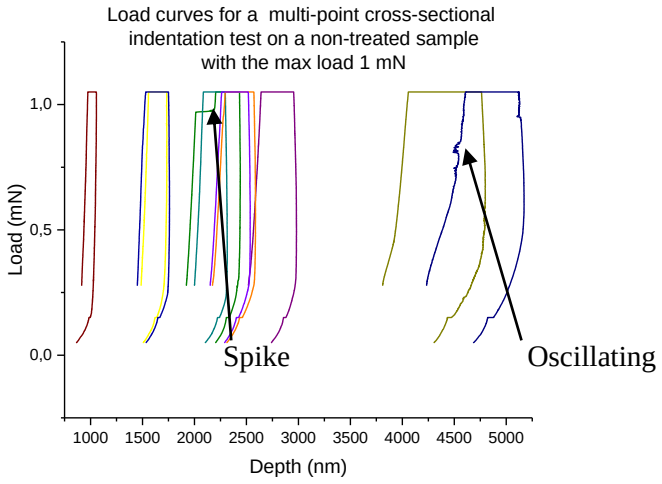

The corresponding curves during holding are shown in Figure 5.48 – Figure 5.53. For 0.05 Max load there is a lot of oscillating behavior. There also seems to be some small spikes, although there are some signs that these spikes transcends from oscillating behavior to spikes. An enlarged image showing this behavior is shown in Figure 5.49.

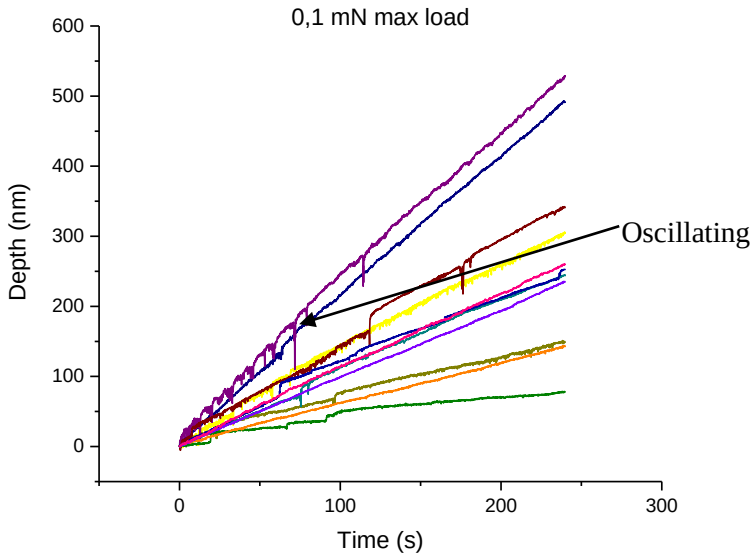

Figure 5.48 *Dwell curves for multi-point indentations of a non-treated sample (sample 3), aimed squarely in the interface with the max load of 0.05 mN.*

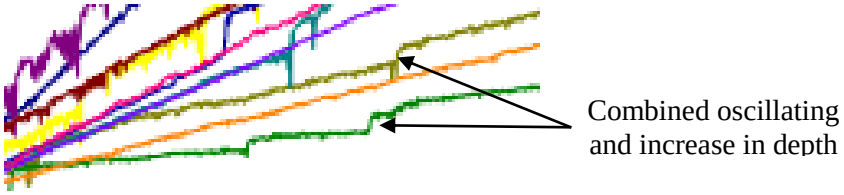

Figure 5.49 *Enlarged image of Figure 5.48 showing what seems to be a combined oscillating behavior and sudden spikes in depth.*

For the curves corresponding to a max load of 0.3 mN there is less oscillating and bigger spikes in depth, although some of the combined oscillating behavior and spike in depth seem to be visible.

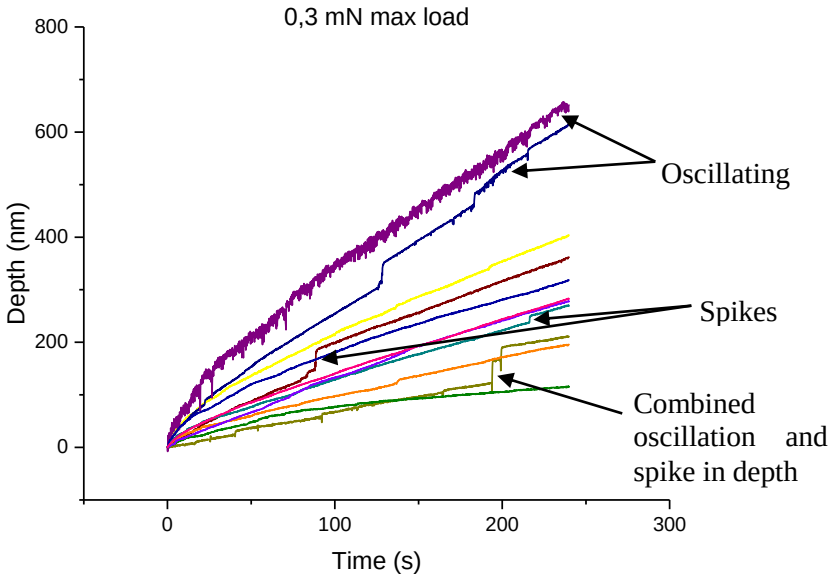

Figure 5.50 *Dwell curves for multi-point indentations of a non-treated sample (sample 3), aimed squarely in the interface with the max load of 0.05 mN.*

For the 0.5 mN max load dwell curves there is a spike in depth bigger than those seen for lower max loads. Further, there seem to be less oscillating and spikes.

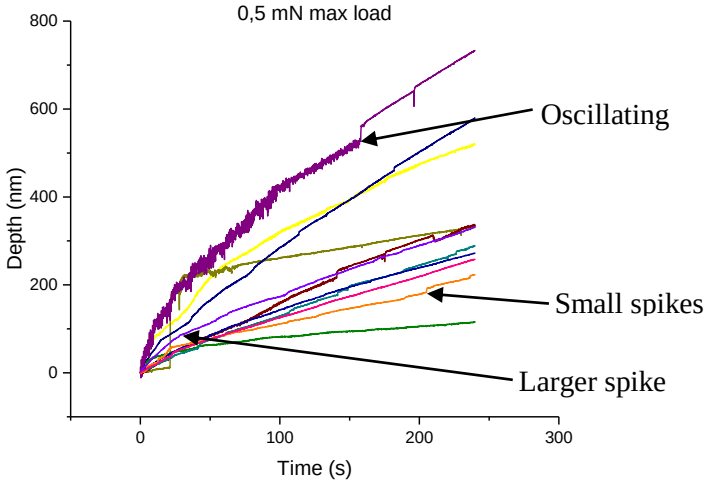

Figure 5.51 *Dwell curves for multi-point indentations of a non-treated sample (sample 3), aimed squarely in the interface.*

Looking at the 0.75 mN one there seem to be less oscillating but some small spikes

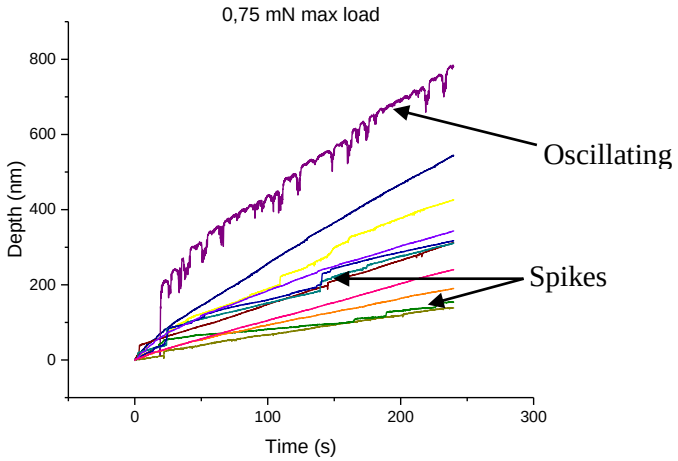

Figure 5.52 *Dwell curves for multi-point indentations of a non-treated sample (sample 3), aimed squarely in the interface.*

For the 1 mN curves there seem to be a smaller variation and the oscillation also seem to decrease. Apart from one small spike and the curve that has been oscillating in the previous graphs, all curve show the trend of a straight line with no irregular behavior.

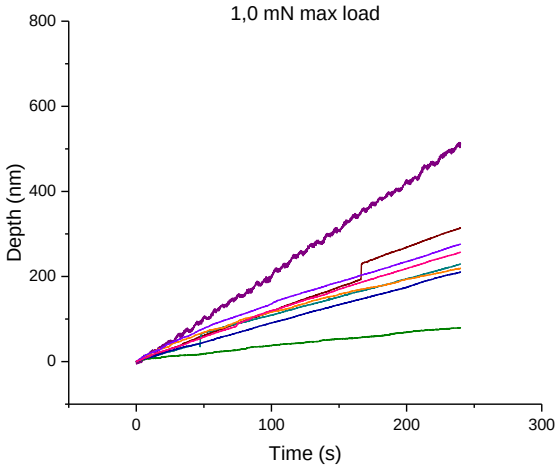

Figure 5.53 *Dwell curves for multi-point indentations of a non-treated sample (sample 3), aimed squarely in the interface.*

The corresponding residual indents are shown in Figure 5.54. It can be clearly seen that the indent has made a half-circular mark in the aluminum layer with the size of

this half circle varying slightly between the indents. There is however no indent that has a clearly deviating appearance from the other.

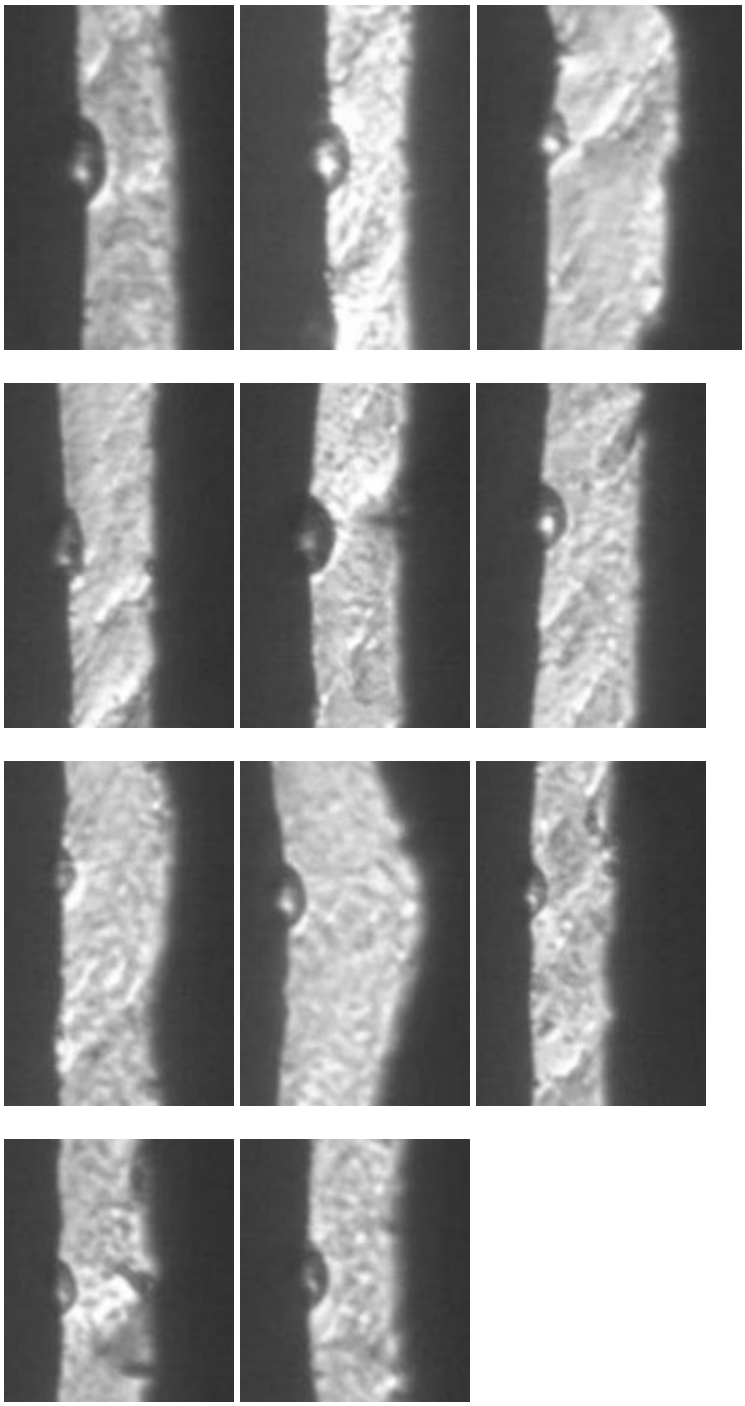

Figure 5.54 *Residual indents for cross-sectional indentation of a non-acid treated sample (sample 3) with aimed squarely into the polymer-aluminum interface.*

Cross-sectional experiments were performed on two separate samples that had been submerged in acid for one day. Unfortunately, reproducing the aim from the previous experiment so the indent hits squarely in the interface proved difficult, but instead most of the times the indent ended up squarely in the aluminum layer or polymer layer. Therefore indents were aimed a few microns into the polymer layer to see if that could induce a placement of the indents into the interface. This strategy mostly resulted in indents in the polymer layer with an offset from the interface of some micron but also some occasional indents in the aluminum layer. The indents analyzed from the first acid treated sample (denoted sample 1) are those that ended up in the polymer layer both intentionally and unintentionally, and the residual indents can be seen in Figure 5.81and Figure 5.82. As the next sample (denoted sample 2 through this chapter) showed the same problems a strategy was employed in which eight indents were offset into the polymer layer about 6 µm from the interface with the intention to exclude as much aluminum influence as possible. It should be noted that this is not ideal since there is an interface between two polymers at that width so it could be some different indentation response due to that fact. Another eight indents were made approximately 3 µm into the polymer layer so that the indenter reaches the polymer as close to the interface as possible but still minimizing the risk of pure aluminum contact. Loading curves for the 6 µm experiments are shown in Figure 5.56 - Figure 5.65 and residual indents are shown in Figure 5.66. The loading curves for the 3 µm experiments are shown in Figure 5.67 - Figure 5.76 and the residual indents are shown in Figure 5.77

Important to note is that there was a considerable difference in height between the aluminum and polymer layer with the aluminum protruding above the polymer layer about 2-3 µm, whereas the untreated showed some signs of a difference in height although not as significant. Further, the surface roughness was considerably worse for the acid-treated samples compared to the non-treated one.

Interestingly, one of the acid-treated samples (sample 2) showed an obvious gap between the polymer and aluminum throughout the length of the sample, while sample 1 showed small occasional gaps but not to the same extent. This gap is shown in Figure 5.55. Also interesting to note is that the gap occurred between “the inside polymer” (the one of interest in the indentation tests) and the aluminum layer. This contradicts the observations from the scratch test where the outer layer could be peeled off by hand but not the inside polymer. This might be because of the gap between the inside polymer and the epoxy resin facilitating room for the polymer to move whereas the outside polymer is fixated between the aluminum foil and adhesive joint to the epoxy resin. It could also be due the gluing process

altering the properties of the outside polymer and enhancing the adhesion to the aluminum.

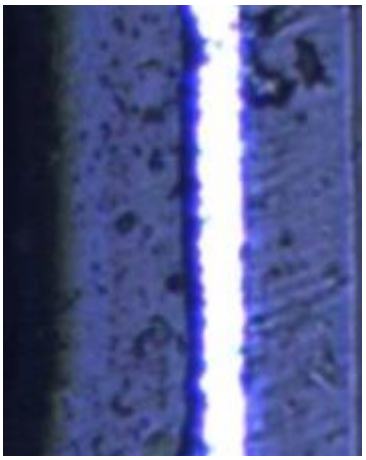

Figure 5.55 *Image showing a gap between the inside polymer (to the left) and the aluminum after submerging the sample in acid one day.*

For the indents that were aimed 6 µm from the interface, with max loads of 0.05 mN shown in the image below, there is considerable oscillation on all curves except two which show smaller indentation depths.

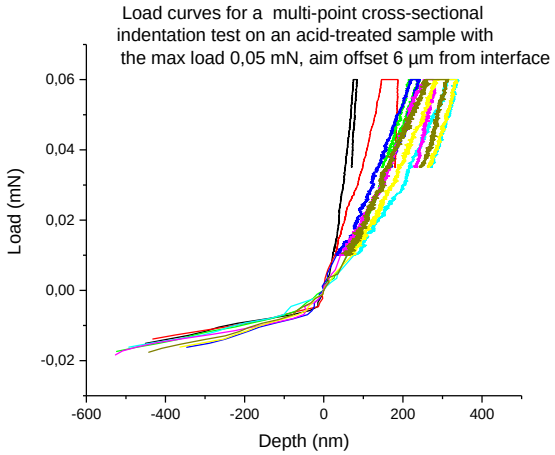

Figure 5.56 *Load curves for multi-point indentations of an acid-treated sample, aimed 6 µm into the polymer layer from the interface.*

This oscillation does seem to diminish when the load is increased to 0.3 mN. The lower indentation depths of the two indents remain however, and the separation is more pronounced.

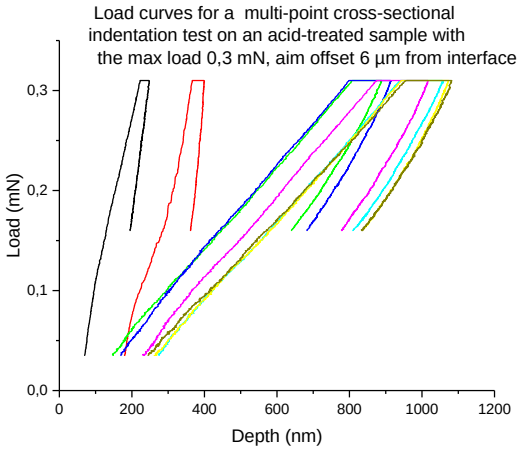

Figure 5.57 *Load curves for multi-point indentations of an acid-treated sample, aimed 6 µm into the polymer layer from the interface.*

Not much difference can be seen for the graph with a max load of 0.5 mN

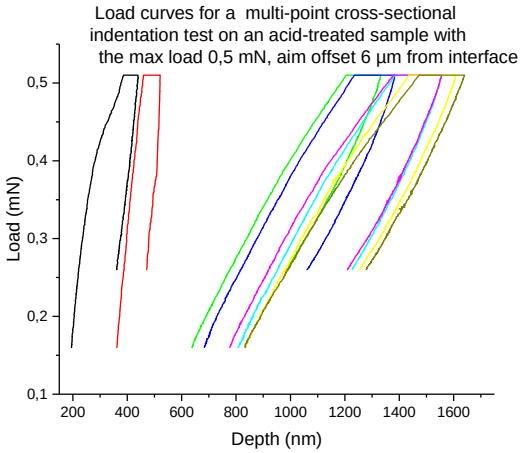

Figure 5.58 *Load curves for multi-point indentations of an acid-treated sample, aimed 6 µm into the polymer layer from the interface.*

Looking at the 0.75 mN graph the two curves with lower indentation depth seem to converge towards each other while maintaining a distinct gap to the other curves. There is a small spike visible for one of the curves but otherwise the overall appearance is similar to the previous graphs.

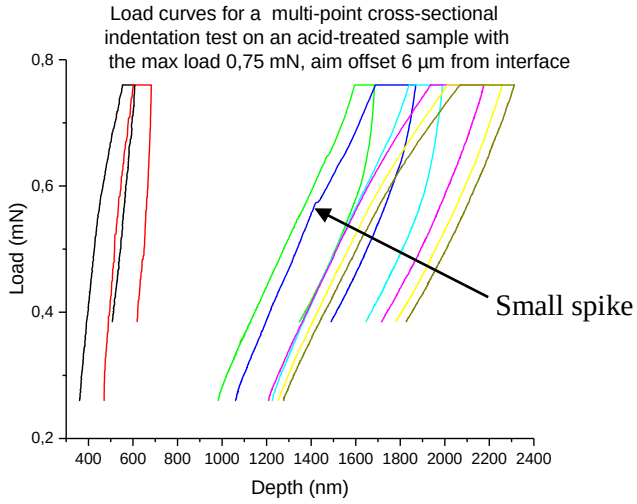

Figure 5.59 *Load curves for multi-point indentations of an acid-treated sample, aimed 6 µm into the polymer layer from the interface.*

For the curves representing the experiments of 1 mN max load the overall appearance does not change. However, there is anomalous behavior for three of the curves near the max load as two curves show a distinct spike in depth and one show a rounded appearance just prior to reaching max load.

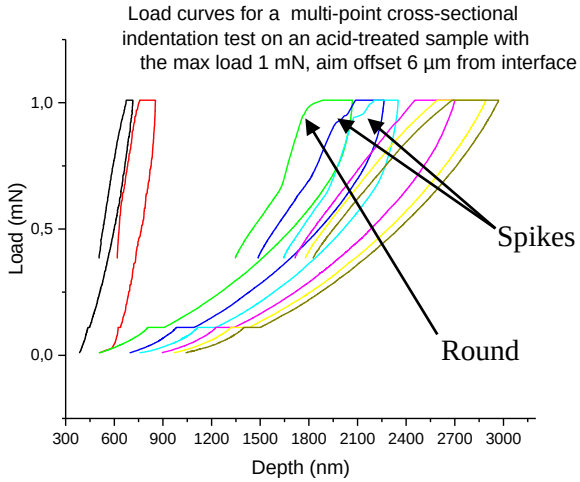

Figure 5.60 *Load curves for multi-point indentations of an acid-treated sample, aimed 6 µm into the polymer layer from the interface.*

The related dwell data shows a highly oscillating behavior with very small depths. This is in stark contrast to the previous experiments in the interface which showed depth of several hundred already for the lowest load.

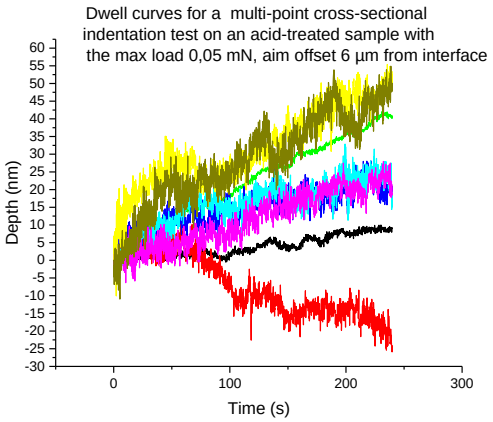

Figure 5.61 *Dwell curves for multi-point indentations of an acid-treated sample (sample 2), aimed 6 µm into the polymer measured from the interface with the max load of 0.05 mN.*

For the 0.3 mN the curves show a logarithm-like appearance with a maximum depth of 20-150 nm. This should be compared with the experiments aimed in the interface which show an appearance of a straight line with depths up to 700 nm. Not much differs from the 0.3 mN to the 0.5 mN graph.

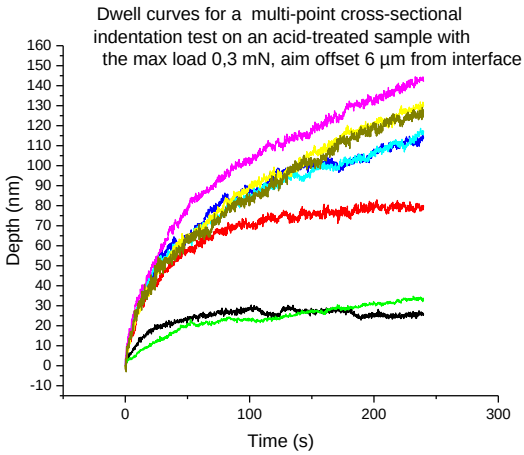

Figure 5.62 *Dwell curves for multi-point indentations of an acid-treated sample (sample 2), aimed 6 µm into the polymer measured from the interface with the max load of 0.3 mN.*

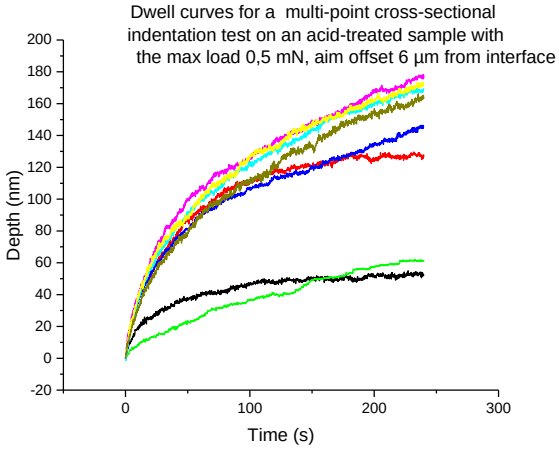

Figure 5.63 *Dwell curves for multi-point indentations of an acid-treated sample (sample 2), aimed 6 µm into the polymer measured from the interface with the max load of 0.5 mN.*

For the 0.75 mN graph, however, the variation starts to increase. The group that have previously been together as a group now starts to deviate from each other. Also, three spikes in depth can be seen.

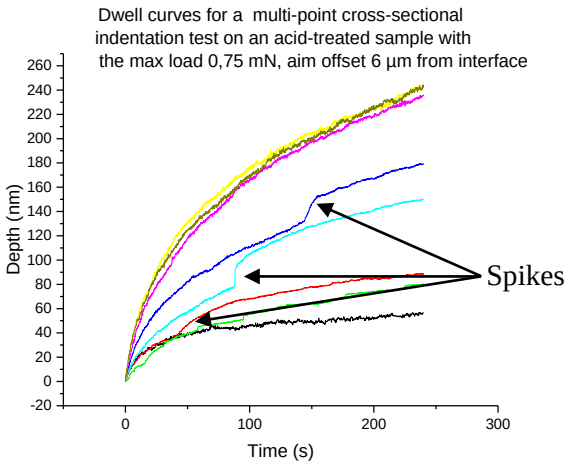

Figure 5.64 *Dwell curves for multi-point indentations of an acid-treated sample (sample 2), aimed 6 µm into the polymer measured from the interface with the max load of 0.75 mN.*

For the 1 mN graph the high variation introduced in the 0.75 mN graph remains, but no spikes or other irregularities can be seen.

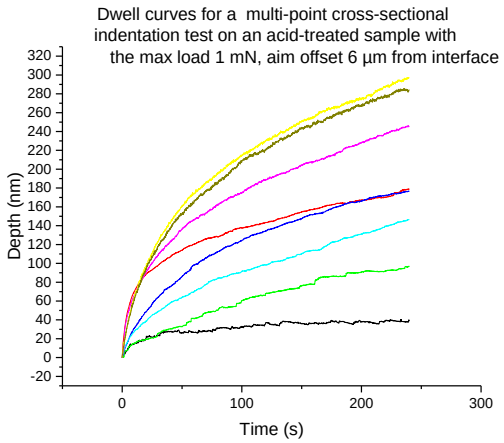

Figure 5.65 *Dwell curves for multi-point indentations of an acid-treated sample (sample 2), aimed 6 µm into the polymer measured from the interface with the max load of 1 mN.*

The residual indents corresponding to the above discussed graphs are shown in Figure 5.66 below. As can be seen the distance from the interface varies slightly between each indents and some even show signs of making contact with the aluminum layer.

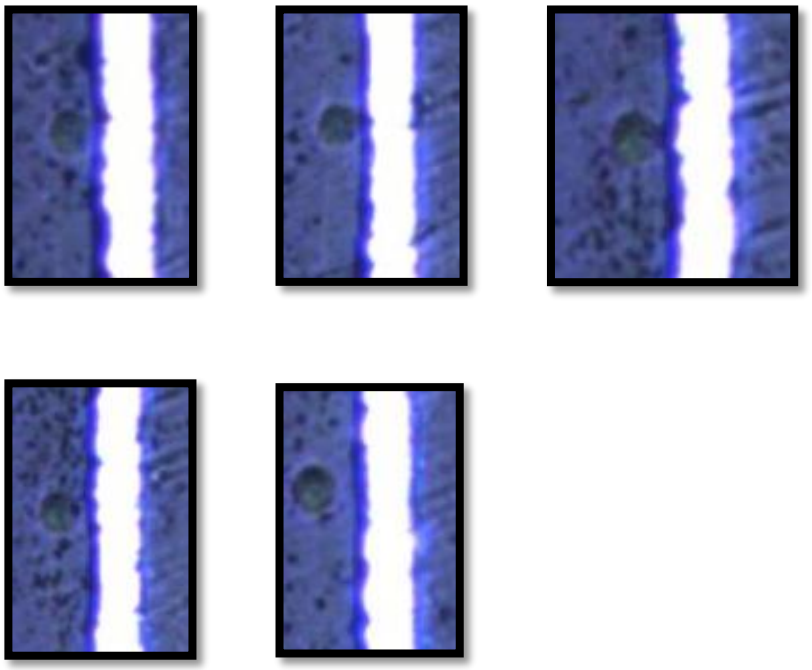

Figure 5.66 *Residual indents for cross-sectional indentation of an acid treated sample (sample 2) with aim offset 6 µm into the polymer from the interface.*

Below are shown the indentation response curves for the experiments where the indents have been aimed 3 µm from the interface. For the max load of 0.05 mN the behavior is very similar to the one seen in Figure 5.56 where indents were aimed 6 µm into the polymer. There are two different groups: one non-oscillating with lower depths and one oscillating group with higher indentation depths.

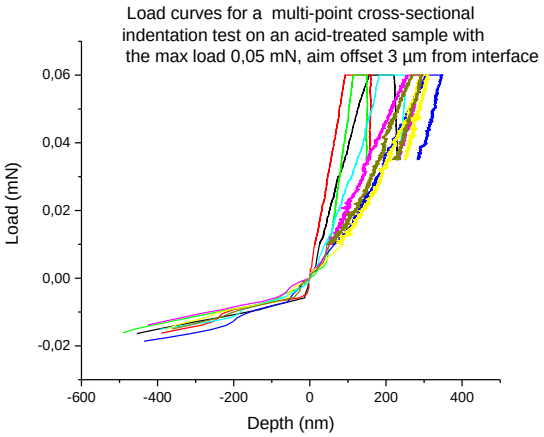

Figure 5.67 *Load curves for multi-point indentations of an acid-treated sample, aimed 3 µm into the polymer layer from the interface.*

For the 0.3 mN one the oscillation seem to have disappeared but there are still two groups divided by their indentation depths. Three spikes can be seen.

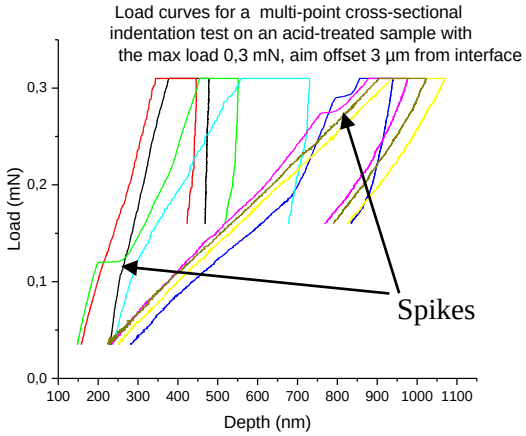

Figure 5.68 *Load curves for multi-point indentations of an acid-treated sample, aimed 3 µm into the polymer layer from the interface.*

For the 0.5 mN graphs two more spikes can be seen.

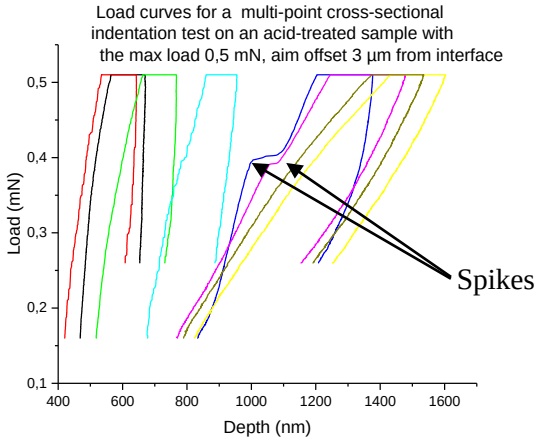

Figure 5.69 *Load curves for multi-point indentations of an acid-treated sample, aimed 3 µm into the polymer layer from the interface.*

For the 0.75 mN the rather big spikes seen in the 0.3 and 0.5 mN graphs is not seen but instead only one minor spike is visible.

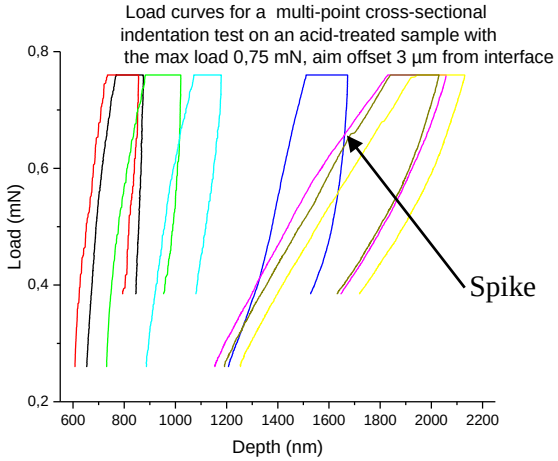

Figure 5.70 *Load curves for multi-point indentations of an acid-treated sample, aimed 3 µm into the polymer layer from the interface.*

For the 1 mN graph there is similarly to the 0.75 mN graph only a small spike and the overall appearance is similar to the graphs of the lower loads.

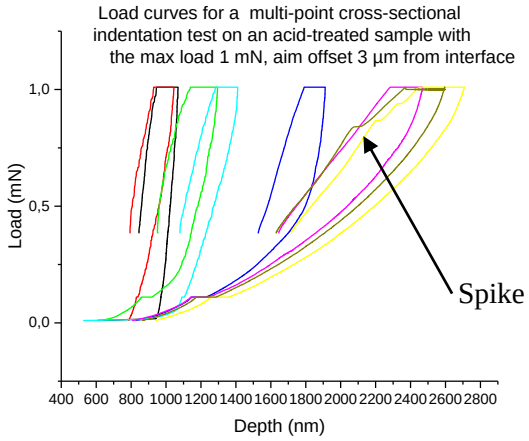

Figure 5.71 *Load curves for multi-point indentations of an acid-treated sample, aimed 3 µm into the polymer layer from the interface.*

The corresponding dwell curves are shown below. For the 0.05 mN graph the appearance is similar to that of the previously shown in Figure 5.61 with high oscillation and low depths.

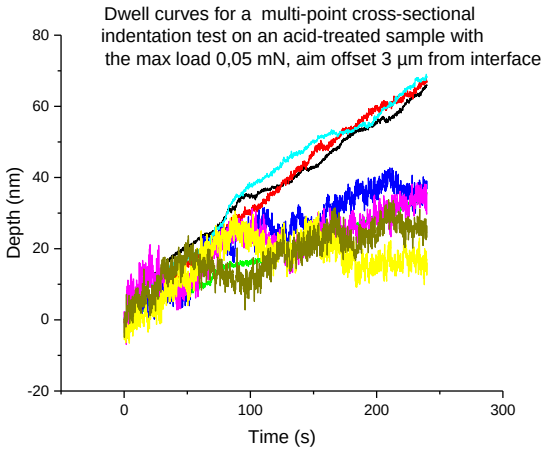

Figure 5.72 *Dwell curves for multi-point indentations of an acid-treated sample, aimed 3 µm into the polymer layer from the interface.*

For the 0.3 mN the appearance is quite similar to the one aimed 6 µm as the curves show the same type of logarithmic-like behavior and similar depths.

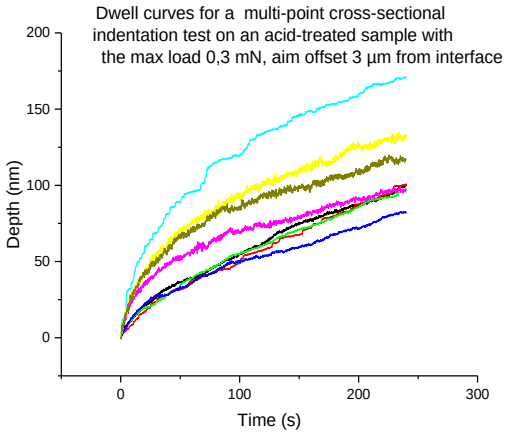

Figure 5.73 *Dwell curves for multi-point indentations of an acid-treated sample, aimed 3 µm into the polymer layer from the interface.*

For the 0.5 mN graph the curve separates into two groups with one group having greater indentation depths than the other. It can clearly be seen a significant spike in depth

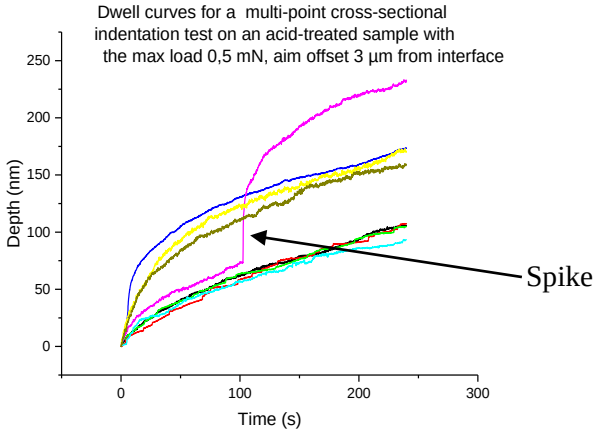

Figure 5.74 *Dwell curves for multi-point indentations of an acid-treated sample, aimed 3 µm into the polymer layer from the interface.*

For the 0.75 mN graph one of the two distinct groups seen in the 0.5 mN graph are shattered as the curves deviates away from each other. No spikes can be seen.

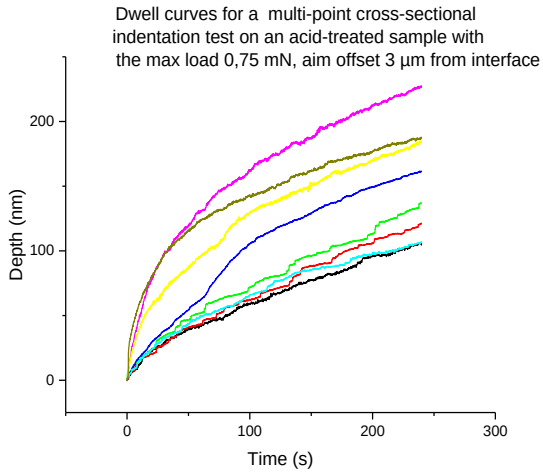

Figure 5.75 *Dwell curves for multi-point indentations of an acid-treated sample, aimed 3 µm into the polymer layer from the interface.*

For the 1 mN graph the appearance is similar to the 0.75 mN graph.

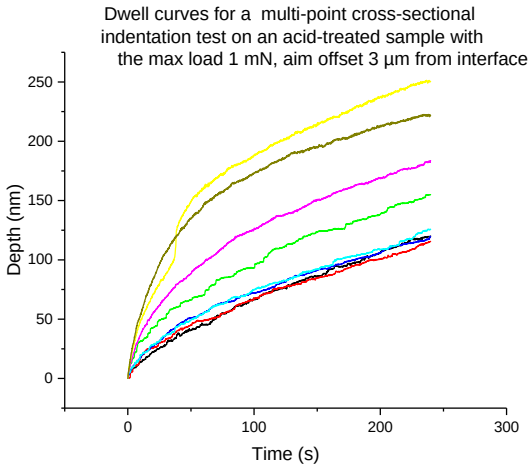

Figure 5.76 *Dwell curves for multi-point indentations of an acid-treated sample, aimed 3 µm into the polymer layer from the interface.*

The corresponding residual indents are shown below. As can be seen the indents does seem to be placed closer towards the interface than for the one offset 6 µm. some indents also show signs of making a mark in the aluminum layer.

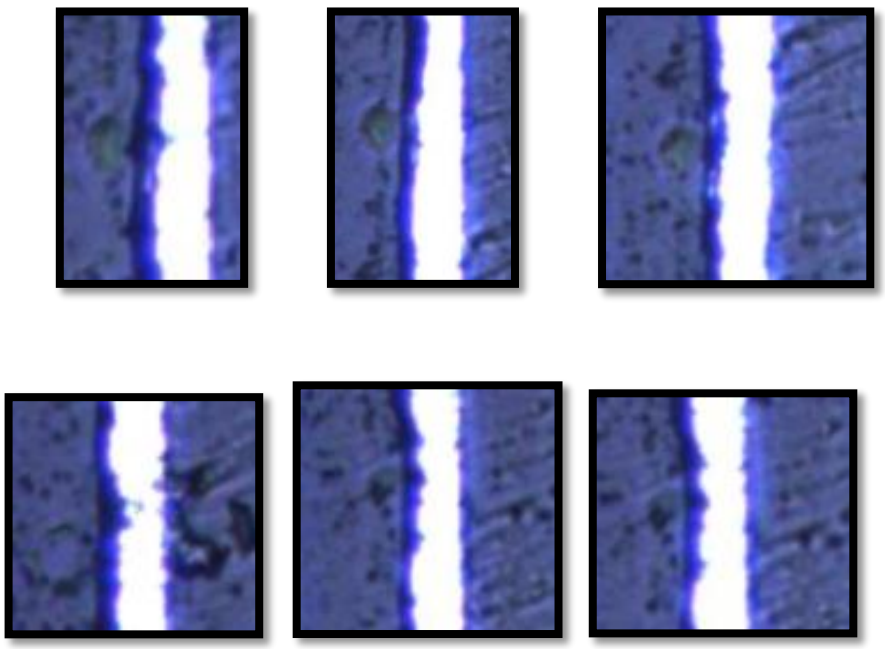

Figure 5.77 *Residual indents for cross-sectional indentation of an acid treated sample (sample 2) with aim offset 3 µm into the polymer from the interface.*

Figure 5.78 shows a graph of hardness for the indentation experiments for both the acid-treated and non-treated samples. As there was problem reproducing the placement into the interface, another loading schedule were tested but were equally unsuccessful. As a result, the figure is not as easily analyzed. The curves with five load cycles ranges from 0.1 mN to 1 mN with the steps 0.1, 0.3, 0.5, 0.75 and 1 mN whereas the one with four load cycles ranges from 0.5 to 2 mN with steps of 0.5 mN in between. Also, two indents with the loading schedule 0.5-2 mN were performed offset into the polymer of the non-treated sample as a reference.

Firstly, the increasing hardness with increasing load is not something that is expected. Usually the opposite is true, with decreasing hardness with increasing load [60]. Potential explanations could be that the bending of the whole laminate structure could influence the hardness response in an unpredictable manner. Another possibility is that the indentation depths are so large that that the material reaches above the point where the spherical tip transcends into a conical behavior which the hardness calculation does not account for.

In any case, the first experiment on the non-acid treated sample show a significantly higher hardness than the others which can be explained by looking at the residual indents which shows indents that shows a half sphere in the aluminum layer, which is not the case for the other experiments which show the whole residual indent in the polymer layer. The indents with a 3 µm offset shows a higher hardness than the one with a 6 µm offset. The non-treated sample with the load schedule 0.5-2 mN that was aimed in the polymer shows a slightly higher hardness than the acid treated sample 1. However, before too much conclusions are drawn, it needs to be compared

to the difference between the two acid treated samples sample 1 and sample 2 which should show the same hardness. To better visualize, these four indentations are shown in Figure 5.79. The difference in hardness between the non-treated sample and the acid treated (sample 1) seem to be close to the same as the difference between the acid treated samples 1 & 2. However, the variation is bigger for the hardness of the two acid treated samples that are compared with each other than that of the non-treated and acid treated that are compared. This could give some basis to argue that there is a significant difference in hardness between the acid-treated and non-treated sample due to the effects of the acid application. However, it does not seem enough to draw those conclusions from this data. Also, it is questionable how interesting that question is since it is doubtful that it shows any adhesion properties.

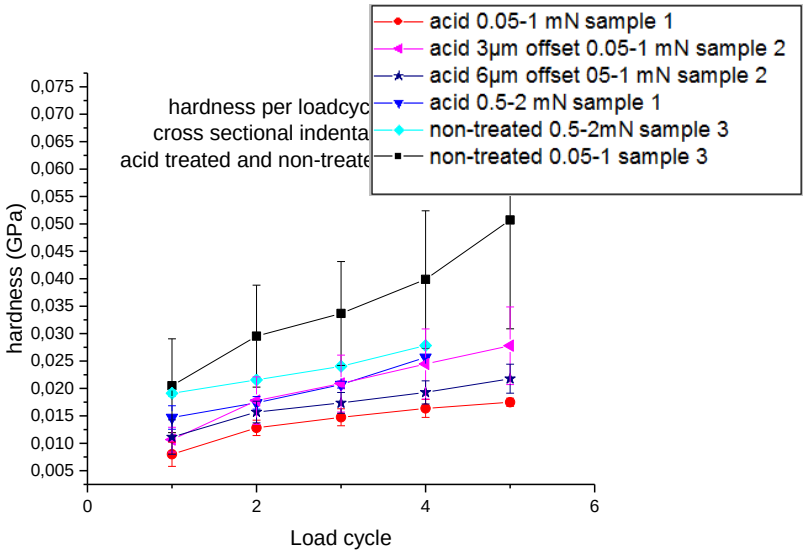

Figure 5.78 *Hardness plots for multi-point hardness tests.*

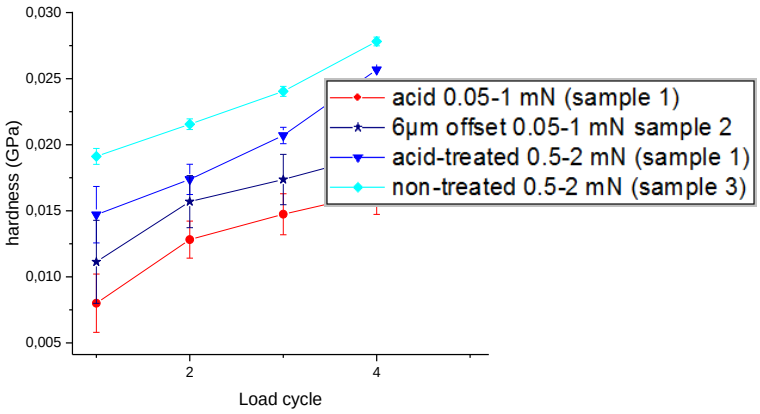

Figure 5.79 *Selected graphs from Figure 5.78.*

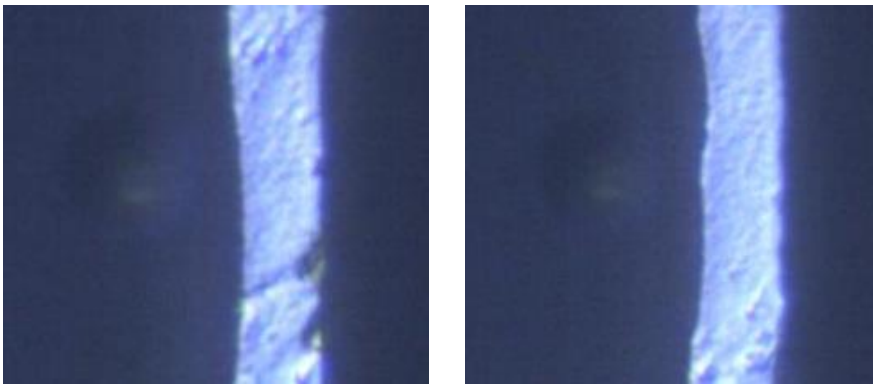

Figure 5.80 *Residual indents of the cross-sectional indents on a non-treated sample (sample 3) with loading schedule 0.05 – 1 mN.*

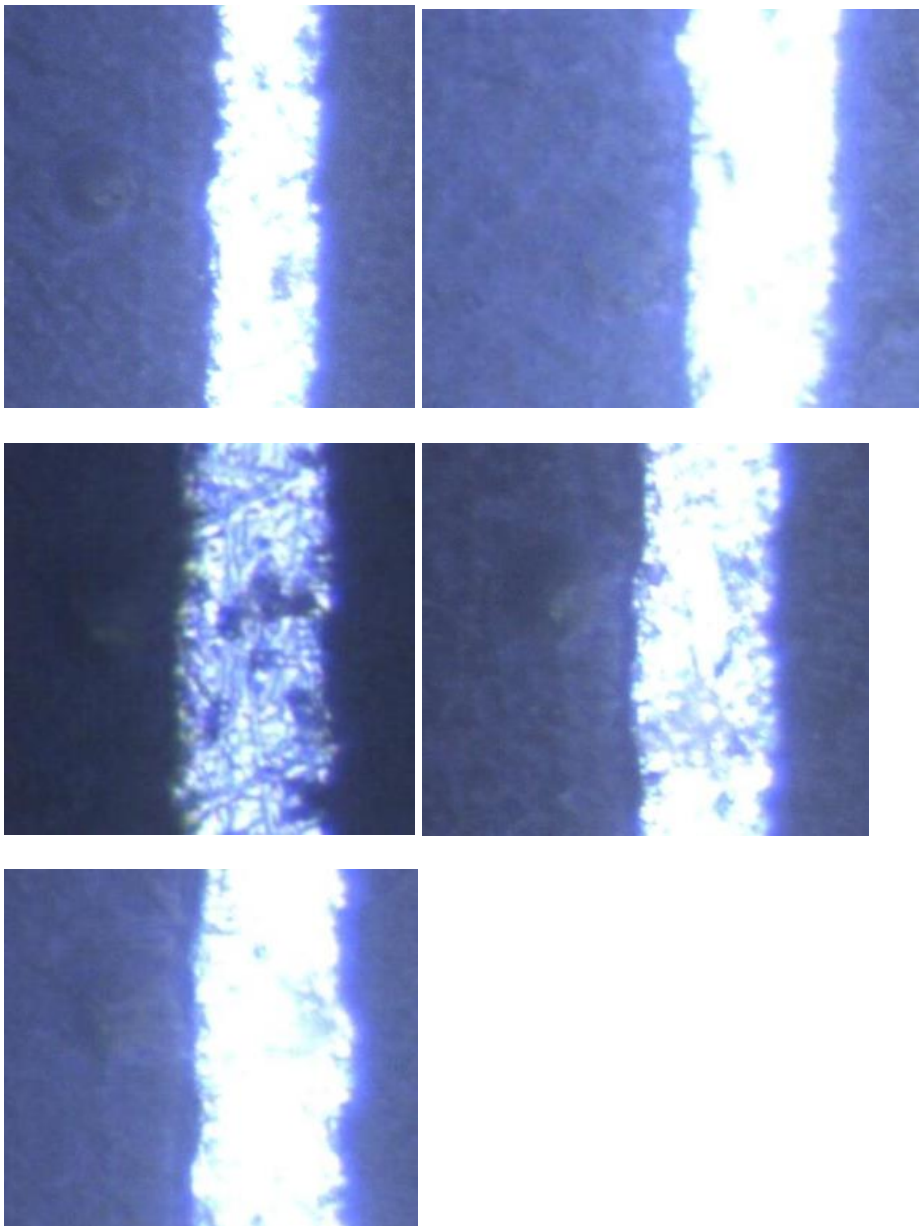

Figure 5.81 *Residual indents for cross-sectional indentation of sample 1 with the loading schedule 0,5 - 2 mN.*

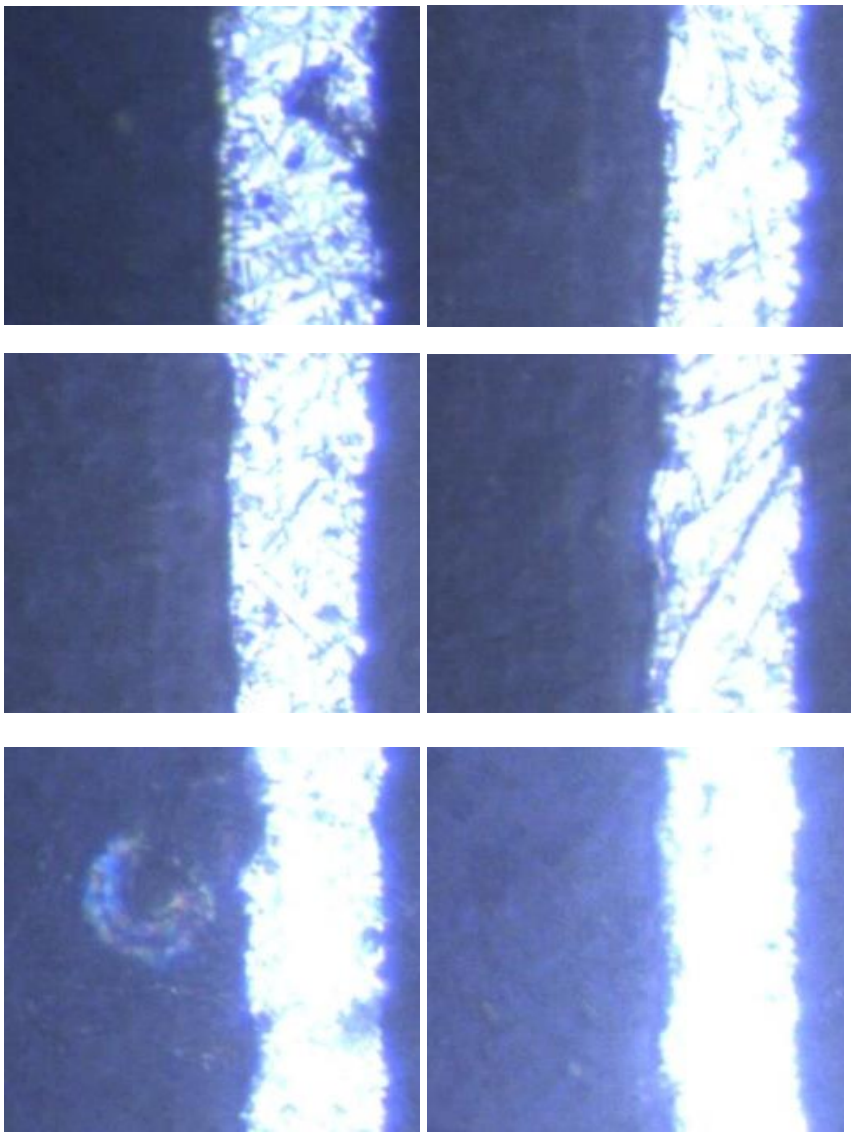

Figure 5.82 *Residual indents for cross-sectional indentation of sample 1 with the load schedule 0.05 - 1 mN. The image on the third row in the left column shows an indent that has (by mistake) been indented twice on the same coordinates.*

6 Summary of findings

6.1 Normal indentation

The hardness of the polymer was measured, and found to be approximately 15 MPa. There was variation due to surface roughness. The holding time was found to be more responsible for hardness value than loading rate.

6.2 Scratch test

Both samples with and without paperboard was investigated via scratch test. No sign of the indenter reaching through to the aluminum was found. No sign of delamination could be found. Applying acid normal to the surface for one day and submerging the sample in one day showed no difference in scratch behavior than an untreated sample. Submerging a sample in acid for two days resulted in a very soft material behavior with very little plastic deformation. No method for determining adhesion properties has been found.

6.3 Cross-sectional indentation

Both samples with and without paperboard has been tested using cross-sectional indentation. Placing the indents in the polymer-aluminum interface has been difficult. There seem to be a trend of higher success with better surface roughness. Loading curves has been analyzed qualitatively and sudden spikes in depth has been discovered. However, these have not been able to be linked with delamination or other adhesion properties. The acid-treated samples could not be indented in the interface and therefore have not been able to be compared to the non-treated ones.

7 Conclusions and future work

In this report the mechanical properties of the polymer and aluminum layer in a package application has been investigated via the nanoindentation technique. Although no obvious measures of adhesion could be found some interesting results have nonetheless been found and a discussion around these will be done in this chapter together with possible future experiments.

7.1 Normal indentation

Indentations were made normal to the polymer surface of two different samples of a carton package with different polymer thickness. Hardness was analyzed from these experiments and it was investigated how the hardness value depended on experimental parameters. It was found that holding time had bigger influence on the hardness value than loading rate. The hardness of the polymer was measured to approximately 15 MPa. However, there was quite significant variation, probably due to a high surface roughness, which was observed in a light microscope. To minimize this effect in future experiments a large number of indentations per measurement are proposed. Hardness has been measured only for a carton sample not treated with acid in the beginning of the work since focus was put on scratch test and cross-sectional indentation. However, it could be a useful approach in the future to perform hardness measurements on acid treated materials to compare these values to the ones from scratch or cross-sectional ones. Since the hardness and other mechanical properties of the polymer are probable to decrease when acid is applied, measuring the hardness in normal indentation could possibly adjust for this decrease in hardness in adhesion measuring tests, hopefully aiding in the task of isolating adhesion properties.

Further, another interesting technique could be to measure the decrease in hardness over time when the sample is subjected to acid. This could potentially be done in a liquid cell which is an alternative in which the sample is submerged in liquid and can be indented while being submerged. The results from these experiments could possibly be compared with other experiments/knowledge regarding migration behavior, adhesion tests and shelf life measurements to get a better grasp of the food-package interaction.

7.2 Scratch test

Scratch test were performed both for paperboard samples and samples without paperboard. A lot of focus was put on finding the optimal parameters regarding max load and loading rate. The max load most used was 50 mN as this gave a maximum depth during scratch close to the instruments maximum displacement limit of 20 µm. The thickness of the polymer layer of the scratched sample was 25 µm, and subtracting scratch curves with initial topography of the sample, which should give a value of the indentation depth into the polymer, produces a displacement into the polymer during scratch very close to these 25 µm at the end of the scratch sequence. However, no signs of the indenter reaching the aluminum or the polymer delaminating from the aluminum has been seen either in the loading curves or in investigations in light microscope. It could be seen in the light microscope up to a certain point that the polymer layer was unbroken but after a while the groove was too dark to conclude anything, probably due to the groove being too deep with the ridges creating a shadow. To overcome this problem a possible approach could be to use an electron microscope. The non-conductive nature of the polymer could give rise to some difficulties so some sample preparation techniques (e.g. coating with a conductive material) might have to be undertaken.

Further, the load curves showed a lot of oscillating behavior which might mask potential adhesion properties. A possible solution could be to investigate the dependence of this behavior on loading rates to see if there is a loading rate that minimizes these oscillations. Also, as these oscillations to some extent depend on the surface roughness, some focus should be put on sample preparation. For example, for the carton-less sample it is important to ensure a good surface finish of the sample holder prior to application and thereafter ensuring a thin evenly spread adhesive layer followed by an evenly applied pressure. Also, as the surface roughness cannot be minimized completely a possible approach could be to perform topography scans of the sample prior to carrying out the scratch tests to see where the surface finish is best.

Generally, a big problem with the scratch tests was to isolate the adhesion properties from the material properties and other possible influences. A possible solution to this could be to include samples with different materials and adhesion to see how the scratch response is changed when a different material is present. For example, a possibility could be to compare the scratch behavior of a sample with an outer layer of polyethylene to one with polypropylene and a sample with insufficient adhesion properties to one produced with optimal parameters. Also, materials with a polymer layer thinner than the instruments maximum displacement limit of 20 µm should be advantageous.

Although the indenter reached 20-25µm into the polymer during the scratch sequence the resulting residual scratch topography only showed a depth of approx. 5 µm that in the case of multiple scratch sequences did not increase more than a few hundred nanometers per each repeated scratch sequence. This is a bit surprising since polymers are not known for their scratch resistance, but rather wear resistance is something associated for harder materials. First one has to consider the accuracy

of the measurement. There is a possibility that the polymer retracts inwards after the scratch blocking the indenter from reaching the entire depth. This could potentially explain why there is so little plastic deformation after the first scratch in the multipass tests. To adjust for this uncertainty one could perform topography scans with an indenter with smaller edge radius and sharper angle. Also, the aforementioned electron microscope investigation might also give some hints about the depth.

Scratch tests on samples submerged in acid for one day showed no detectable difference to that of untreated ones. Samples submerged for two days gave a scratch response with a very soft material behavior as the indenter sank into the polymer rapidly to the instruments maximum displacement limit. However, the plastic deformation was significantly small and for the single scratch at times non-existent (which was in accordance with microscopic examinations) or otherwise on the order of 300 nm. Repeated scratching did not result in any change in scratch behavior or significant increase in plastic deformation, but rather each scratch yielded an increase of the depth of approx. 300 nm even up to fifteen times. Also of importance is that the surface topography was completely flat. The reason for the changed scratch response could be due to swelling of the polymer, which is a phenomena in which polymers after contact with solvent starts to increase its volume by absorption of the solvent. This leads to the polymer becoming soft and rubbery [58]. However, this behavior vanished after one day as the scratch behavior reverted back to the one seen for non-treated materials. This shows that the behavior of acid is time-dependent and decreases with time. In future experiments this detail therefore needs to be taken into account so that experiments are performed as soon after acid removal as possible.

In summary, it has been shown that an effect of the acid treatment is detectable by the nanoindentation instrument using nano-scratch. It therefore gives some credibility to the approach of measuring the polymer degradation via normal indentation as proposed in chapter 0. However, isolating the adhesion properties from the material properties seem difficult. As mentioned, a first step of isolating adhesion properties should be to choose the samples to test carefully in order to create an understanding of how varying material and adhesion properties affect the scratch response. Also, some comparison to normal indentation studies of acid treated samples could be done. This way, a method to account for the decreased hardness could potentially be found, thus inching closer to a way of isolating adhesion properties.

7.3 Cross-sectional indentation

For the cross-sectional indentation tests the biggest struggle was to get the indenter to hit squarely in the interface consistently. It was possible on some samples but not all. It seems to be a correlation between surface roughness and the ability to hit the interface as samples with a high surface roughness have had lower success at hitting the interface.

One explanation for the difficulty of indenting the interface could be that the aluminum layer protrudes above the polymer layer so that the indenter first reaches the edge of the aluminum layer. Thereafter, the indenter can slide towards the polymer layer or into the aluminum layer. The sliding can be caused both by instabilities in the instrument or by the aluminum layer bending outwards or inwards. This sliding could also partly explain the spikes in depth seem for some indentation experiments, predominantly those closer to the interface.

A protruding aluminum layer was observed for the acid treated samples but for the fresh sample, determining exact focus of the polymer was difficult due to the smoothness and lack of details. The difference in height was at least not as apparent as for the acid samples. For one of the acid treated samples the aluminum layer was measured to protrude from the polymer layer with approximately 2-3 µm. Therefore, emphasis has to be put on sample preparation if future experiments are to be undertaken. A possible method could be to explore the possibility of cutting instead of grinding. For example, a microtome cutter can cut very thin samples on a sub-micron scale and perhaps the surface of the sample after cutting could be sufficient for nanoindentation testing. Otherwise, careful grinding with a lot of focus on trying to determine the surface roughness should be performed, to hopefully develop a protocol where consistently satisfactory surface finish is obtained.

It cannot be ruled out that the spikes seen in some experiments are in fact a sign of delamination between the polymer and aluminum but no conclusive evidence to support that theory has been found. One finding that somewhat contradicts that idea is that some experiments there seemed to be a combined effect of oscillation and spikes. The oscillation does not have an obvious explanation but it seems likely that it is some kind of instability rather than material property. The combination of oscillation and spikes in the same curve therefore indicates that the spikes and oscillation might be two symptoms of errors. It therefore casts some doubt on the viability on using those spikes as a measure of adhesion.

The hardness for indents reaching the interface squarely were found to be larger than those in the polymer layer, and the variation in hardness were larger for the indents reaching the interface than those reaching the polymer. No indents reached the interface squarely for the samples subjected to acid, instead hardness comparisons were done with non-treated samples with indents offset from the interface. Although the hardness were higher for the non-treated one than the acid-treated one the difference were comparable to the one between hardness measurements of two acid treated samples. This casts some doubt about the validity of that difference. Also, analogous to the discussion for scratch test a method for

isolating adhesion properties were not found. It is possible that hardness is a viable measure, but since the samples submerged in acid was not possible to indent squarely in the interface, a comparison could not be made which renders an investigation on the viability on hardness as a measure impossible.

If the theory of a protruding aluminum causing the indenter to slide is true, a possible solution could be to use an indenter with a smaller edge radius and smaller angle that would hopefully avoid the protruding aluminum layer to a greater extent than the comparably blunt 5 µm tip used in the experiments. It is possible to get tips with edge radiuses down to some tens of nanometers. Also some thought could be put on the appearance of the indenter. It is for example possible to use a wedge type indenter which could perhaps be better at creating delamination in cross-sectional indentation. Another method that would aid in understanding the behavior during cross-sectional indentation is the use of an electron microscope which could give some insight in whether the aluminum protrudes above the polymer layer and perhaps also give some insight in whether the indenter slides during indentation or if drift renders the indent placement randomized.

7.4 Suggestion for future work

In conclusion, although the nanoindentation technique in theory seem to be well-equipped to measure the adhesion in thin film multilayer structures this report has not been able to find a method to measure the adhesion properties. Firstly, the soft viscoelastic properties of the polymer layer is something that the instrument is not well equipped to model. Secondly, sample preparation has proven to be of vital importance as too high surface roughness has proven to make testing difficult. Further, a big challenge which has yet to find a solution is to find an approach to isolate the adhesion properties. A few suggestions for future experiments are proposed below.

- For normal indentation: Investigate how the hardness of the polymer changes with acid application and investigate if this can be connected to other properties (e.g. migration, shelf life, adhesion).
- Choose material with care: different polymer materials, different adhesion.
- For the scratch test, use a material with a polymer thickness lower than 20 µm.
- For the cross-sectional tests, use a sharp indenter with low angle.

8 References

1. Fusions, 2015, *Estimates of european food waste levels, http://www.eu-fusions.org/phocadownload/Publications/Estimates%20of%20European%20food%20waste%20levels.pdf*
2. Marsh, K. and B. Bugusu, *Food packaging - Roles, materials, and environmental issues.* Journal of Food Science, 2007. **72**(3): p. R39-R55.
3. Sivaramakrishna, V., et al., *Development of a timesaving leak detection method for brick-type packages.* Journal of Food Engineering, 2007. **82**(3): p. 324-332.
4. Lamberti, M. and F. Escher, *Aluminium foil as a food packaging material in comparison with other materials.* Food Reviews International, 2007. **23**(4): p. 407-433.
5. Hernandez-Munoz, P., R. Catala, and R. Gavara, *Food aroma partition between packaging materials and fatty food simulants.* Food Additives and Contaminants, 2001. **18**(7): p. 673-682.
6. Tuominen, M., et al., *The Effect of Flame Treatment on Surface Properties and Heat Sealability of Low-Density Polyethylene Coating.* Packaging Technology and Science, 2013. **26**(4): p. 201-214.
7. Wagner Jr, J.R., *Multilayer Flexible Packaging*. 2009: Elsevier.
8. Hsu, C.L. and K.S. Chang, *Development of a novel method for detecting the integrity of aseptic paperboard laminate packages containing aluminium foil.* Food Control, 2007. **18**(2): p. 102-107.
9. Wolf, R., *A Technology Decision - Adhesive Lamination or Extrusion Coating/Lamination?*, in *TAPPI PLACE CONFERENCE 2010*. 2010: Albuquerque, New Mexico USA.
10. Enercon. *Improve Lamination Adhesion with Surface Treating*. Available from: http://www.enerconind.com/treating/library/applications/laminating-adhesion-improves-with-treatment.aspx.
11. Wolf, R.A., *MODIFYING SURFACE FEATURES Extrusion Coating and Lamination*, in *TAPPI PLACE CONFERENCE 2007 - "Polymers, Laminations, Adhesives, Coatings, Extrusions"* St. Louis, MO, United States
12. Britt, K.W. *Papermaking.* Encyclopaedia Brittanica online; Available from: http://global.britannica.com/topic/papermaking#ref625114.
13. Yang, Y.K., et al., *A study of Taguchi and design of experiments method in injection molding process for polypropylene components.* Journal of Reinforced Plastics and Composites, 2008. **27**(8): p. 819-834.
14. Kostic, M.R.L.G. *Extrusion Die Design*. Encyclopedia of Chemical Processing 2005; page 641-643]. Available from: http://www.kostic.niu.edu/extrusion_die_design-echp-1.pdf.
15. Sprang, N., D. Theirich, and J. Engemann, *Plasma and ion beam surface treatment of polyethylene.* Surface & Coatings Technology, 1995. **74-75**(1-3): p. 689-695.

16. Zhang, D., Q. Sun, and L.C. Wadsworth, *Mechanism of corona treatment on polyolefin films.* Polymer Engineering and Science, 1998. **38**(6): p. 965-970.
17. Tehrany, E.A. and S. Desobry, *Partition coefficients in food/packaging systems: a review.* Food Additives and Contaminants Part a-Chemistry Analysis Control Exposure & Risk Assessment, 2004. **21**(12): p. 1186-1202.
18. Rodushkin, I. and A. Magnusson, *Aluminium migration to orange juice in laminated paperboard packages.* Journal of Food Composition and Analysis, 2005. **18**(5): p. 365-374.
19. Schubert, G., *Adhesion of Aluminium Foil to Coatings – Stick With it*, in *TAPPI European PLACE Conference*. 2003: Budapest.
20. Gnanasekharan, V. and J.D. Floros, *Migration and sorption phenomena in packaged foods.* Critical Reviews in Food Science and Nutrition, 1997. **37**(6): p. 519-559.
21. Olafsson, G. and I. Hildingsson, *Sorption of Fatty-Acids into Low-Density Polyethylene and Its Effect on Adhesion with Aluminum Foil in Laminated Packaging Material.* Journal of Agricultural and Food Chemistry, 1995. **43**(2): p. 306-312.
22. Willige van, R.W.G., *Effects of flavour absorption on foods and their packaging materials*. 2002, Wageningen University.
23. Olafsson, G., et al., *Delamination of Polyethylene and Aluminum Foil Layers of Laminated Packaging Material by Acetic-Acid.* Journal of Food Science, 1993. **58**(1): p. 215-219.
24. Olafsson, G., et al., *Effects of Different Organic-Acids on the Adhesion between Polyethylene Film and Aluminum Foil.* Food Chemistry, 1993. **47**(3): p. 227-233.
25. *Fatty Acid.* Encyclopaedia Brittanica online.
26. *Fatty-acic nomenclature*. Oxford Dictionary of Biochemistry and Molecular Biology; Available from: http://www.oxfordreference.com/view/10.1093/acref/9780198529170.001.0001/acref-9780198529170-e-6838.
27. Fowkes, F.M., *Acid-Base Interactions in Polymer Adhesion*, in *Tribology Series*, J.M. Georges, Editor. 1981, Elsevier. p. 119-137.
28. Bell, R.P. *Acid-Base reaction*. Encyclopaedia Brittanica online]. Available from: http://www.britannica.com/science/acid-base-reaction.
29. *The Lewis Definitions of Acids and Bases*. Available from: http://chemed.chem.purdue.edu/genchem/topicreview/bp/ch11/lewis.php.
30. Sun, C. and J.C. Berg, *A review of the different techniques for solid surface acid–base characterization.* Advances in Colloid and Interface Science, 2003. **105**(1–3): p. 151-175.
31. van den Brand, J., *On the adhesion between aluminum and polymers*, in *Delft University of Technology*. 2004.
32. Kucukpinar, E. and H.C. Langowski, *Adhesion Aspects in Packaging.* Journal of Adhesion Science and Technology, 2012. **26**(20-21): p. 2317-2324.

33. Mittal, K.L., *Adhesion Measurement of Thin-Films.* Electrocomponent Science and Technology, 1976. **3**(1): p. 21-42.
34. Jesdinszki, M., et al., *Evaluation of Adhesion Strength Between Thin Aluminum Layer and Poly(ethylene terephthalate) Substrate by Peel Tests - A Practical Approach for the Packaging Industry*. Journal of Adhesion Science and Technology, 2012. **26**(20-21): p. 2357-2380.
35. Cohen, S.R. and E. Kalfon-Cohen, *Dynamic nanoindentation by instrumented nanoindentation and force microscopy: a comparative review*. Beilstein Journal of Nanotechnology, 2013. **4**: p. 815-833.
36. Fischer-Cripps, A.C., *Nanoindentation*. 2011, New York Dordrecht Heidelberg London: Springer.
37. Cheneler, D. and J. Bowen, *Degradation of polymer films.* Soft Matter, 2013. **9**(2): p. 344-358.
38. Chen, L., *Nanoindentation characterization of high chromium white cast iron for assessment of machining performance*, in *Production and Materials Engineering*. 2015, Lund University.
39. Oliver, W.C. and G.M. Pharr, *An Improved Technique for Determining Hardness and Elastic-Modulus Using Load and Displacement Sensing Indentation Experiments.* Journal of Materials Research, 1992. **7**(6): p. 1564-1583.
40. Cinar, E., F. Sahin, and D. Yablon, *Development of a novel nanoindentation technique by utilizing a dual-probe AFM system.* Beilstein Journal of Nanotechnology, 2015. **6**: p. 2015-2027.
41. Mencik, J. and L. Benes, *Determination of viscoelastic properties by nanoindentation.* Journal of Optoelectronics and Advanced Materials, 2008. **10**(12): p. 3288-3291.
42. VanLandingham, M.R., et al., *Nanoindentation of polymers: An overview.* Macromolecular Symposia, 2001. **167**: p. 15-43.
43. Fang, T.H. and W.J. Chang, *Nanoindentation characteristics on polycarbonate polymer film.* Microelectronics Journal, 2004. **35**(7): p. 595-599.
44. Briscoe, B.J., L. Fiori, and E. Pelillo, *Nano-indentation of polymeric surfaces.* Journal of Physics D-Applied Physics, 1998. **31**(19): p. 2395-2405.
45. Beake, B.D. and G.J. Leggett, *Nanoindentation and nanoscratch testing of uniaxially and biaxially drawn poly(ethylene terephthalate) film.* Polymer, 2002. **43**(2): p. 319-327.
46. Strojny, A., et al., *Techniques and considerations for nanoindentation measurements of polymer thin film constitutive properties.* Journal of Adhesion Science and Technology, 1998. **12**(12): p. 1299-1321.
47. Spinks, G.M., H.R. Brown, and Z. Liu, *Indentation testing of polystyrene through the glass transition.* Polymer Testing, 2006. **25**(7): p. 868-872.
48. Cakmak, U.D., T. Schoberl, and Z. Major, *Nanoindentation of polymers.* Meccanica, 2012. **47**(3): p. 707-718.
49. Schuh, C.A., *Nanoindentation studies of materials.* Materials Today, 2006. **9**(5): p. 32-40.

50. Tranchida, D., et al., *Mechanical characterization of polymers on a nanometer scale through nanoindentation. A study on pile-up and viscoelasticity.* Macromolecules, 2007. **40**(4): p. 1259-1267.
51. Oyen, M.L. and R.F. Cook, *Load-displacement behavior during sharp indentation of viscous-elastic-plastic materials.* Journal of Materials Research, 2003. **18**(1): p. 139-150.
52. Hochstetter, G., A. Jimenez, and J.L. Loubet, *Strain-rate effects on hardness of glassy polymers in the nanoscale range. Comparison between quasi-static and continuous stiffness measurements.* Journal of Macromolecular Science-Physics, 1999. **B38**(5-6): p. 681-692.
53. Djokic, J.D., et al., *Processing and nanomechanical properties of chitosan/poly(ethylene oxide) blend films.* Journal of the Serbian Chemical Society, 2012. **77**(12): p. 1723-1733.
54. Zhou, B.a.P., B.C. *The Manifestation of Substrate Effects in Thin Film Nanoindentation*. in *Proceedings of the SEM Annual Conference*. 2009. Albuquerque New Mexico USA: Society for Experimental Mechanics Inc.
55. Liu, Z.H., et al., *Interfacial characteristics of polyethylene terephthalate-based piezoelectric multi-layer films.* Thin Solid Films, 2013. **531**: p. 284-293.
56. Kassavetis, S., S. Logothetidis, and I. Zyganitidis, *Nanomechanical Testing of the Barrier Thin Film Adhesion to a Flexible Polymer Substrate.* Journal of Adhesion Science and Technology, 2012. **26**(20-21): p. 2393-2404.
57. Li, M., et al., *Adhesion of polymer-inorganic interfaces by nanoindentation.* Journal of Materials Research, 2001. **16**(12): p. 3378-3388.
58. Callister, William D and Rethwisch, David G., 2013, *Materials Science and Engineering*. 4th ed., ISBN: 9781118322697
59. Davidson, M.W. *Resolution*. Available from: http://www.microscopyu.com/articles/formulas/formulasresolution.html.
60. Pharr, G.M., E.G. Herbert, and Y.F. Gao, *The Indentation Size Effect: A Critical Examination of Experimental Observations and Mechanistic Interpretations.* Annual Review of Materials Research, Vol 40, 2010. **40**: p. 271-292.